

COMPACT AND ROBUST MEMBRANE BIOREACTOR FOR SOURCE-SEPARATED URINE RESOURCE RECOVERY FOR A CIRCULAR ECONOMY

by JIAXI JIANG

Thesis submitted in fulfilment of the requirements for
the degree of

Doctor of Philosophy

under the supervision of Prof Hokyong Shon and
Dr Sherub Phuntsho

University of Technology Sydney
Faculty of Engineering and Information Technology

February 2022

Certificate of Original Authorship

I, Jiayi Jiang declare that this thesis, is submitted in fulfilment of the requirements for the award of Doctor of Philosophy, in the School of Civil and Environmental Engineering, Faculty of Engineering and Information Technology at the University of Technology Sydney.

This thesis is wholly my own work unless otherwise referenced or acknowledged. In addition, I certify that all information sources and literature used are indicated in the thesis.

This document has not been submitted for qualifications at any other academic institution.

This research is supported by the Australian Government Research Training Program.

Production Note:

Signature: Signature removed prior to publication.

Date: 23/02/2022

Acknowledgements

I would like to express my sincere appreciation to my principal supervisor Prof. Hokyong Shon and co-supervisor Dr. Sherub Phuntsho for their continuous support of my Ph.D. study and encourage me in pursuing my research interests. My deepest thanks to Dr. Pema Dorji, Dr. Ugyen Dorji, Dr. Jiawei Ren, Dr. Federico Volpin, Mr. Umakant Badeti and Mr. Abdulaziz Yousef B Almntashiri for their guidance and collaborations. Thanks to my family for supporting me all the time, always uplift me, comfort me, and bring joy to my soul.

List of Publications

1. U. Badeti, **J. Jiang**, A. Almuntashiri, N. Pathak, U. Dorji, F. Volpin, S. Freguia, W.L. Ang, A. Chanan, S. Kumarasingham, H.K. Shon, S. Phuntsho, Impact of source-separation of urine on treatment capacity, process design, and capital expenditure of a decentralised wastewater treatment plant, *Chemosphere*, 300 (2022) 134489.
2. **J. Jiang**, S. Phuntsho, N. Pathak, Q. Wang, J. Cho, H.K. Shon, Critical flux on a submerged membrane bioreactor for nitrification of source separated urine, *Process Safety and Environmental Protection*, 153 (2021) 518-526.
3. J. Ren, D. Hao, **J. Jiang**, S. Phuntsho, S. Freguia, B.-J. Ni, P. Dai, J. Guan, H.K. Shon, Fertiliser recovery from source-separated urine via membrane bioreactor and heat localized solar evaporation, *Water Research*, 207 (2021) 117810.
4. F. Volpin, U. Badeti, C. Wang, **J. Jiang**, J. Vogel, S. Freguia, D. Fam, J. Cho, S. Phuntsho, H.K. Shon, Urine treatment on the international space station: current practice and novel approaches, *Membranes*, 10 (2020) 327.
5. F. Volpin, **J. Jiang**, I. El Saliby, M. Preire, S. Lim, M.A. Hasan Johir, J. Cho, D.S. Han, S. Phuntsho, H.K. Shon, Sanitation and dewatering of human urine via membrane bioreactor and membrane distillation and its reuse for fertigation, *Journal of Cleaner Production*, 270 (2020) 122390.

Journal Articles Under Review

1. W. Shon, **J. Jiang**, S. Phuntsho, H.K. Shon. (Under review). Nutrient in a Circular Economy: Role of urine separation and treatment.
2. **J. Jiang**, A. Almuntashiri, W. Shon, S. Phuntsho, Q. Wang, S. Freguia, I, El-Saliby, H.K. Shon. (Under review). Feasibility study of powdered activated carbon membrane bioreactor (PAC-MBR) for source-separated urine treatment: a comparison with MBR.

Conferences

1. The 11th International Membrane Science and Technology Conference (IMSTEC 2022), 4-8 December 2022. Australia & online. Poster presentation
2. 2022 Rich Earth Summit, 1- 3 November 2022. USA & online. Oral presentation
3. The International Workshop on Membrane in Kobe (IWMK 2021), 18-19 November 2021 online. Poster presentation
4. 2021 Rich Earth Virtual Summit, 3-5 November 2021 online. Attended
5. North American Membrane Society (NAMS 2020), 18-21 May 2020 online. Attended
6. The 2021 International Conference on the "Challenges in Environmental Science and Engineering" (CESE-2021), 6-7 November 2021 online. Oral presentation
7. The 4th International Conference on capacitive Deionization and Electrosorption (CDI&E 2019), 20-23 May China. Poster presentation

Table of Contents

Certificate of Original Authorship	i
Acknowledgements	ii
List of Publications	iii
Journal Articles Under Review	iv
Conferences.....	v
List of Figures	x
List of Tables	xiii
Abstract	xiv
1 Introduction.....	1
1.1 Research background.....	1
1.2 Contribution to the existing knowledge.....	2
1.3 Research aims and objectives.	4
1.4 Thesis structure outline.....	5
2. Literature review.....	7
2.1 Urine composition and properties.....	7
2.2 Why reusing the nutrients in the urine.....	9
2.3 Types and Implementations of Urine Diversion.....	12
2.3.1 Urine-Diverting Flush Toilet (UDFT)	13
2.3.2 Urine-Diverting Dry Toilet (UDDT)	18

2.4	Review of current membrane technologies for urine resource utilization....	19
2.4.1	Pressure driven membrane process	20
2.4.2	Forward osmosis (FO)	21
2.4.3	Electrodialysis (ED).....	22
2.5	Review of alternative membrane-based process for source-separated urine resource utilization	24
2.5.1	Forward osmosis-reverse osmosis (FO-RO).....	24
2.5.2	Membrane bioreactor (MBR) and MBR-combined treatment process	25
2.5.3	Membrane distillation (MD).....	28
2.6	Nitrification.....	29
3.	Critical flux on a submerged membrane bioreactor for nitrification of source separated urine	32
3.1	Abstract.....	32
3.2	Introduction.....	33
3.3	Materials and methods	36
3.3.1	MBR set-up and operation.....	36
3.3.2	Characteristics of stored source separated urine	39
3.3.3	Determination of critical flux and the critical flux for irreversibility.....	40
3.3.4	Analytical methods	42
3.4	Results and discussion	44
3.4.1	UF-MBR start-up and operation	44
3.4.2	Effect of step length and height on critical flux.....	49

3.4.3	Effect of aeration intensity on critical flux	50
3.4.4	Effect of sludge concentration on critical flux.....	51
3.4.5	Fouling reversibility	52
3.5	Conclusions.....	56
4	Effects of PAC concentration in membrane bioreactor (MBR) for source-separated urine treatment	57
4.1	Materials and methods.....	57
4.1.1	Laboratory scale PAC-MBR operation.....	57
4.1.2	Analytical methods	59
4.2	Results and discussion	61
4.2.1	Effect of PAC dosage on membrane permeate water quality	61
4.2.2	Effect of PAC dosage on organic matter removal	62
4.2.3	Effect of PAC dosage on micropollutant removal	64
4.2.4	Effect of PAC dosage on sludge mixture properties.....	65
4.3	Conclusions.....	66
5.	Feasibility study of powdered activated carbon membrane bioreactor (PAC-MBR) for source-separated urine treatment: a comparison with MBR	67
5.1	Abstract.....	67
5.2	Introduction.....	68
5.3	Materials and methods	69
5.3.1	Experimental setup.....	69
5.3.2	Water quality analysis	72

5.3.3	Micropollutant analysis.....	73
5.3.4	Fouling models analysis.....	75
5.4	Results and discussion	78
5.4.1	Comparison of permeate water quality.....	78
5.4.2	Comparison of organic matter removal	79
5.4.3	Comparison of biomass growth.....	80
5.4.4	Membrane performance.....	82
5.4.5	Removal of micropollutants by MBR.....	87
5.5	Conclusion.....	91
6	Conclusions and recommendations	92
6.1	Conclusions.....	92
6.2	Limitations and recommendations.....	93
	Bibliography.....	95
	Appendix A Code for fouling model simulations and automatically calculating sum of squared error (SSE) and model fitting constants.....	111
	Appendix B Theoretical fouling models results (Control MBR).....	123
	Appendix C Theoretical fouling models results (Hybrid PAC-MBR)	127

List of Figures

Figure 2.1 World and regional potential nutrient balance between 2016 and 2020. Modified from FAO (2017).	10
Figure 2.2 Scheme of flow streams separation, treatment, and reuse for urine diversion flush toilets (UDFT) with sewerage system and urine diversion dry toilets (UDDT). Adapted with permission granted by the copyright holder Tilley et al. (2014).....	16
Figure 2.3 Two-phase collaborative project for implementation of novel sanitation systems in an urban office, funded by the Federal Ministry of Education and Research, Germany. Modified from Winker and Saadoun (2011).....	17
Figure 2.4 Pressure driven membrane filtration types	21
Figure 2.5 Schematic diagram of forward osmosis.....	22
Figure 2.6 Schematic diagram of membrane capacitive deionization (MCDI)	23
Figure 2.7 Schematic diagram of hybrid forward osmosis-reverse osmosis (FO-RO) system.....	24
Figure 2.8 Schematic diagram of two common MBR configurations. (a) side-stream MBR, (b) submerged MBR.....	26
Figure 2.9 Schematic diagram of MD system.....	29
Figure 3.1 Schematic diagram of the lab scale UF-MBR	37
Figure 3.2 Pure water flux (PWF) of potted UF membrane module at different TMP...	37
Figure 3.3 Typical flux profile in (a) continues and (b) improved flux-step method.	41
Figure 3.4 (a) pH profile during the MBR start-up and stable operation stages. (b) all-time concentration of inorganic nitrogen compounds in feed urine and MBR permeate	46
Figure 3.5 Concentration of FA and FNA during the MBR start-up period and stable operation, and corresponding nitrite accumulation phenomenon.	48

Figure 3.6 Effects of various flux step length and step height on critical flux when aeration intensity at 0.2 m ³ h ⁻¹ , biomass concentration at 3.5 g. L ⁻¹ , initial flux rate at 4 Lm ⁻² h ⁻¹ , and reference flux rate at 0.5 Lm ⁻² h ⁻¹	50
Figure 3.7 Effects of various aeration intensity and biomass concentration on critical flux when initial flux rate at 4 Lm ⁻² h ⁻¹ , reference flux rate at 0.5 Lm ⁻² h ⁻¹ , flux step length at 15 min, and step height at 6 Lm ⁻² h ⁻¹	51
Figure 3.8 Profile of TMP, total fouling rate (F _{Total}), irreversible fouling rate (F _{Irr}) and critical fouling rate (F _{Crit}) on membrane determined by the improved flux-step method among various aeration intensity (a) 0.1 m ³ h ⁻¹ , (b) 0.2 m ³ h ⁻¹ , and (c) 0.4 m ³ h ⁻¹ . The biomass concentration at 3.5 g.L ⁻¹ , initial flux rate at 4 Lm ⁻² h ⁻¹ , reference flux rate at 0.5 Lm ⁻² h ⁻¹ , flux step length at 15 min, and step height at 6 Lm ⁻² h ⁻¹	55
Figure 4.1 Schematic diagram of proposed hybrid PAC-MBR.....	59
Figure 4.2 Variation of COD removal efficiencies in (a) low PAC-MBR and (b) high PAC-MBR overtime	63
Figure 4.3 Overall micropollutants removal rate in low PAC-MBR and high PAC-MBR	64
Figure 4.4 Variation of MLSS concentration and MLSS/MLVSS ratio in (a) low PAC-MBR and (b) high PAC-MBR overtime	66
Figure 5.1 Schematic diagram of (a) control MBR and (b) hybrid PAC-MBR.....	71
Figure 5.2 Variation of COD removal efficiencies in (a) control MBR, and (b) hybrid PAC-MBR in 73 days	80
Figure 5.3 Variation of MLSS concentration and MLSS/MLVSS ratio in (a) control MBR and (b) hybrid PAC-MBR in 73 days	81

Figure 5.4 Theoretical and experimental Pt/P0 versus time profiles and corresponding SSE values for single and combined membrane fouling models in (a) control MBR and (b) hybrid PAC-MBR..... 86

Figure 5.5 Targeted micropollutant removal rate and logD_{6.2} value in control MBR and hybrid PAC-MBR 88

List of Tables

Table 2.1 The composition of fresh and stored human urine (Udert et al., 2006, Rose et al., 2015, Udert and Wachter, 2012)	8
Table 2.2 World and regional potential balance of ammonia as N, phosphate as P, potash as K between 2016 and 2020 (million tonnes). Modified from FAO (2017)	10
Table 3.1 Properties of the potted UF membrane module	38
Table 3.2 Composition and corresponding ion concentrations in each 40 L stored raw urine at room temperature	39
Table 3.3 Proposed experimental operation conditions and control parameters for membrane critical flux study.....	41
Table 3.4 The linear relationship between various aeration intensity and its corresponding critical flux value.....	52
Table 4.1 Composition and corresponding ion concentrations in source-separated urine, low PAC-MBR permeate and high PAC-MBR permeate.....	61
Table 5.1 Composition and corresponding ion concentrations in source-separated urine, control MBR permeate, and hybrid PAC-MBR permeate.....	71
Table 5.2 MRM table for proposed LC-MS/MS analysis.....	74
Table 5.3 Membrane fouling models and corresponding equations at constant flux.....	76
Table 5.4 Theoretical model fitting results and SSE values for the single and combined membrane fouling modules.....	84
Table 5.5 Physicochemical properties of targeted micropollutants and their corresponding removal efficiencies	89

Abstract

Human urine contains essential nutrient – nitrogen (N), phosphorus (P) and potassium (K) - for crop cultivation. However, using raw human urine as a direct agricultural fertilizer source is limited, due to its distinct odour, high pH condition, pathogen risk associated with faecal cross-contamination, and the possible presence of high concentrations of pharmaceuticals. Biological nitrification, a two-step biological oxidation process, is therefore a promising technology to covert volatile and odorous ammonia into stable odour-free nitrate, while still preserving all the nutrients. Although biological nitrification is a well-understood process, only a few research groups have studied the application of this process with undiluted human urine, and the experiences to optimize the nitrification of source-separated urine without addition of alkalinity are even less.

In addition, micropollutants such as pharmaceuticals and personal care products are a group of emerging environmental contaminants, which are structurally complex and can cause adverse physiological effects on human health even at low concentration when exposed for long-term. However, the current wastewater treatment technologies are not designed to remove these compounds, and hence most of these residual pharmaceuticals and hormones remain in the treated effluent. Therefore, it is very important that we remove the residual micropollutants by a natural biological process.

The combined processes of powdered activated carbon - microfiltration membrane bioreactor (PAC-MF-MBR) is thereby proposed in this work to optimize the efficiency

of biological nitrification, control membrane fouling, improve organic removal efficiency from 88% to 96%, achieve greater than 99% removal efficiency among all targeted micropollutants (metronidazole, acetaminophen, naproxen, ibuprofen carbamazepine and estriol), promote more rapid biomass growth, increase sludge floc size growth by 17% and achieve complete nutrient recovery from source-separated urine. This study demonstrates the potential application of full-scale PAC-MF-MBR plant in treating source-separated urine at building level for complete nutrient recovery.

Keywords: membrane bioreactor (MBR); powdered activated carbon (PAC); source-separated urine; circular economy; resource recovery; nitrification; micropollutant; fouling

1 Introduction

1.1 Research background

Human urine contributes 85-90% of nitrogen load, 50-80% of phosphorus load, and 80-90% of potassium load in only 1% of the total wastewater volume (Le et al., 2020, Wilsenach and Van Loosdrecht, 2004). The unique composition makes it, at the same time, a heavy burden for conventional biological sanitation. The conventional wastewater treatment plants (WWTPs) focus on the removal of N and P to mitigate or prevent the risk of eutrophication in the receiving water body (Preisner et al., 2021, Zhou et al., 2022). Maurer et al. (2003) calculated that biological oxidation of NH_4^+ into NO_2^- and NO_3^- and then the reduction into N_2 gas consumes $12.5 \text{ kWh kgN}^{-1}$, while chemical precipitation of PO_4^{3-} consumes 8.1 kWh kgP^{-1} . As urine contains high concentration of nitrogen (on average 8180 mgN.L^{-1}), phosphorous (on average 670 mgP.L^{-1}) and potassium (on average 2160 mgK.L^{-1}) (Randall and Naidoo, 2018b, Maurer et al., 2003, Maurer et al., 2006, Simha and Ganesapillai, 2017, Bhattacharyyab, 2010), the cost of treating urine is significant (Wilsenach and Loosdrecht, 2006). Wilsenach and Loosdrecht 2006 even demonstrated that, if 50% or more urine is treated separately, conventional wastewater treatment can achieve higher effluent quality and even being a source of net-energy production (Wilsenach and Loosdrecht, 2006).

On the other hand, source separation of human urine has been proposed for over two decades as a sustainable alternative solution for total nutrients recovery and reuse. For instance, the idea to integrate sewerage system with Urine-Diverting Flush Toilet (UDFT)

was firstly invented in the late 20th century in Sweden (Kvarnström et al., 2006). The practical application of using such water-based system includes the SANIRESCH (SANitaryRecycling ESCHborn) project in Germany and the UTS Sustainable Sanitation project in Australia. Above projects investigated the barriers associated with replacing existing sanitation systems to more sustainable urine diversion (UD) systems (Mitchell et al., 2013). The SANIRESCH project concluded that the struvite and compost received from the system is hygienic and safe to use for agricultural fertilization purpose and is considered economically feasible in favourable conditions (Winker and Saadoun, 2011). Moreover, the use of alternative sanitation system - Urine-Diverting Dry Toilet (UDDT) - in higher density areas is of important in many ways. The Ecological Sanitation Ethiopia project in Ethiopia concluded that the reuse of human excrete produces in agriculture would contribute to self-sufficiency and food-security - about 25% capital and operational cost reduction was achieved by using such waterless urine diverting systems, compared to conventional sanitation systems. The urine application could replace or reduce the chemical fertilizer usage and provide household additional incomes.

1.2 Contribution to the existing knowledge

Although, many studies have shown the reuse of human excrete produces in agriculture would contribute to self-sufficiency and food-security, using raw human urine as a direct agricultural fertilizer source is limited, due to its distinct odour, wide range of pH, pathogen risk associated with faecal cross-contamination, the possible presence of pharmaceuticals, and product transportability and application efficiency. Urine nitrification via membrane bioreactor (MBR) is therefore a promising technology to overcome these drawbacks. It can recover all nutrients that is beneficial for self-

sufficiency and food security, especially for crops with nitrogen deficiency. At the present, only a few research groups have studied this process with undiluted human urine, and the experiences to optimize the nitrification of very concentrated human urine without addition of alkalinity are even less.

In addition, the presence of micropollutants (MPs) such as pharmaceuticals and personal care products in wastewater streams is an emerging health and environmental concern (Kumari et al., 2020). These compounds are structurally complex and can cause adverse physiological effects on human health at low concentration (Gavrilescu et al., 2015, Luo et al., 2014). However, the current wastewater treatment technologies are not designed to remove these compounds, which leads to many residual pharmaceuticals and hormones in treated effluents (Samal et al., 2022). Hence, it is important that we can clean off the residual with nature and biological purification method (Chtourou et al., 2018, Qrenawi and Rabah, 2023, Tadkaew et al., 2010).

The post-treatment such as granular activated carbon (GAC) adsorption is introduced for additional MBR effluent purification, given that the physiochemical interactions between adsorbent and adsorbate can effectively remove MPs. However, such approach is unattractive due to high consumption of GAC, reduction in MPs removal efficiency due to the competitive adsorption between nutrients and MPs, decline of GAC adsorption capacity over time, and additional space requirement (Boehler et al., 2007, Almunashiri et al., 2021, Nguyen et al., 2013b, Asif et al., 2020). In contrast, the powdered activated carbon membrane bioreactor (PAC-MBR) is an attractive alternative to remove micropollutant via physical adsorption and biodegradation in a single step, as biological powdered activated carbon (BPAC) formed over time via growth of stable microbial film

on PAC surface (Stoquart et al., 2012, Zhang et al., 2015). The additional benefits for PAC-MBR system include: 1) increase urine nitrification efficiency (Ma et al., 2012, Thuy and Visvanathan, 2006, Hu et al., 2014b); (2) control and mitigate membrane fouling (Yang et al., 2016, Huang et al., 2021, Guo et al., 2008); (3) improve organic matter and micropollutant removal efficiency (Chtourou et al., 2018, Qrenawi and Rabah, 2023, Tadkaew et al., 2010); and (4) promote more rapid biomass growth (Hu et al., 2014b, Alvarino et al., 2017).

The compact and robust powdered activated carbon and microfiltration membrane bioreactor (PAC-MBR) process is therefore proposed in this work to optimize urine nitrification efficiency, control membrane fouling, improve organic matter and micropollutant removal efficiency, promote more rapid biomass growth and achieve complete nutrient recovery from source-separated urine.

1.3 Research aims and objectives.

This study aimed at exploring the potential application of integrating membrane bioreactor with powdered activated carbon additive for complete nutrient recovery and effective micropollutant removal from source-separated urine.

The specific objectives of the research were to:

- Conduct literature review on the membrane-based technologies in water and wastewater treatment and its application potential for source-separated urine resource utilization.

- Investigate the influence of nitrifying conditions on urine nitrification efficiencies and fouling behaviour in MBR treating source-separated urine.
- Investigate the effects of PAC concentration in MBR for source separated urine nutrient recovery in terms of treated permeate quality, micropollutant removal, and sludge mixture properties.
- Conduct a feasibility study for proposed hybrid MBR-PAC. Compare its performance with control MBR in terms of treated permeate quality, emerging contaminants removal, membrane fouling, and sludge mixture property.

1.4 Thesis structure outline

This dissertation contains six chapters, some of which includes published materials during the research tenure as a PhD candidate. The structure outline of the thesis is:

- Chapter one provides a brief background on the need and motivation for the research, and the main research objective and the scope of research.
- Chapter two provides a detailed literature review on the application of membrane-based technologies on urine source separation and resource utilization, challenges, and future developments. A part of this chapter is submitted for publication as “Nutrient in a Circular Economy: Role of urine separation and treatment.”
- Chapter three assesses the application of membrane bioreactor (MBR) for source-separated urine resource utilization. The result of this chapter was published in Process Safety and Environmental Protection titled as “Critical flux on a submerged membrane bioreactor for nitrification of source separated urine”. The results from this study were also presented during the CESE International

Conference 2021, 6-7 November 2021 and awarded the best student oral presentation (first place).

- Chapter four studies the effect of PAC concentration in lab-scale PAC-MBR combination process on biological and micropollutant removal performance. Chapter five compares the performance between a powdered activated carbon - membrane bioreactor (PAC-MBR-MF) and control MBR-MF for source-separated urine resource utilization in terms of treated permeate quality, emerging contaminants removal, membrane fouling, and sludge mixture property. These chapters are submitted for publication as “Feasibility study of powdered activated carbon membrane bioreactor (PAC-MBR) for source-separated urine treatment: a comparison with MBR”.
- Chapter six provides a summary of major conclusions from the research and provides recommendations for further improvement of system performance in compact and robust membrane bioreactor.

2. Literature review

[Notes: A part of this chapter has been submitted for publication and is currently under review]

W. Shon, **J. Jiang**, S. Phuntsho, H.K. Shon. (Under review). Nutrient in a Circular Economy: Role of urine separation and treatment

2.1 Urine composition and properties

Human urine contributes 85-90% of nitrogen load, 50-80% of phosphorus load and 80-90% of potassium load in only 1% of the total wastewater volume. The biological and chemical composition of fresh urine varies with recent fluid intake, diet, temperature, blood pressure, general health, etc. The chemical composition of source separated urine can change during storage (Table 2.1), as urea ($\text{CO}(\text{NH}_2)_2$) is hydrolysed to ammonia and bicarbonate by naturally occurring bacterial urease (Equation 2.1). The urine hydrolysis leads to an increase in pH (around 9), conductivity and osmotic pressure. Subsequently, resulting at least 30% of phosphorous is precipitated to the form of calcium phosphate, struvite, and calcite (Udert et al., 2003b, Udert et al., 2003a, Randall et al., 2016). Source separated urine can be collected by using urine diversion, also known as source-separated toilets and water free urinals. It helps separate collection and treatment of urine from feces, exemplifying the high potential of energy and resource recovery from source-separated urine at the level of a single household device.



Table 2.1 The composition of fresh and stored human urine (Udert et al., 2006, Rose et al., 2015, Udert and Wachter, 2012)

Component (unit)	Fresh urine		Hydrolyzed urine	
	Udert et al., 2006	Rose et al., 2015	Udert et al., 2006	Udert and Wachter, 2012
Total nitrogen (mgN.L ⁻¹)	9200	4000-13900	9200	
Total ammonia (mgN.L ⁻¹)	480	125-600	8100	2390 ± 250
Ammonia NH ₃ (mgN.L ⁻¹)	0.3		2700	
Urea (mgN.L ⁻¹)	20	9300-23300	0	
Total phosphate (mgP.L ⁻¹)	740	250-760	540	208 ± 49
COD (mgO ₂ .L ⁻¹)	10000	6270-17500	10000	4500 ± 910
Calcium (mg L ⁻¹)	190	32-320	0	16 ± 3
Magnesium (mg L ⁻¹)	100	70-120	0	< 5
Potassium (mg L ⁻¹)	2200	750-2610	2200	1410 ± 320
Total carbonate (mgC.L ⁻¹)	0		3200	
Sulphate (mgSO ₄ .L ⁻¹)	1500		1500	
Chloride (mg L ⁻¹)	3800		3800	

Sodium (mg L ⁻¹)	2600		2600	
Alkalinity (mM)	22		490	
Conductivity (mS cm ⁻¹)		160-270		
pH	6.2	5.5-7.0	9.1	8.69 ± 0.11

2.2 Why reusing the nutrients in the urine

The Food and Agriculture Organization of the United Nations (FAO, 2017) reported that the global fertilizer demand of the three primary plant nutrients - ammonia (NH₃) as N, phosphate (P₂O₅) as P, potash (K₂O) as K– reached 201.66 million tonnes in 2020/21 (FAO, 2017). From 2015 to end of 2020, the N demand increased annually by 1.5%, while the demand for P and K grown at an average annual rate of 2.2% and 2.4%, respectively. The world nitrogen capacity of fertilizers reached 160 million metric tons (mmt) in 2022. The report for world and regional potential nutrient balance – the difference between supply and total demand - suggested that regions such as Latin America & Caribbean, South Asia, West Europe, and Oceania are solely relied on fertilizer import from 2006 (Figure 2.1 and Table 2.2). In addition, Maurer et al. (2003) reported that the energy consumption in the conventional biological ammonium removal processes and struvite precipitation to remove phosphorous is 12.5 kWh kgN⁻¹ and 8.1 kWh kgP⁻¹, respectively. Urine has a high concentration of essential nutrients (N, P, K) which makes the treatment of urine costly (Randall and Naidoo, 2018b, Maurer et al., 2003, Maurer et al., 2006, Simha and Ganesapillai, 2017, Bhattacharyyab, 2010). Wilsenach and Loosdrecht (2006) found that treating 50% or more of the urine separately can result in improved effluent quality and even net-energy production in conventional wastewater treatment. Therefore,

urine fertilization is beneficial for self-sufficiency and food security, especially for crops with nitrogen deficiency. The urine application could replace or reduce the chemical fertilizer usage; provide household additional incomes.

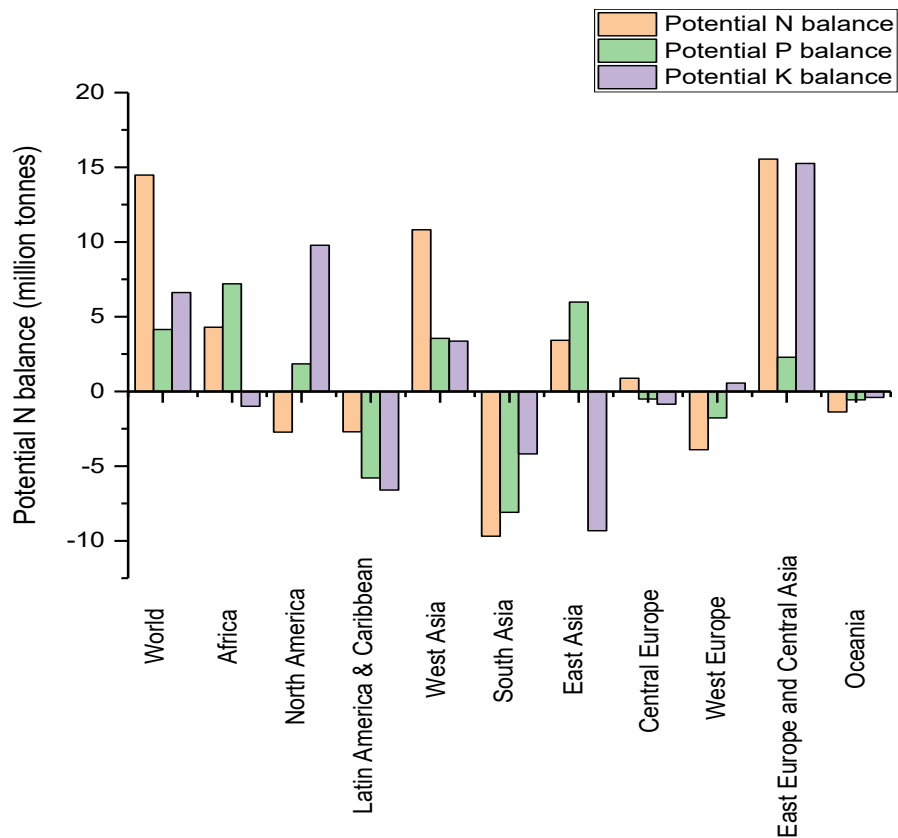


Figure 2.1 World and regional potential nutrient balance between 2016 and 2020. Modified from FAO (2017).

Table 2.2 World and regional potential balance of ammonia as N, phosphate as P, potash as K between 2016 and 2020 (million tonnes). Modified from FAO (2017)

Potential nutrient balance		2016	2018	2020
World	N	12.77	17.40	14.48

	P	3.98	4.19	4.14
	K	4.10	6.70	6.62
Africa	N	3.53	4.46	4.30
	P	5.23	6.46	7.20
	K	-0.76	-0.87	-1.0
North America	N	-3.67	-2.67	-2.73
	P	1.96	1.90	1.84
	K	7.61	9.35	9.78
Latin America & Caribbean	N	-1.97	-2.09	-2.70
	P	-4.78	-5.33	-5.79
	K	-5.76	-5.94	-6.60
West Asia	N	7.44	10.88	10.82
	P	2.51	3.14	3.55
	K	3.30	3.30	3.37
South Asia	N	-7.86	-8.99	-9.69
	P	-6.48	-7.42	-8.09
	K	-3.36	-3.75	-4.18
East Asia	N	5.45	4.56	3.42
	P	5.71	5.85	5.98

	K	-8.87	-8.58	-9.32
Central Europe	N	1.06	0.98	0.88
	P	-0.42	-0.46	-0.51
	K	-0.70	-0.81	-0.86
West Europe	N	-4.00	-3.97	-3.90
	P	-1.76	-1.82	-1.78
	K	1.00	0.75	0.56
East Europe and Central Asia	N	14.00	15.51	15.55
	P	2.52	2.40	2.29
	K	12.01	13.64	15.26
Oceania	N	-1.19	-1.27	-1.38
	P	-0.50	-0.53	-0.56
	K	-0.39	-0.39	-0.40

2.3 Types and Implementations of Urine Diversion

Urine diversion, also known as source separation, helps separate collection and treatment of urine from faeces, exemplifying the high potential of energy and resource recovery from source-separated urine at the level of a single household device (Larsen et al., 2016, Panesar et al., 2006). In addition, the urine diversion systems contribute less to toilet-

related groundwater contamination than conventional sanitation systems (Hanak et al., 2016). The most common types of urine diversion in urban areas are urine diversion flush toilets (UDFT) and urine diversion dry toilets (UDDT) which have been commercially available worldwide. Figure 2.2 shows the scheme of flow streams separation, treatment, and reuse for (a) urine diversion flush toilets treatment, and reuse for (a) urine diversion flush toilets (UDFT) with sewerage system (b) urine diversion dry toilets (UDDT).

2.3.1 Urine-Diverting Flush Toilet (UDFT)

The idea to integrate sewerage system with UDFT was firstly invented in the late 20th century in Sweden (Kvarnström et al., 2006). The practical application of using such water-based system include the SANIRESCH (SANItaryRecycling ESCHborn) in Germany and the UTS Sustainable Sanitation project in Australia.

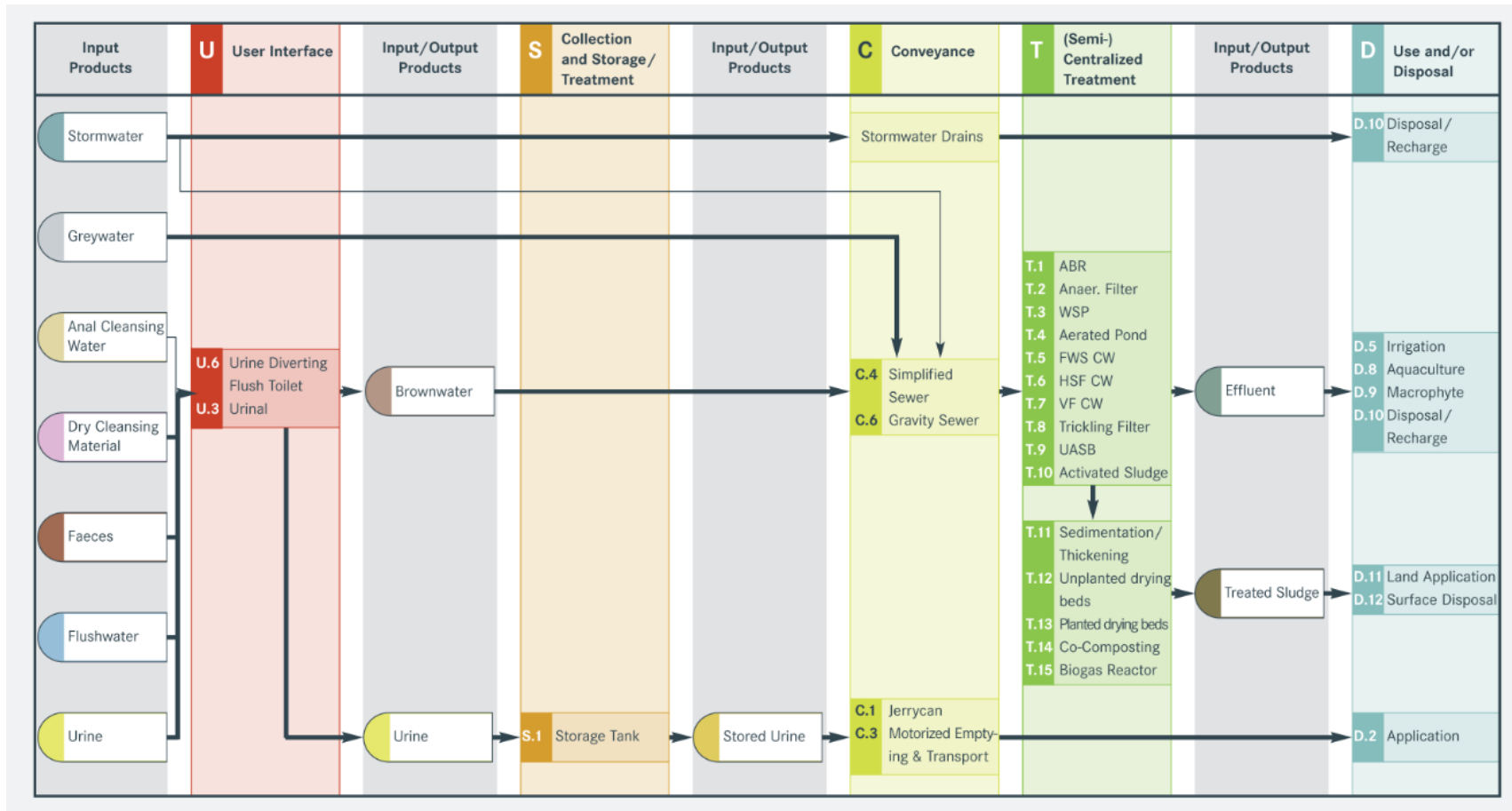
GTZ and SANIRESCH program

The Federal Ministry of Education and Research funded two-phase collaborative project for implementation of novel sanitation concepts in an urban office (Figure 2.3). The objective of first stage GTZ program (2005-2006) was to design and construct the urine separating system in GTZ main building. The followed SANIRESCH program executed by Maßalsky GmbH institution, studied the feasibility of implementing ecological sanitation (ecosan) concept for separate treatment and recycling of urine, brown- and greywater from an urban office building (Winker and Saadoun, 2011). The system performance was analysed in according with health and hygiene concerns, environmental impact and local resources availability, operation and implementation complexity, financial and economic feasibility, and social-culture acceptance. It was found upon

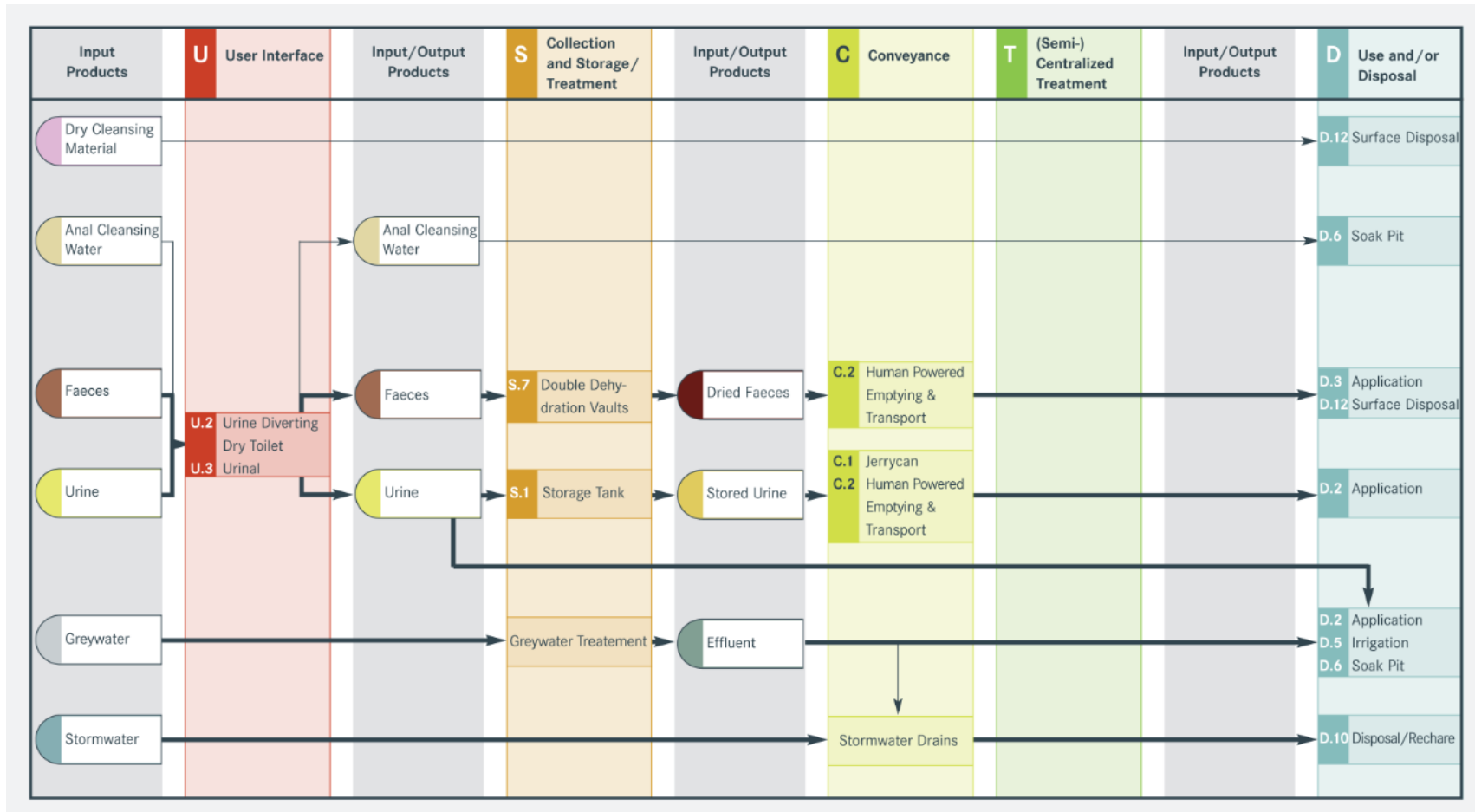
concluding the project that, (1) the product received from the system is hygienic and safe to use for agricultural fertilization purpose; (2) the social acceptance of such system is sound, both farmers' and consumers' show the willingness to use urine as a liquid fertilizer; (3) the project is considered economically feasible in favourable conditions. However, integration of advanced wastewater treatment technologies, such as struvite precipitation, have not been studied yet. In addition, the technologies for reuse product in agriculture as well as increase its transportability and application efficiency need to investigate further.

UTS Sustainable Sanitation project

The UTS Sustainable Sanitation project conducted by the Institute for Sustainable Futures (ISF) at the University of Technology, Sydney (UTS), in 2013, Australia, investigated the barriers associated with replacing existing sanitation systems to more sustainable urine diversion (UD) systems (Mitchell et al., 2013). The project consisted of UDFT, water free urinals, piping systems for urine sampling, and tanks for urine storage and transportation. The performances of project were analysed in accordance with regulations and institutions, user practices, operation and implementation, agriculture trials, market, and socio-cultural acceptance. It was found that the development of urine diversion system could be hampered by: (1) lack policies to support or promote the urine diversion and reuse; (2) no guidelines to regulate source-separated urine practices; (3) low market share in sustainable sanitation business could slow down development of existing product.



(a)



(b)

Figure 2.2 Scheme of flow streams separation, treatment, and reuse for urine diversion flush toilets (UDFT) with sewerage system and urine diversion dry toilets (UDDT). Adapted with permission granted by the copyright holder Tilley et al. (2014)

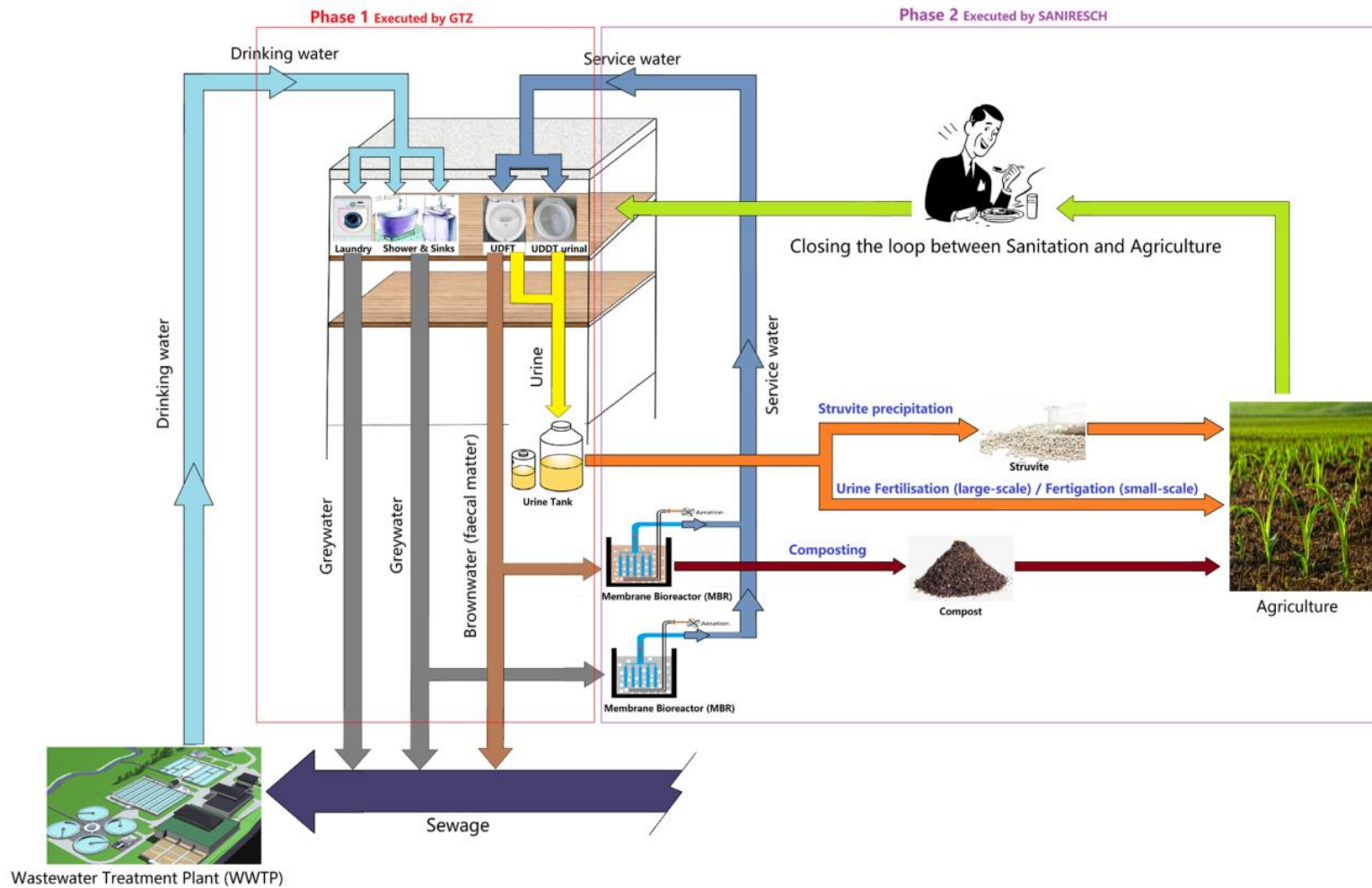


Figure 2.3 Two-phase collaborative project for implementation of novel sanitation systems in an urban office, funded by the Federal Ministry of Education and Research, Germany. Modified from Winker and Saadoun (2011)

2.3.2 Urine-Diverting Dry Toilet (UDDT)

Kvarnström et al. (2006) reported that the first modern version of the waterless system with urine diversion became available in 1970s. As a sustainable sanitation system, UDDT is of importance in many ways. It minimizes unpleasant odours and decreases the occurrence of flies. It can be made from locally available materials and is suitable for use by all users, regardless of location or personal preferences, including sitters, squatters, washers, and wipers. The system ensures safe and hygienic handling of feces and has a longer product lifespan compared to traditional toilets. However, issues such as pipe blockage due to inappropriate maintenance, presence of foul-smelling, and visible excreta pile constrain its application and promotion (Randall and Naidoo, 2018a).

Ecological Sanitation Ethiopia Project

The Ecological Sanitation Ethiopia Project funded by the German agency for technical cooperation (GTZ) started in 2006, Ethiopia, has been demonstrated the technical requirements and economic benefit from UDDT implementation in high population density areas. It was concluded that the use of UDDT in multi-storey buildings and reuse of human excrete produces in agriculture would contribute to self-sufficiency and food-security as well as provide additional income in terms of 1.4 times higher crop yield and productivity. About 25% capital and operational cost reduction was achieved compared to conventional sanitation systems. This shows an advantage for use alternative sanitation system in higher density areas (Meinzinger et al., 2009a, Meinzinger et al., 2009b, Simpson-Hebert, 2007, Fry et al., 2015).

Compost Toilet Trial Project

The Compost Toilet Trial Project conducted by the Wellington Regional Emergency Management Office (WREMO) in 2012, New Zealand, has been undertaken to evaluate the service reliability of urine separating emergency compost toilets under crisis situations where sewage system is damaged and conventional toilet may not be functioning, such as earthquake (WREMO, 2013). The trial was conducted for one month. 11 households and workplaces were engaged during that time. It was found that, the compost toilet is safe and hygiene for use inside during exceptional circumstances. A user acceptance evaluation results shown an increase in users' satisfaction as the trial progressed. For instance, all 11 participants shown positive attitudes after short term (1 - 2 weeks) trial period. 7 out of 11 participants chosen very comfortable or comfortable for 3 months trial. No negative feedback (uncomfortable) was received at the end. It has been also noticed, however, that the issue of using such waterless urine diverting system could potentially lies in high-density cities. As here space is limited for the urine and the compost disposal as well as manual removal of compost is required at all-time which is labour intensive (O'Neill, 2015, Zakaria et al., 2018). The true operation cost and implementation difficulties of composting toilets have only been researched under household level or at the single household device level, but lack of investigation at the large scale (Anand and Apul, 2014).

2.4 Review of current membrane technologies for urine resource utilization

Membrane filtrations utilize membrane to separate the dissolved solids from liquid streams. It is commonly used in wastewater treatment to remove microorganisms or

desalination to remove salts. It is a physical separation process with no chemical introduced. Membrane process can be summarized in 3 categories: pressure driven membrane process, forward osmosis (FO) process, and electrodialysis (ED) and electrodialysis reversal (EDR) process.

2.4.1 Pressure driven membrane process

The pressure driven membrane processes include micro-filtration (MF), ultra-filtration (UF), nano-filtration (NF) and reverse osmosis (RO). Specifically, MF is usually used to remove particulate or suspended material which have particle size between 0.1 and 10 μm . UF and NF can separate particles and materials ranged in size from 0.01 to 0.1 μm and 0.001 to 0.01 μm , respectively. RO is normally deal with dissolved solids less than 0.001 μm . As the pressure required for membrane to separate water from other dissolved material increase while the pore size of membrane gets smaller, RO usually requires highest pressure among other pressure driven membrane processes to overcome the osmotic pressure. For instance, the pressure used in RO can sometimes up to 150 bar, while the pressure applied in MF and UF is in the 0.1 to 10 bar range. Consequently, MF, UF, and NF could be served as pre-treatment process to RO (Figure 2.4)(Bonnélye et al., 2008, Cox et al., 2008, Kaya et al., 2015).

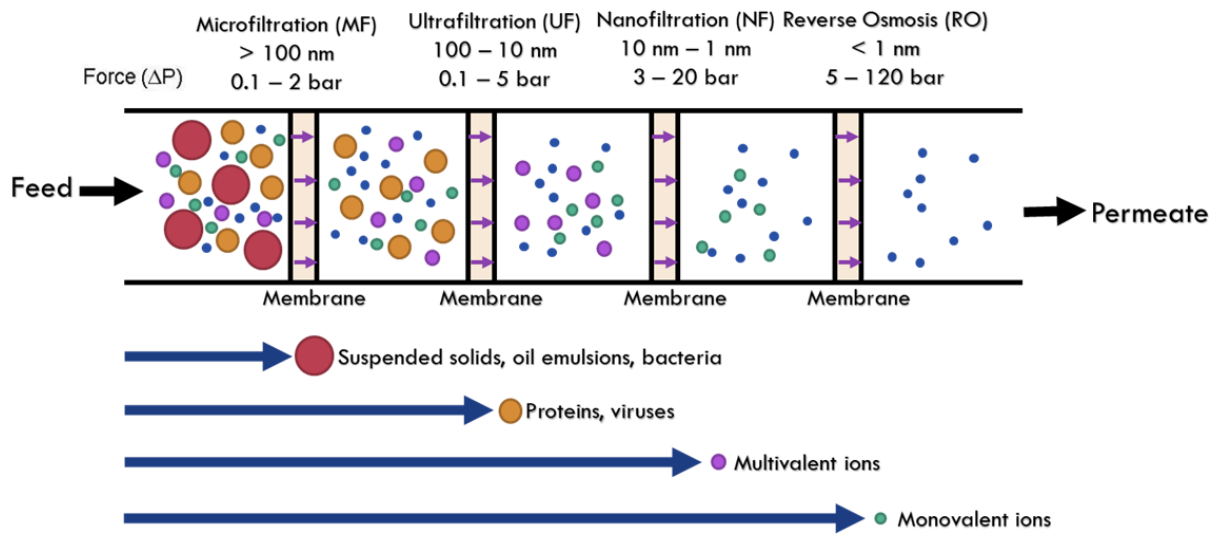


Figure 2.4 Pressure driven membrane filtration types

2.4.2 Forward osmosis (FO)

Compare to pressure driven membrane process utilizes hydraulic pressure to against the osmotic pressure between the feed side to draw side. The FO technology relies on the natural osmotic pressure to drive water molecules from the feed solution to draw solution. This technology has been widely used for ammonium recovery in human urine. The drawback associated with this application is that the ammonium recovery efficiency is gradually decreased as draw solution become diluted (Figure 2.5).

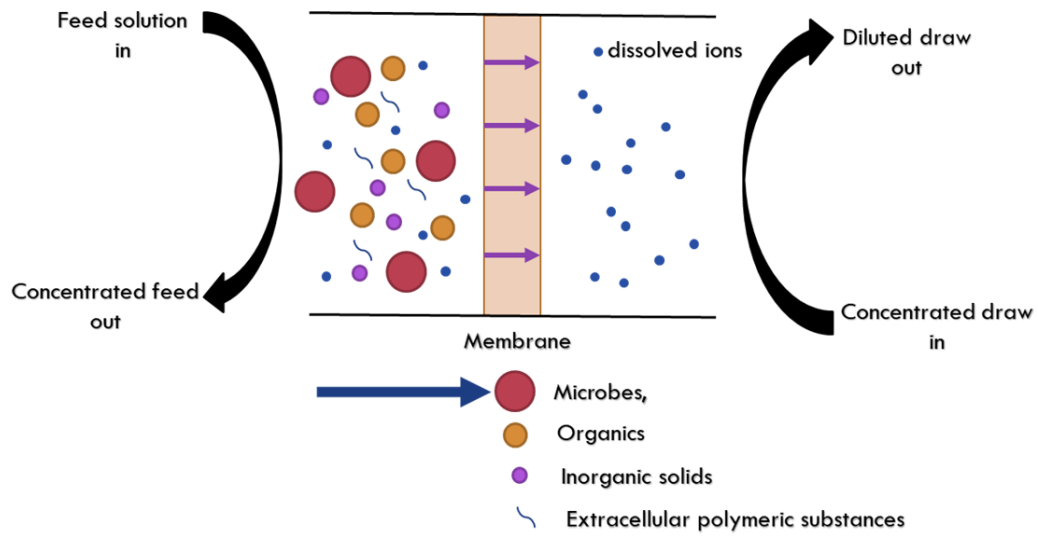


Figure 2.5 Schematic diagram of forward osmosis

2.4.3 Electrodialysis (ED)

Unlike other wastewater treatment measures, electrodialysis (ED) is an evolving technology that removes ions from the water due to the formation of an electric double layer (EDL) on the surface of the charged electrodes (Pekala et al., 1998, AlMarzooqi et al., 2014, Kim and Choi, 2010a). Capacitive deionization (CDI) for instance, can remove a wide range of charged contaminants and has been increasingly investigated for desalination and the removal and recovery of target ions from different water sources. Compared with other desalination technology, the CDI is determined to be efficient for desalination of low saline water (Suss et al., 2012, Farmer et al., 1995). CDI technology also does not require excessive chemical usage for practical application, which can be achieved by a simple reversal of polarity for ion desorption. There are currently three most common types of CDI in use (1) conventional CDI that uses a pair of static electrodes, (2) membrane CDI (MCI) which uses ion exchange membranes in

combination with static carbon electrodes (Lee et al., 2006) and (3) Flow CDI (FCDI) which uses, slurry electrodes (Jeon et al., 2013). Among these, the MCDI with coated layer of ion exchange polymer directly on the surface of the electrode is commonly used by various manufacturers. The use of ion-exchange membranes with CDI drastically improves desalination and energy efficiency (Kim and Choi, 2010b, Li and Zou, 2011). Currently, more than half of the research activities in ED and EDR processes are focused on developing new electrodes to improve ion desorption/adsorption performance and reduce energy consumption. Figure 2.6 shows a schematic diagram of membrane capacitive deionization (MCDI) set-up.

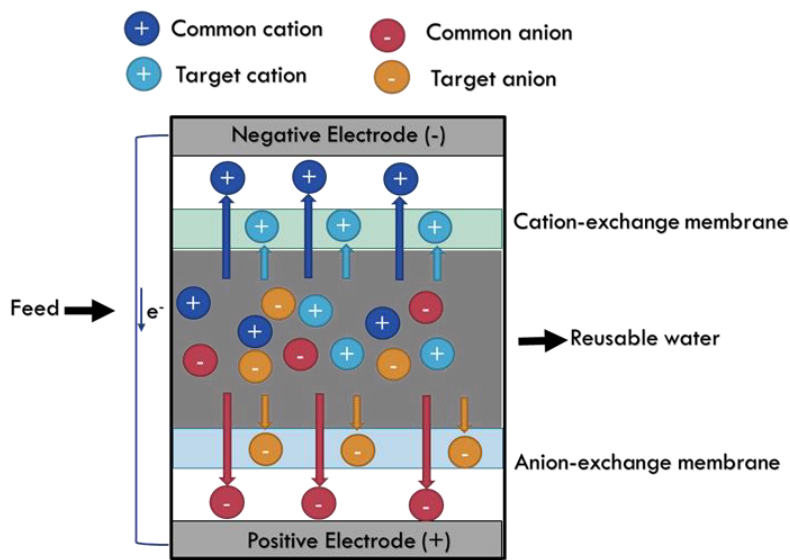


Figure 2.6 Schematic diagram of membrane capacitive deionization (MCDI)

2.5 Review of alternative membrane-based process for source-separated urine resource utilization

2.5.1 Forward osmosis-reverse osmosis (FO-RO)

The hybrid forward osmosis-reverse osmosis (FO-RO) system is firstly developed to treat wastewater and desalination simultaneously. Through the contacted membrane, FO generates clean water meanwhile RO desalt the undilute seawater. Figure 2.7 shows a schematic diagram of hybrid FO-RO system.

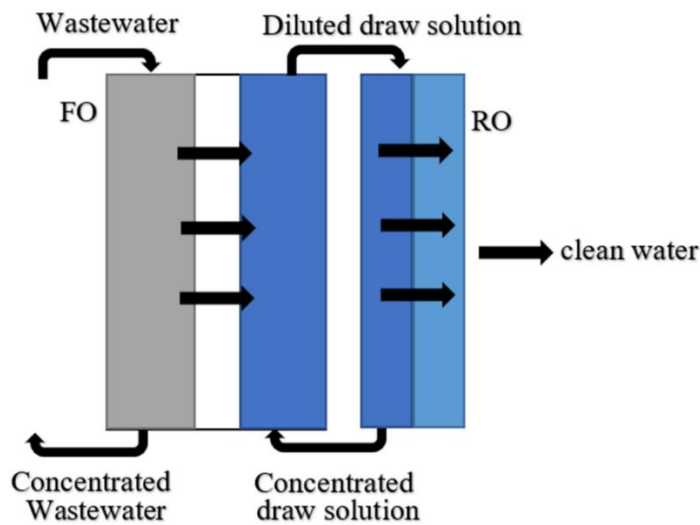


Figure 2.7 Schematic diagram of hybrid forward osmosis-reverse osmosis (FO-RO) system

2.5.2 Membrane bioreactor (MBR) and MBR-combined treatment process

Membrane bioreactor (MBR)

Membrane bioreactor is a technology that combines membrane filtration processes (UF, NF, MF, etc.) with a biological process (activated sludge) to treat wastewater or recover nutrients from it. Side-stream MBR and submerged MBR are two common configurations used in MBR. Specifically, the membrane filtration module is placed outside the bioreactor for easy membrane module access and cleaning. The submerged MBR has membrane module inside the bioreactor, which requires less energy compared to the side stream MBR but disadvantages in membrane accessibility and cleaning. Like any membrane-assisted technologies, membrane fouling in MBR is a primary barrier to the widespread application. It causes transmembrane pressure (TMP) increase, decline of permeate quality and membrane performance, increase of membrane operation and maintenance cost, and decrease of membrane module usage lifespan (Park et al., 2018b, Kang et al., 2018). Figure 2.8 shows a schematic diagram of two common MBR configurations.

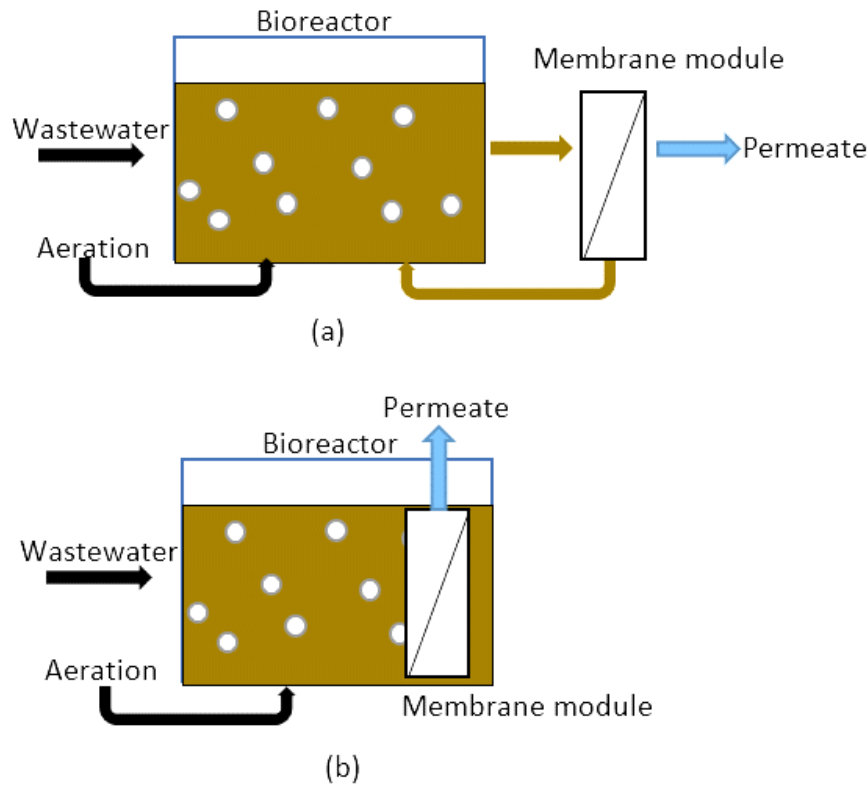


Figure 2.8 Schematic diagram of two common MBR configurations. (a) side-stream MBR, (b) submerged MBR.

MBR-combined technology

There are also studies to combine biological nitrification with consecutive treatment technology for nitrogen stabilization and complete nutrient recovery in human urine. Udert and Wächter (2012) combined a lab-scale membrane-aerated biofilm reactor (MABR) with thermal distillation to produce a nutrient-rich dry powder urine fertilizer. However, such process is energy intensive; the thermal stability of recovery solid products with high ammonium nitrate content could cause safety hazards during production and processing. Volpin et al. (2020) investigated to dewater the nitrified urine up to 20 times of its initial concentration by low-temperature direct contact membrane distillation (DCMD) process. It was proven that the nitrified urine fertilizer and

commercially available fertilizer have similar yield rate in lettuce and park choy growth. However, significant organic fouling and cake layer formation was observed on the DCMD membrane surface; the potential cost on membrane chemical cleaning needs to be considered in long-term operation.

The studies on the removal of total antibiotics in five wastewater treatment plants (WWTPs) showed that 22.5% - 38.2% of total antibiotics were adsorbed on the surface of activated sludge particles, and 61.8% – 77.5% of which were degraded by bacteria. The removal efficiency of hydrophobic MPs ($\log K_{ow} > 3.2$) in aerobic MBR were greater than 85% while the removal capacity of hydrophilic MPs ($\log K_{ow} < 3.2$) varied significantly (Wang et al., 2020, Chtourou et al., 2018). To further purify MBR effluent and remove micropollutants, post-treatment methods such as granular activated carbon (GAC) adsorption have been introduced, as they can effectively remove MPs through physiochemical interactions. However, this method has several disadvantages, including high consumption of GAC, reduced efficiency in removing MPs due to competition with nutrients, decreased GAC adsorption capacity over time, and the need for additional space (Boehler et al., 2007, Almutashiri et al., 2021, Nguyen et al., 2013b, Asif et al., 2020). There have also been reports of noticeable loss in essential nutrients during physical adsorption on GAC (Köpping et al., 2020, Almutashiri et al., 2021). On the other hand, the powdered activated carbon membrane bioreactor (PAC-MBR) process is a more attractive alternative as it can remove micropollutants through physical adsorption and biodegradation in a single step. This is achieved by the growth of a stable microbial film on the PAC surface, forming biological powdered activated carbon (BPAC) (Stoquart et al., 2012, Zhang et al., 2015). The PAC-MBR system offers additional benefits such as increased urine nitrification efficiency (Ma et al., 2012, Thuy and Visvanathan, 2006, Hu

et al., 2014b), mitigated membrane fouling propensities fouling (Yang et al., 2016, Huang et al., 2021, Guo et al., 2008), improved removal efficiency of organic matter and micropollutants (Chtourou et al., 2018, Qrenawi and Rabah, 2023, Tadkaew et al., 2010), and more rapid biomass growth (Chtourou et al., 2018, Qrenawi and Rabah, 2023, Tadkaew et al., 2010).

2.5.3 Membrane distillation (MD)

Membrane distillation (MD) is an emerging alternative membrane-based technology driven by vapor pressure to separate volatile substances based on their volatilities. In this application, only vapor molecules can move across hydrophobic membrane pores from hot temperature side to low temperature side. MD has the potential advantage of being operated at low temperatures (30 - 80°C) compared to conventional distillation and low pressure (maximum 100 psi) compared to other pressure-driven membrane separations (Alkudhiri et al., 2012, Onsekizoglu, 2012), thereby reducing energy use and cost. In comparison with RO, MD is less affected by concentration polarisation (CP) or membrane pollution, thus achieving 100% retention of non-volatile solute. The membrane pore wetting in MD is the primary obstacle to large scale or commercial use. Figure 2.9 shows the common configurations in MD.

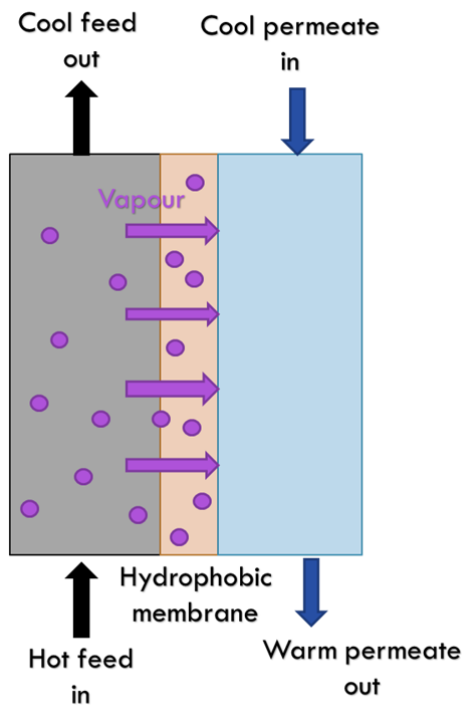
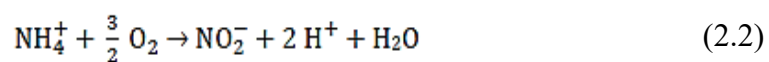
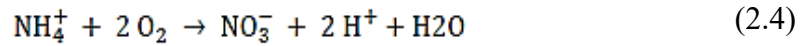


Figure 2.9 Schematic diagram of MD system

2.6 Nitrification

Nitrification is two step sequential biological oxidation process where ammonia is oxidised to nitrate. The first step of this process involves ammonia oxidizing bacteria (AOB). It oxidises ammonia to hydroxylamine and hydroxylamine then converting to nitrite (Equation. 2.2). The second step involves the oxidation of nitrite to nitrate by nitrite oxidizing bacteria (NOB) according to equation 2.3. The complete nitrification process is shown by equation 2.4. The formation of nitrous acid releases hydrogen ions, consumes alkalinity and cause the pH decrease (Koops et al., 2006).





The desired product of stable urine nitrification is a solution contains equal parts of ammonium and nitrate, which requires that nitrite is oxidised at the same rate as ammonia (Udert et al., 2003a). The growth of both AOB and NOB bacteria can be inhibited by temperature, pH, organic load, DO concentration, free ammonia and nitrous acid concentration, alkalinity, hydraulic and sludge retention time, and the previous history of the biosystem (Rusten et al., 2006, Bock and Wagner, 2013).

It reported that the main substrate for AOB is ammonia and the favourable substrate for NOB growth is nitrite. For instance, the AOB is inhibited when FA concentration ranged between 8 and 120 mg/L and FNA concentration ranged between 0.08 and 0.82 mg/L. The NOB bacteria activity is inhibited when FA concentration ranged between 0.08 and 0.82 mg/L and FNA concentration ranged between 0.06 and 0.83 mg/L.

The nitrification rate is temperature dependent. Nitrification rates are hampered at temperatures below 20 °C and will close to zero at temperatures above 40 °C (Grunditz and Dalhammar, 2001). Hellinga (1999) also reported that NOB grow faster than AOB in lower temperature, while AOB grow more rapidly at temperature above 16 °C.

pH represents the acid-base equilibria of NH₃, NO₂ and hydroxylamine (Udert et al., 2003a) during nitrification process. The pH fluctuation indicates the instabilities of nitrification process. Suthersand and Ganczarczyk (1986) reported that NOB have great pH resistance than AOB. AOB will suffer irreversible activity loss during pH shocks, while NOB activity stays unaffected. The nitrite accumulation may occur if AOB activity is more favourable than NOB activity. The build-up of nitrite can be problematic, as it

will poison both AOB and NOB bacteria. Therefore, it is recommended to operate nitrification process at relatively low temperature and pH (Udert & Wächter, 2012; Edefell, 2017).

3. Critical flux on a submerged membrane bioreactor for nitrification of source separated urine

[Notes: This chapter was published in *Process Safety and Environmental Protection* (2021)]

Jiang, J., S. Phuntsho, N. Pathak, Q. Wang, J. Cho and H. K. Shon (2021). "Critical flux on a submerged membrane bioreactor for nitrification of source separated urine." Process Safety and Environmental Protection **153**: 518-526.

3.1 Abstract

Membrane fouling is the biggest challenge in membrane-based technology operation. Studies on critical flux mainly focused on membrane bioreactor for municipal wastewater and/or greywater treatment, which can significantly differ from the ultrafiltration membrane bioreactor (UF-MBRs) to treat source separated urine. In this work, the inhibitory factors on nitrifying bacteria activity were investigated for fast acclimation of nitrifying bacteria with high ammonium concentration and optimization of a high-rate partial nitrification MBR. The maximum nitrification rate of $447 \pm 50 \text{ mgN} \cdot \text{L}^{-1} \cdot \text{d}^{-1}$ was achieved when concentration of ammonia in feed urine is approximately $4006.3 \pm 225.8 \text{ mgN} \cdot \text{L}^{-1}$ by maintaining desired pH around 6.2 and FA concentrations below 0.5 mgL^{-1} . Furthermore, for the first time, the impact of different operational and filtration conditions (i.e., aeration intensity, filtration method, imposed flux, intermittent relaxation, biomass concentration) on the reversibility of membrane fouling was carried out for enhancement of membrane flux and fouling mitigation. Fouling mechanisms for minor irreversible

fouling observed under sub-critical condition were pore blocking and polarization. To mitigate membrane fouling, the UF module with effective membrane surface area of 0.02 m² is recommended to be operated at the aeration intensity of 0.4 m³h⁻¹, intermittent relaxation of 15 min, biomass concentration of 3.5 g.L⁻¹.

Keywords: submerged ultrafiltration membrane bioreactor (UF-MBR); critical flux; critical flux for irreversibility; fouling reversibility; source separated urine, improved flux-step method

3.2 Introduction

Human urine contributes up to 90% of the nitrogen, more than half of the phosphorus and around 90% of the potassium and yet it constitutes only about 1% of the total wastewater volume at the wastewater treatment plants (WWTPs). This unique composition makes it, at the same time, a heavy burden for conventional biological sanitation (Randall and Naidoo, 2018b, Maurer et al., 2003, Maurer et al., 2006, Simha and Ganesapillai, 2017, Bhattacharyyab, 2010). The contribution of urine to the wastewater treatment cost is significant, since the conventional WWTPs focus on the removal of *nitrogen* (N) and *phosphorus* (P) to meet the more stringent effluent discharge standards with the aim to prevent the risk of eutrophication in the receiving water body (Wilsenach and Loosdrecht, 2006). Maurer et al. (2003) calculated that biological oxidation of ammonium (NH₄⁺) into nitrite (NO₂⁻) and nitrate (NO₃⁻), following with the reduction of nitrogen gas, consumes 12.5 kWh per kg of N. While chemical precipitation of phosphate (PO₄³⁻) consumes only 8.1 kWh per kg of P. Wilsenach and Loosdrecht (2006) even summarized that, if treat half

of urine separately, conventional wastewater treatment can achieve higher effluent quality and even have a potential for a net-energy production. In fact, source separation of human urine has been proposed for over decades as a perfect solution for total nutrients recovery and reuse. Existing projects concluded that the source-separated urine is hygienic and safe to use for agricultural fertilization purpose. Such application is considered economically feasible in favourable conditions, in which would replace or reduce the chemical fertilizer usage; provide household additional incomes; and contribute to self-sufficiency and food-security (Winker and Saadoun, 2011, Mitchell et al., 2013, Fry et al., 2015). Given that using raw human urine as a direct agricultural fertilizer source is limited to its distinct odour, wide range of pH, pathogen risk associated with faecal cross-contamination, and the possible presence of high concentrations of pharmaceuticals. Source separated urine nitrification by membrane bioreactor is therefore a promising technology to overcome these drawbacks and achieve complete nutrient recovery (Fumasoli et al., 2015, Udert et al., 2015, Volpin et al., 2020, Udert and Wächter, 2012).

Like any membrane-assisted technologies, membrane fouling will continue to be a major challenge for the application of the MBR for urine nitrification. The membrane fouling can lead to transmembrane pressure (TMP) increase, decline of permeate quality and membrane performance, increase of membrane operation and maintenance cost, and decrease of membrane module usage lifespan (Park et al., 2018b, Kang et al., 2018). The concept of critical flux and critical flux for irreversibility in submerged MBRs has been proposed to control the membrane fouling and optimize the system treatability (Field et al., 1995, Le Clech et al., 2003). Unfortunately, no publication has yet investigated the reversibility of membrane fouling in UF-MBR feed with hydrolysed human urine. Most of previous literature evaluated membrane filtration performance in submerged MBRs for

municipal wastewater and/or greywater treatment, which has substantially different fouling propensities (Park et al., 2018a, Khanzada et al., 2020, Hube et al., 2020, Tiranuntakul et al., 2011). Given the reason that fouling in submerged MBR is relate to membrane configuration and characteristics (i.e. pore size, configuration, material, etc.), operation conditions (i.e. aeration intensity, membrane physical cleaning and/or filtration method, imposed flux, etc.), and biomass characteristics (floc parameters, extracellular polymeric substances, feed solution characteristics, etc.). Compare to municipal wastewater and/or greywater, urine is nutrients enriched in natural, but has low chemical oxygen demand/nitrogen (COD/N) ratio and insufficient alkalinity, leading to maximum half of the ammonia ultimately oxidized to nitrate in urine nitrification reactor without introduction of additional alkalinity (Tian et al., 2019).

As such, for the first time, an investigation of the critical flux and critical flux irreversibility in UF-MBR feed with undiluted source-separated urine was conducted by an improved flux-step method incorporating with various fouling mitigation strategies. This aspect is of major interest for membrane flux enhancement and fouling mitigation in nitrifying MBR. Moreover, the impact of free ammonia (FA) and free nitrous acid (FNA) concentration on nitrifying bacteria activity during UF-MBRs' start-up and stable operating stage was studied, for fast acclimation of nitrifying bacteria with high ammonium concentration and optimization of a high-rate partial nitrification MBR.

3.3 Materials and methods

3.3.1 MBR set-up and operation

A lab scale UF-MBRs with total effective working volume of 4.5L was operated to treat hydrolysed source separated urine. The seeding activated sludge containing mixed nitrifying bacteria strains was taken from the Central Park Wastewater Treatment Plants, Sydney, Australia, to initiate the cultivation of urine nitrifying sludge. Figure 3.1 shows the schematic diagram of designate lab scale UF-MBR. The feed stream constitutes an automatic pH controller and pump (BL7916-1, Hanna Instruments, Australia) and a pH meter (HI6100405, Hanna, Australia) to achieve the precise dosage of stored urine and maintain the pH of sludge mixture at approximately 6.2 during the entire operation period. An air diffuser was placed at the bottom of the bioreactor to diffuse the incoming compressed air from the single tubing into finer air bubbles. An air flow rate of 4 L.min⁻¹ was set to maintain the dissolved oxygen level in a range between 4.3 and 4.5 mg. L⁻¹. The sludge retention time (SRT) was set at infinite by discharging 5 mL of sludge mixture in a daily basis for sampling purpose only, accounting for 0.11% of total working volume. Measurement of conductivity and pH were conducted in every 5 minutes in this study. The probes were cleaned with commercial cleaning solution and calibrated with corresponding pH/conductivity standard solution in every two weeks. The commercially available braid-reinforced polyvinylidene fluoride (PVDF) hollow fibre, manufactured by Lotte Chemical, South Korea, were used for potting UF membrane modules in this study. It has nominal pore size diameter at 0.03 µm, inner diameter at 0.8mm and outer diameter at 2.1 mm. Each UF membrane module that was potted in UTS lab has a total effective area of 0.02 m² (Table 3.1). The timely TMPs were measured by Druck pressure

transmitter PTX 1400. The LogBox-AA (Novus Automation, UK) and LogChart II software were used for continuous data logging, data configuration recording and retrieval, and further data plotting and analyses. Figure 3.2 shows the pure water flux (PWF) of potted UF membrane modules as a function of various TMP.

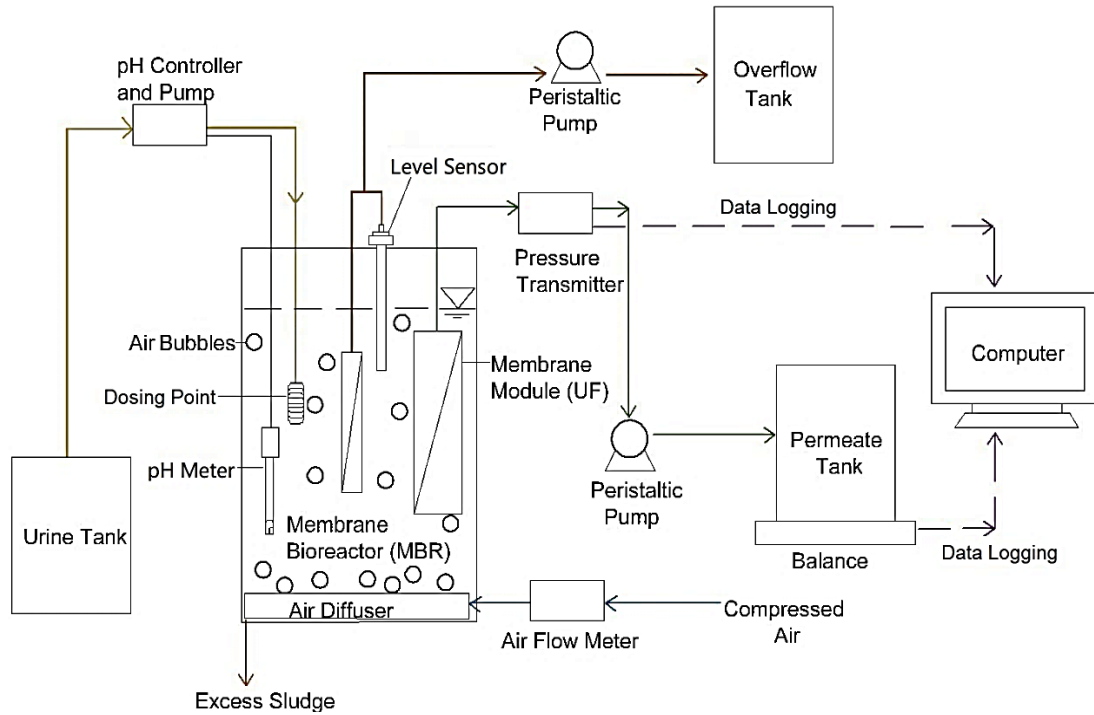


Figure 3.1 Schematic diagram of the lab scale UF-MBR

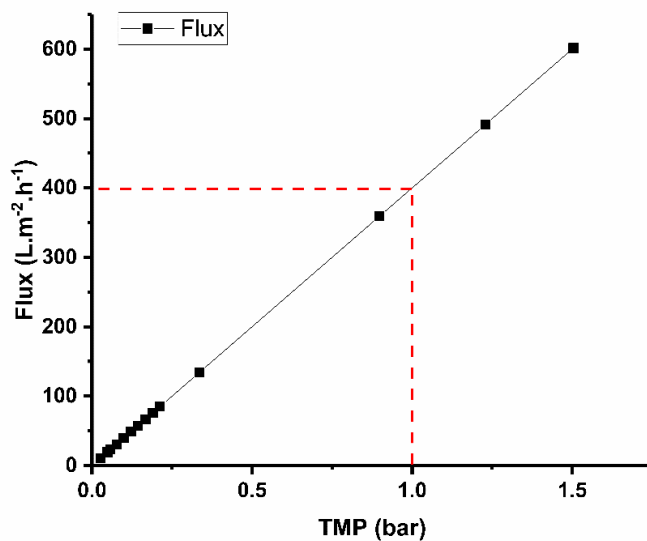


Figure 3.2 Pure water flux (PWF) of potted UF membrane module at different TMP

Table 3.1 Properties of the potted UF membrane module

	Characteristics
Material	PVDF (braid-reinforced)
Type	Hollow fiber membrane
Nominal pore size (μm)	0.03
Outer diameter (mm)	2.1
Inner diameter (mm)	0.8
Number of fibres	4
Effective surface membrane area (m^2)	0.02

An additional set of the potted UF membrane module was connected to an automatic water level controller and a peristaltic pump (Cole-Parmer, UK) in series to control the minimum and maximum water level. When water level inside the bioreactor rises well above a maximum fixed level, the peristaltic pump is automatically switched on by the water level sensor to pump the excess amount of nitrified urine permeate out of the bioreactor. When the working volume decreases below a minimum fixed level, it will refill permeate that previously stored in overflow tank back to its minimum fixed level.

3.3.2 Characteristics of stored source separated urine

The University of Technology Sydney (UTS) installed sustainable urine diversion (UD) systems in the Faculty of Engineering and IT building in 2013 (Mitchell et al., 2013). The systems consist of urine-diverting flush toilet, water free urinals, piping systems for urine sampling, and tanks for urine storage and transportation. The proposed nitrifying membrane bioreactor was continuously fed with stored source-separated urine collected from the urine storage tanks. The composition and corresponding ion concentrations in stored raw urine (40 L per batch) are given in Table 3.2.

Table 3.2 Composition and corresponding ion concentrations in each 40 L stored raw urine at room temperature

Component	Batch 1	Batch 2	Batch 3	Batch 4	Average
Total Ammonia Nitrogen (mg. L ⁻¹)	3900.0	4300.0	3775.0	4050.0	4006.3± 225.8
Total Phosphate (mg. L ⁻¹)	262.0	298.0	245.0	289.0	273.5± 24.4
Potassium (mg. L ⁻¹)	1185.0	1288.0	1048.0	1209.0	1182.5± 99.9
Calcium (mg. L ⁻¹)	44.0	56.0	37.0	50.0	46.8± 8.1
Magnesium (mg. L ⁻¹)	1.0	2.0	1.0	4.0	2.0± 1.4

Sodium (mg. L ⁻¹)	1463.0	1919.0	1670.0	1798.0	1712.5± 194.9
Chloride (mg. L ⁻¹)	1510.0	1576.0	1521.0	1555.0	1540.5± 30.4
Total Organic Carbon (mg. L ⁻¹)	1644.0	1924.0	1622.0	1764.0	1738.5± 138.5
Conductivity (mS.cm ⁻¹)	37.9	39.6	37.5	38.3	38.3± 0.9
pH (-)	9.2	9.2	9.1	9.2	9.2

3.3.3 Determination of critical flux and the critical flux for irreversibility

The critical flux and its irreversibility were experimentally determined using an improved flux-step method rather than continues flux-step method in literature (Le Clech et al., 2003, Wu et al., 2008, van der Marel et al., 2009, Lan et al., 2017). Figure 3.3 shows the typical flux versus time profile in (a) continues and (b) improved flux-step method. Specifically, intermittent flux of 0.5 Lm⁻²h⁻¹ is applied in this work to incorporate the physical cleaning technology between consecutive flux step height, allowing the determination of critical flux and the critical flux for irreversibility with intermittent relaxation cycle. The initial flux of 4 Lm⁻²h⁻¹ is adopted to eliminate severe fouling deposition on membrane at the initiation period. The maximum flux rate of 58 Lm⁻²h⁻¹ is selected in experiments, which is more than tripled of the value in actual submerged MBR. The effect of filtration frequency, air scouring, biomass concentration, intermittent relaxation frequency, and imposed flux on the irreversibility of membrane fouling was individually investigated by performing consecutive experiments. The proposed control

and operating parameters can be found in Table 3.3. The TMPs data were measured in every 30 s by pressure transmitter. The potted UF membrane modules were carefully cleaned prior to conducting critical flux experiments. All used membrane modules were firstly cleaned by 5 minutes of backwashing at $40 \text{ Lm}^{-2}\text{h}^{-1}$ to remove the reversible fouling on the membrane surface, followed by soaking in 0.1 M sodium hypochlorite (NaClO) solution for 1 hour to remove the irreversible fouling on the membrane caused by pore blocking and plugging.

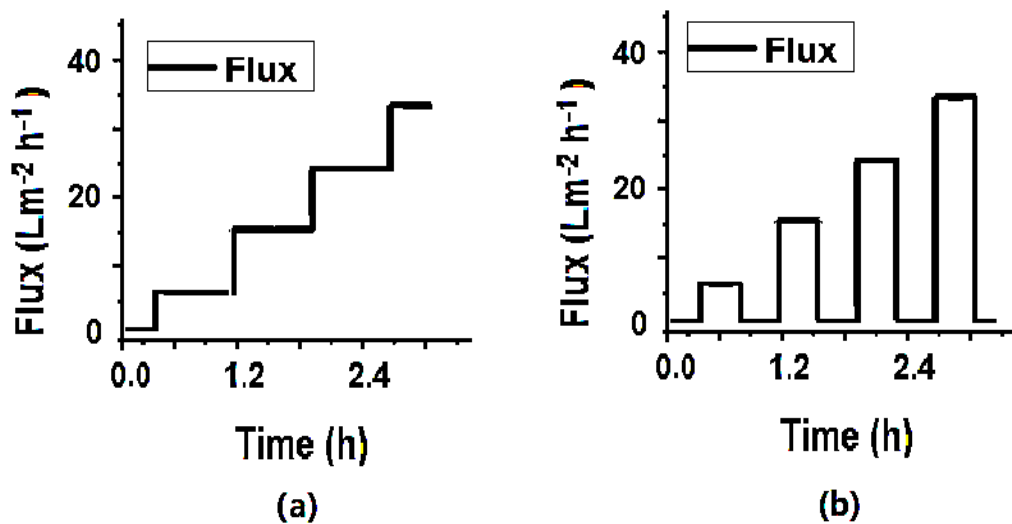


Figure 3.3 Typical flux profile in (a) continues and (b) improved flux-step method.

Table 3.3 Proposed experimental operation conditions and control parameters for membrane critical flux study

Control	Corresponding	Operating Conditions
	Fouling	

Corresponding Section in This Paper	Parameters	Mitigation Strategies				
			Aeration intensity (m ³ h ⁻¹)	MLSS (g.L ⁻¹)	Step length (min)	Step height (Lm ² h ⁻¹)
3.2	Step length	Filtration frequency	0.2	3.5	15, 20, 25, 30	6
	Step height	Imposed flux	0.2	3.5	15	3, 6, 9, 12
3.3	Aeration intensity	Air scouring	0.1, 0.2, 0.4	3.5	15	6
3.4	MLSS	Biomass concentration	0.1, 0.2, 0.4	2, 3.5, 5	15	6

3.3.4 Analytical methods

The validity of experimental results was guaranteed by taking raw urine feed solution, sludge mixture and MBR permeate samples in every 24-hour cycle; centrifuged and filtered through 0.2 µm filter immediately after collection, then stored at 4°C for triplicated analyses. All samples were individually digested with corresponding Merck Millipore ammonia (ammonium), nitrate, nitrite, and phosphate spectroquant test kit. The concentration of total ammonia/ammonium nitrogen (NH₃-N/ NH₄-N), nitrate nitrogen

(NO₃⁻N), nitrite nitrogen (NO₂⁻N), and total phosphate (PO₄-P) was then measured by Merck Millipore UV/VIS Spectrophotometer (Spectroquant^R NOVA 60, USA). The concentration of chloride ion (Cl⁻) was measured by Ion Chromatography (IC, Thermo Fisher Scientific, USA), while the concentration of major cations (i.e., K⁺, Ca²⁺, Mg²⁺, Na⁺) were analysed via Microwave Plasma Atomic Emission Spectroscopy (MP-AES 4100, Agilent, USA).

The concentration of total organic carbon (TOC) was measured by a TOC analyser (Analytik Jena AG, Germany). 5 mL sludge mixture samples were taken from the reactor fortnightly to measure the concentration of mixed liquor suspended solids (MLSS) and mixed liquor volatile suspended solids (MLVSS) inside the bioreactor. MLSS and MLVSS concentrations were measured and calculated according to the standard method in biological wastewater treatment literatures (Basile et al., 2015, Baird, 2017).

$$MLSS = 1000 * \frac{(b-a)}{V} \quad (3.1)$$

where a (g) represents the weight of glass microfiber filter before filtration, b (g) represents the weight of glass microfiber filter after drying at 110 °C for 60 minutes, and V (mL) is the sample volume.

$$MLVSS = 1000 * \frac{(b-c)}{V} \quad (3.2)$$

where c (g) represents the weight of glass microfiber filter after drying at 550 °C for 30 minutes

The FA and FNA calculated by following equations:

$$FA = \frac{17}{14} * \frac{NH_4^+ - N * 10^{pH}}{e^{\left(\frac{6.344}{273} + 0C\right)} * 10^{pH}} \quad (3.3)$$

$$FNA = \frac{46}{14} * \frac{NO_2^- - N}{e^{\left(\frac{2.300}{273} + 0C\right)} * 10^{pH}} \quad (3.4)$$

where FA and FNA are measured as ammonia (mg.L⁻¹) and nitric acid (mg.L⁻¹), respectively.

The total fouling rate and irreversible fouling rate were calculated by following equations.

$$Total \ fouling \ rate = \frac{P_f - P_i}{\eta J_H} \frac{1}{\Delta t} \quad (3.5)$$

$$Irreversible \ fouling \ rate = \frac{P_2 - P_1}{\eta J_L} \frac{1}{\Delta t} \quad (3.6)$$

where P represents the pressure (Pa), η (Pa.s) represents the MBR permeate viscosity at 21.5 °C. J_H is the applied flux; J_L is the benchmark flux; t is the flux step length (s).

3.4 Results and discussion

3.4.1 UF-MBR start-up and operation

Given that the FA and FNA concentrations in municipal wastewater are about 100 times lower than that in urine, it is necessary to dilute the initial feed solution at a desired concentration, to avoid the irreversible activity loss of nitrifying bacteria during shock loading. The reactor was initially fed at a total ammonia nitrogen concentration ranged between 100 and 150 mg. L⁻¹. The pH was manually adjusted by dosing hydrochloric acid

and sodium bicarbonate to keep the pH between the desired levels of 6 and 6.6 at the first stage operation.

It reports that the main substrate ammonia oxidizing bacteria (AOB) is ammonia and the favourable substrate for nitrite oxidizing bacteria (NOB) growth is nitrite. AOB is inhibited when FA concentration ranged between 8 and 120 mg. L⁻¹ and FNA concentration above 0.08 mg. L⁻¹. On the other hand, NOB bacteria activity is inhibited when FA concentration listed between 0.08 and 0.82 mg.L⁻¹ and FNA concentration exceed 0.06 mg.L⁻¹ (Zhang et al., 2014, Anthonisen et al., 1976). Cho et al. (2016) concluded that NOB have a higher growth rate than AOB and are more resistant to pH changes. AOB will suffer irreversible activity loss during pH shocks, while NOB have a relatively good recovery of nitrifying activity (Kurisu et al., 2007, Im et al., 2014, Liu et al., 2015).

The nitrite accumulation occurs when AOB activity is more favourable than NOB activity. The build-up of nitrite can be problematic, as it will poison both AOB and NOB bacteria (Udert & Wächter, 2012; Edefell, 2017). The desired product of stable urine nitrification is a solution that contains equal parts of ammonium and nitrate. For this to happen, ammonia is oxidised to nitrite at the same rate as nitrite transferred to nitrate (Udert et al., 2003a). The growth of both AOB and NOB bacteria can be inhibited by several factors including temperature, pH, organic load, dissolved oxygen (DO) concentration, FA and FNA concentration, alkalinity, hydraulic and sludge retention time, and the previous history of the biosystem (Rusten et al., 2006, Bock and Wagner, 2013).

To investigate the influence of the pH and ammonia nitrogen dosage on AOB and NOB bacteria activity, pH data was continuously recorded in every 5 minutes during the experimental period, while the concentration of nitrogen compounds ($\text{NH}_3\text{-N}/\text{NH}_4\text{-N}$, $\text{NO}_3\text{-N}$, $\text{NO}_2\text{-N}$) in the urine feed tank, bioreactor and permeate tank was analysed in every 24-hour cycle. It can be observed in Figure 3.4 that the reactor pH firstly increased and then decreased every time after change to the new total ammonia nitrogen loading (i.e., day 0, 11, 17, 22). This is because the nitrifying bacteria have an inefficient cell growth and therefore needed more time to adapt to the new feed environment and total nitrogen loading (Fumasoli et al., 2017, Anthonisen et al., 1976).

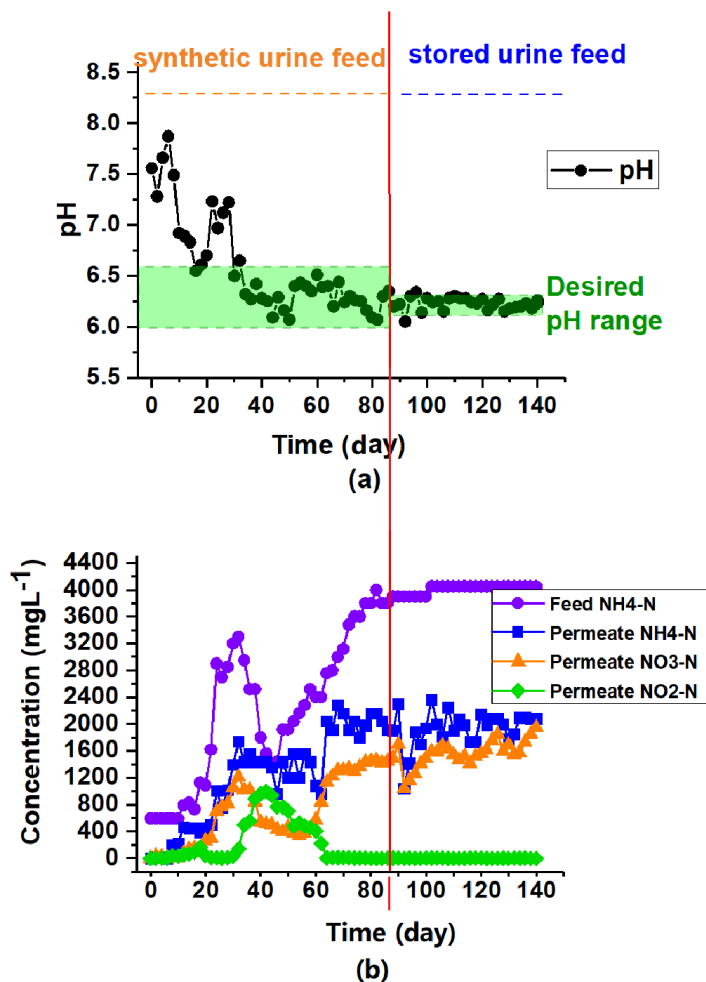


Figure 3.4 (a) pH profile during the MBR start-up and stable operation stages. (b) all-time concentration of inorganic nitrogen compounds in feed urine and MBR permeate

The impact of FA and FNA concentration on AOB and NOB also showed profound pH changes in UF-MBR. It can be observed from Figure 3 that the first nitrite accumulation occurred within the first 19 days of operation when pH of reactor fluctuated at relatively higher range. This implies that the pH change could lead to the FA and FNA inhibition on nitrifying bacteria activity (AOB and NOB). The specific growth rate of AOB is higher compared to that of NOB growth rate within the discussed pH range, resulting in the accumulation of nitrite intermediate.

The second nitrite accumulation was observed from day 30 to 64 when the reactor pH was maintained at the desired pH value of around 6.2. One reason for this observation could be due to the large amount of FA available in the reactor. The increase of FA to 2.3 mgN.L⁻¹ concentration under ammonium nitrogen shock loading inhibited the NOB activity, resulting unbalanced growth between AOB and NOB (Zhang et al., 2018). The permeate water quality in Figure 3.4(b) and Figure 3.5 also demonstrates this effect of shock ammonium nitrogen loading on nitrification performance and nitrifying bacteria activity. For instance, the ammonium nitrogen loading increased from 1,010 to 3,200 mg. L⁻¹ between day 22 and 30, which caused the excess amount of FA presents in system. As a result, the nitrate nitrogen concentration decreased from 1,180 to 395 mg. L⁻¹ between day 32 and 58 after the nitrite concentration reached to more than 200 mg. L⁻¹. It matches with above discussion - NOB is less FA tolerant than AOB. The NOB growth was inhibited by the high FA concentration. Three measures then used between day 32 and 42 to mitigate the nitrite accumulation: 1) reduce the SRT from infinite to 150 days by discharging 30 mL of sludge mixture every day; 2) reduce the feed nitrogen concentration by switching off feed pump every other day; 3) add sodium bicarbonate as external alkalinity dosage to boost the AOB and NOB activity, thus increase the nitrification rate.

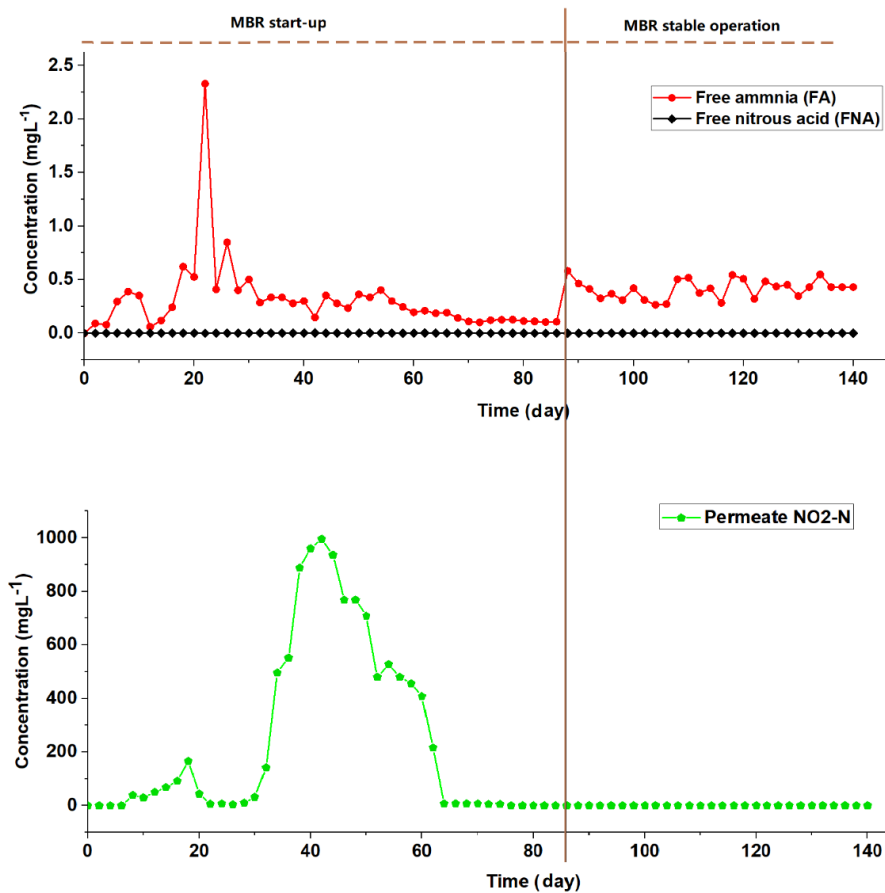


Figure 3.5 Concentration of FA and FNA during the MBR start-up period and stable operation, and corresponding nitrite accumulation phenomenon.

The UF-MBR adopted full strength stored human urine from day 87 and the system was maintained at the desired pH level at around 6.2 for stable operation. pH readings always fluctuate after the pH electrode cleaning and calibration, while the nitrification process remains stable. This is evidence that the pH reading in urine nitrification process is extremely sensitive. The pH fluctuation can be an indicator that reflects the instabilities of nitrification to some extent. But FA and FNA concentrations are more useable to control inhibitory effects and maintain the system stability. For instance, there is no sign of the excess amount of FA and FNA in the system between day 87 and 140 at the pH shocking moment (Figure 3.5). The changes in pH does not necessary imbalance the

system and cause nitrite accumulation. The system remained to its optimal equilibrium condition from day 106 that approximately 50% of ammonia in the feed is converted to nitrate by nitrification, without the introduction of additional alkalinity. The ammonium nitrogen and nitrate nitrogen in the nitrified urine reached a concentration ratio of 1:1. The optimal urine nitrification rate of $447 \pm 50 \text{ mg N} \cdot \text{L}^{-1} \cdot \text{d}^{-1}$ was achieved with a total nitrogen concentration of approximately $4006.3 \pm 225.8 \text{ mg N} \cdot \text{L}^{-1}$ in the feed.

3.4.2 Effect of step length and height on critical flux

The effect of various step length and step-height on UF-MBR critical flux was assessed in consecutive experiments, while the other operating parameters remain unchanged. It can be seen from Figure 3.6 that the critical flux values decrease with longer filtration duration. The critical flux is about $58 \text{ Lm}^{-2}\text{h}^{-1}$ under step length of 15 min but decreases to $54 \text{ Lm}^{-2}\text{h}^{-1}$ at a step length of 30 min. On the other hand, the higher the step height, the lower the critical flux value was observed. For example, the critical flux value dropped by $8 \text{ Lm}^{-2}\text{h}^{-1}$ as the step height increased from 3 to $12 \text{ Lm}^{-2}\text{h}^{-1}$. The critical flux was $59 \text{ Lm}^{-2}\text{h}^{-1}$ under step height at $3 \text{ Lm}^{-2}\text{h}^{-1}$, in contrast with that value of $53 \text{ Lm}^{-2}\text{h}^{-1}$ under $12 \text{ Lm}^{-2}\text{h}^{-1}$ step height. Above results imply that the faster and mostly irreversible fouling deposition is formed on the membrane by the increased step height or step length (Le Clech et al., 2003) at the initiation period in an UF-MBR feed with full strength stored urine. Subsequent experiments for critical flux assessment were therefore conducted at moderate step length (15 min) and relatively small step height ($6 \text{ Lm}^{-2}\text{h}^{-1}$) to avoid large error of flux averaging and rapid irreversible fouling on membrane at the early stage. In

addition, it is important to use constant step height and step length between consecutive experiments when verifying the effects of other parameters on critical flux.

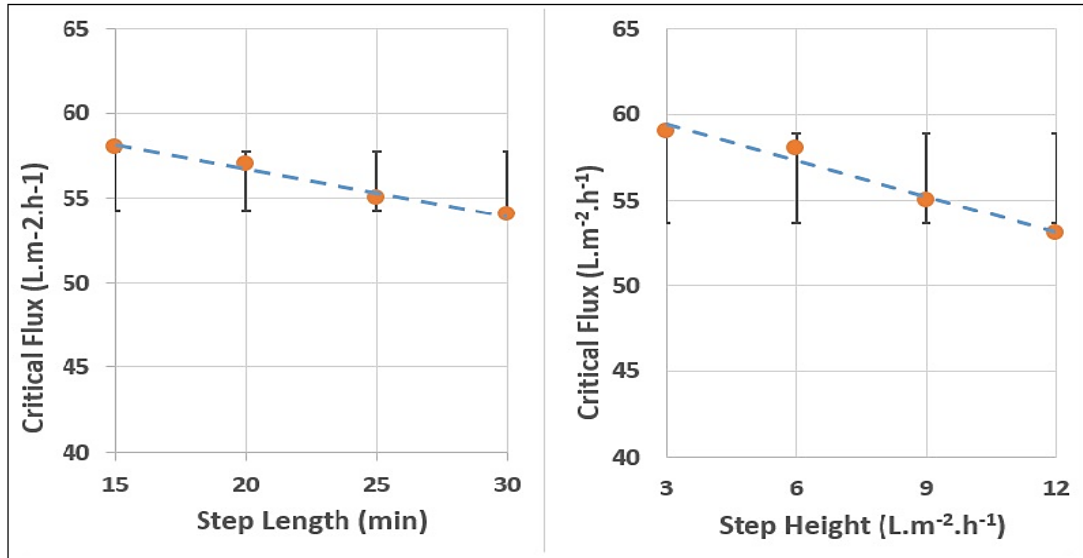


Figure 3.6 Effects of various flux step length and step height on critical flux when aeration intensity at 0.2 m³h⁻¹, biomass concentration at 3.5 g. L⁻¹, initial flux rate at 4 Lm⁻²h⁻¹, and reference flux rate at 0.5 Lm⁻²h⁻¹.

3.4.3 Effect of aeration intensity on critical flux

The continuous aeration supplies dissolved oxygen for micro-organisms growth without oxygen transfer limitation and assists membrane bioreactor to be operated at higher biomass concentration. Moreover, it functions as air scouring that helps remove or slow down solid build-up on the membrane surface, and thus reduced the problematic membrane reversible fouling and improved the membrane's critical flux value. From results presented in Figure 3.7, the range of critical flux was improved from 40-46 Lm⁻²h⁻¹ to 52-58 Lm⁻²h⁻¹ when the aeration intensity is raised from 0.1 m³h⁻¹ to 0.4 m³h⁻¹ at

MLSS concentration set at 3.5 g. L⁻¹. Similar trend also observed when biomass concentration at 2 and 5 g.L⁻¹. The aeration intensity has therefore a positive effect on critical flux.

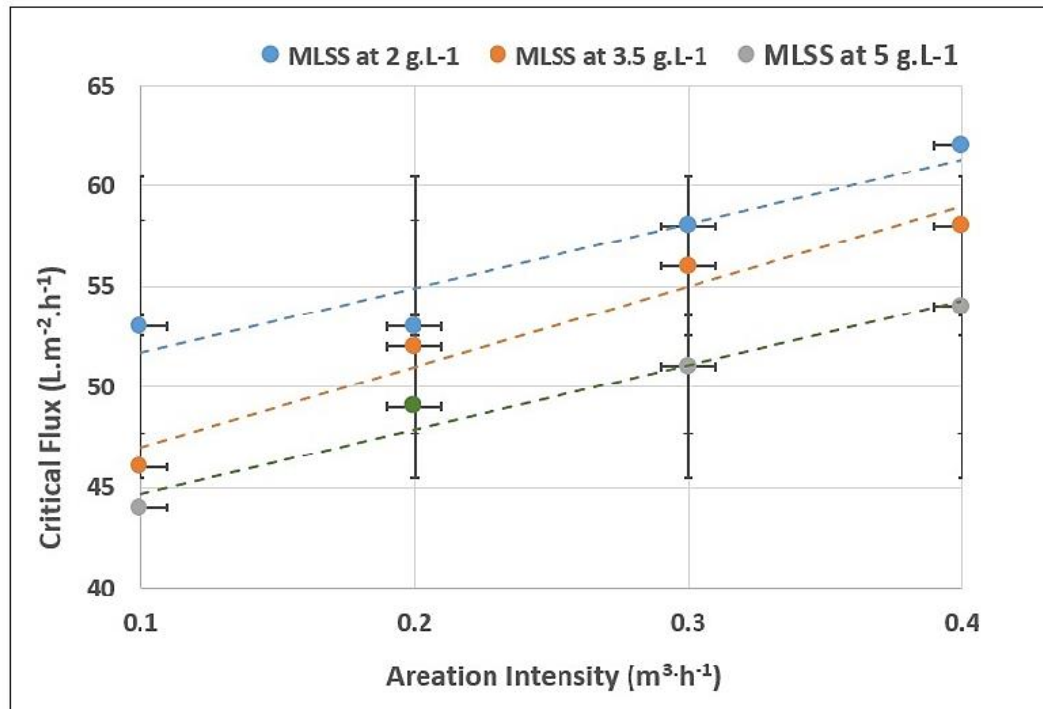


Figure 3.7 Effects of various aeration intensity and biomass concentration on critical flux when initial flux rate at 4 Lm⁻²h⁻¹, reference flux rate at 0.5 Lm⁻²h⁻¹, flux step length at 15 min, and step height at 6 Lm⁻²h⁻¹

3.4.4 Effect of sludge concentration on critical flux

Figure 3.7 also shows that the critical flux increases at higher aeration intensities and lower sludge concentrations. For instance, under the same aeration intensity at 0.3 m³h⁻¹, the critical fluxes for the sludge concentrations at 2, 3.5, and 5 g.L⁻¹ are 58, 56, and 51

$\text{Lm}^{-2}\text{h}^{-1}$, respectively. The relationships between critical flux and aeration intensity (i.e., 0.1, 0.2, 0.3, 0.4 m^3h^{-1}) under various biomass concentration (2, 3.5, 5 g.L^{-1}) were then fitted by linear mathematic equations as presented in Table 3.4. At a sludge concentration of 2, 3.5, and 5 g.L^{-1} , their R^2 values are 0.898, 0.952, and 0.966, respectively. Based on the profile of various aeration intensity on critical flux under different biomass concentrations, it implies that the critical flux decreases with increasing sludge concentration, and it can be improved through intensive aeration irrespective of biomass concentrations. Higher aeration intensity is more favourable for a sludge-rich submerged UF-MBRs to maintain critical flux at certain values and eliminate the degree of membrane fouling.

Table 3.4 The linear relationship between various aeration intensity and its corresponding critical flux value

Sludge concentration (g.L^{-1})	Linear Regression equations	R^2
2	$y = 32x + 48.5$	0.898
3.5	$y = 40x + 43$	0.952
5	$y = 32x + 41.5$	0.966

3.4.5 Fouling reversibility

The profile of critical flux and its irreversibility at various aeration intensities is discussed in this section in accordance with Figure 3.8. At the aeration intensity of 0.1 m^3h^{-1} for

instance – shown in Figure 6(a) - the real time TMP values proportionally increased between the first 5 consecutive flux heights (4 to 28 Lm⁻²h⁻¹); the total fouling rates (F_{Total}) remain zero before flux reached to 28 Lm⁻²h⁻¹. This indicates that the reversible fouling was predominantly on the membrane surface at the early stage of improved flux-step assessment. The physical cleaning method using intermediate flux of 0.5 L m⁻²h⁻¹ is effective in reducing the influence of fouling history on membrane. However, an increase in real time TMP was observed from flux-step 6, suggesting fouling cannot be physically removed by proposed intermittent relaxation cycle. Once imposed flux exceed 28 Lm⁻²h⁻¹, the membrane irreversible fouling starts.

It is worth mentioning that the initial TMP did not completely return back to its original baseline TMP after flux step 5, 6 and 7. For instance, after flux step 5, there was a small amount of irreversible fouling occurred at the irreversible fouling rate (F_{Irr}) of 0.00089 m⁻¹s⁻¹. After flux step 6, the irreversible fouling on membrane continually increased with slower irreversible fouling rate (0.00045 m⁻¹s⁻¹). The initial TMP then returned to a new baseline after flux step 7 without the presence of additional irreversible fouling (zero irreversible fouling rate). This observation could be due to the combination process of pore blocking and concentration polarization. Specifically, due to the interaction between membrane and soluble particles (colloidal and macromolecular matters), the local deposition is build-up within membrane pores. Then ultimately deposits on membrane surface. The development of polarization layer adjacent to the membrane surface will increases the filter resistance and consequently reduces membrane flux, which would exacerbate this phenomenon further.

Furthermore, the incremental irreversible fouling rate and total fouling rate does not exceed the critical fouling rate (F_{Crit}) at all times when aeration intensity is $0.1 \text{ m}^3\text{h}^{-1}$. This implies that neither critical flux nor critical flux for irreversibility were reached among all flux-stepping. The formation of cake layer on membrane surface remains removable up to the maximum imposed flux of $58 \text{ Lm}^{-2}\text{h}^{-1}$. Similar observations have been found in the other two sets of aeration intensity as presented in Fig 3.8 (b) and (c). Hence, the conclusion can be drawn that due to adsorption of macromolecular or colloidal organic matter inside membrane pores and formation of polarization layer at adjacent membrane surface, a small amount of irreversible fouling was gradually build-up on the membrane, despite the membrane filtration was operated at sub-critical conditions. To operate nitrifying UF-MBR under sub-critical rate does not prevent the gradual development of the fouling on membrane. This finding is consistent with previous works on the sub-critical filtration method regardless MBR type, i.e. Ognier et al. (2002), Ognier et al. (2004), Wu et al. (2018), Jang et al. (2021).

In addition, the influence of fouling on membrane can be alleviated by intermediate relaxation and/or moderate aeration intensity (air scouring). The measurement of critical flux and the critical flux for irreversibility in Figure 3.8 showing almost no fouling occurrence when aeration intensity of $0.4 \text{ m}^3\text{h}^{-1}$ and intermediate flux of $0.5 \text{ Lm}^{-2}\text{h}^{-1}$ were adopted.

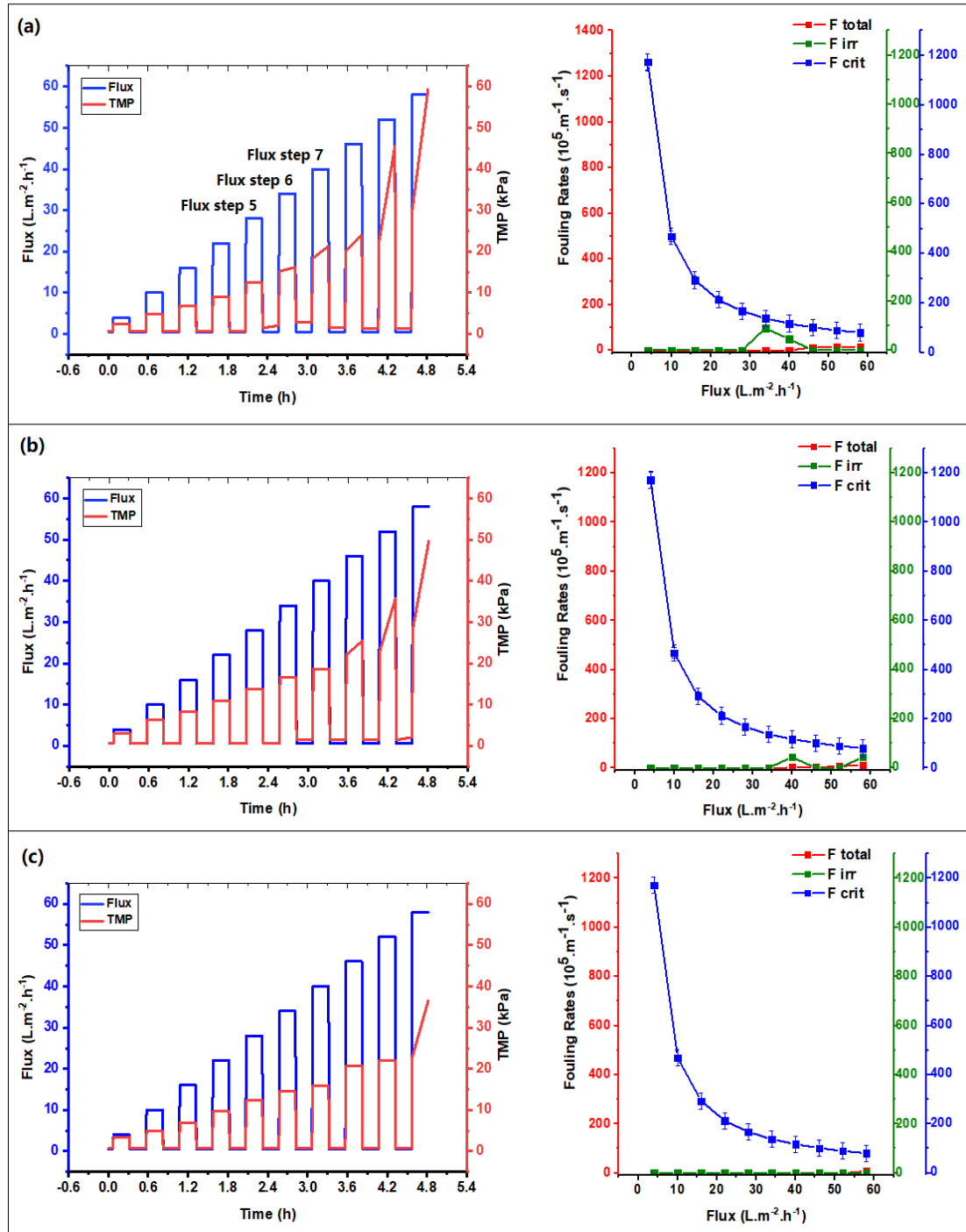


Figure 3.8 Profile of TMP, total fouling rate (FTotal), irreversible fouling rate (Firr) and critical fouling rate (FCrit) on membrane determined by the improved flux-step method among various aeration intensity (a) 0.1 m³h⁻¹, (b) 0.2 m³h⁻¹, and (c) 0.4 m³h⁻¹. The biomass concentration at 3.5 g.L⁻¹, initial flux rate at 4 Lm⁻²h⁻¹, reference flux rate at 0.5 Lm⁻²h⁻¹, flux step length at 15 min, and step height at 6 Lm⁻²h⁻¹.

3.5 Conclusions

The UF-MBR feed with source separated stored urine has been operated at a maximum nitrification rate of $447 \pm 50 \text{ mgN} \cdot \text{L}^{-1} \cdot \text{d}^{-1}$ in this work. The critical flux and flux for irreversibility were evaluated by conducting consecutive flux-step experiments. The effects of parameters such as aeration intensity, biomass concentration, step length, and step height of incremental flux on the critical flux have been successfully identified. It can be concluded that the aeration intensity has a positive effect on critical irrespective of sludge concentrations, while the critical flux decreases at higher biomass concentrations. Higher aeration intensity is therefore recommended for UF-MBRs containing higher MLSS concentration. The critical flux also decreased by the increased step height or step length, due to rapid fouling on membrane surface at initial flux-step. It is recommended to choose the moderate step length (15-20 min) and small step height ($3\text{-}6 \text{ Lm}^{-2}\text{h}^{-1}$) to initiate the critical flux study under same sludge concentrations. The influence of fouling on membrane surface can be reduced by introducing intermediate relaxation or large aeration intensity. A small amount of irreversible fouling is observed in all the cases studied where applied flux is below the critical flux, due to adsorption of macromolecules, pore blocking and plug, and cake layer formation on membrane surface.

The limitation of this work is that the filtration performance and critical flux analyses were studied with lab-scale UF-MBRs. Although the system was fed with full strength raw urine, the fouling behaviours and corresponding mechanisms may not closely reflect the real case scenario. The critical flux and its irreversibility on membrane were measured for the short-term operations in this study.

4 Effects of PAC concentration in membrane bioreactor (MBR) for source-separated urine treatment

[Notes: A part of this chapter has been submitted for publication and is currently under review]

J. Jiang, A. Almuntashiri, W. Shon, S. Phuntsho, Q. Wang, S. Freguia, I, El-Saliby, H.K. Shon. (Under review). Feasibility study of powdered activated carbon membrane bioreactor (PAC-MBR) for source-separated urine treatment: a comparison with MBR.

4.1 Materials and methods

4.1.1 Laboratory scale PAC-MBR operation

Two lab scale membrane bioreactors, labelled ‘low PAC-MBR’ (0.5 g. L^{-1} of PAC) and ‘high PAC-MBR’ (2 g. L^{-1} of PAC), were operated in parallel to treat hydrolysed source separated urine for 73 days. Each of them has total effective working volume of 26 L (Figure 4.1). The composition of source-separated urine is shown in Table 4.1. The dissolved oxygen (DO) level is monitored by DO meter in a range between 4.3 and 4.5 mg. L^{-1} . The sludge retention time (SRT) was set at 62.5 days by discharging 415 mL of sludge mixture every day. The hydraulic retention time (HRT) was maintained at 3.5 days. Measurement of conductivity and pH were conducted in every 5 minutes in this study. The probes were cleaned with commercial cleaning solution and calibrated with corresponding pH/conductivity standard solution in every two weeks.

The commercially available braid-reinforced polyvinylidene fluoride (PVDF) hollow fibre, manufactured by Lotte Chemical, South Korea, were used for potting MF membrane modules in this study. It has nominal pore size diameter at 0.1 μm , inner diameter at 0.8mm and outer diameter at 2.1 mm. Each MF membrane module that was potted in UTS lab has a total effective area of 0.02 m^2 . The timely TMPs were measured by Druck pressure transmitter PTX 1400. The LogBox-AA (Novus Automation, UK) and LogChart II software were used for continues data logging, data configuration recording and retrieval, and further data plotting and analyses.

The wood-based powdered activated carbon used in this work was purchased from local shop with mean particle size (D50) of 34.2 μm and 1110 m^2/g specific surface area. The PAC was firstly rinsed with DI water to remove the impurity. After that, dried it out in oven at 105 $^\circ\text{C}$ for 1 hour. Then cooled down to the room temperature inside a desiccator before directly dose proposed PAC concentration into the hybrid PAC-MBR. An extra 0.21 g pre-treated PAC was added into the proposed low PAC-MBR every day, corresponding a PAC replenishment ratio at 1.6%. Similarly, an extra 0.83 g pre-treated PAC was added in high PAC-MBR in the same time interval to maintain the same frequency of PAC replacement.

Six pharmaceuticals - carbamazepine (CBZ), naproxen (NPX), acetaminophen (ACE), ibuprofen (IBP), metronidazole (MDZ) and estriol (E3) - were selected in this work according to their molecular size, structural complexity, and the likelihood in source-separated urine.

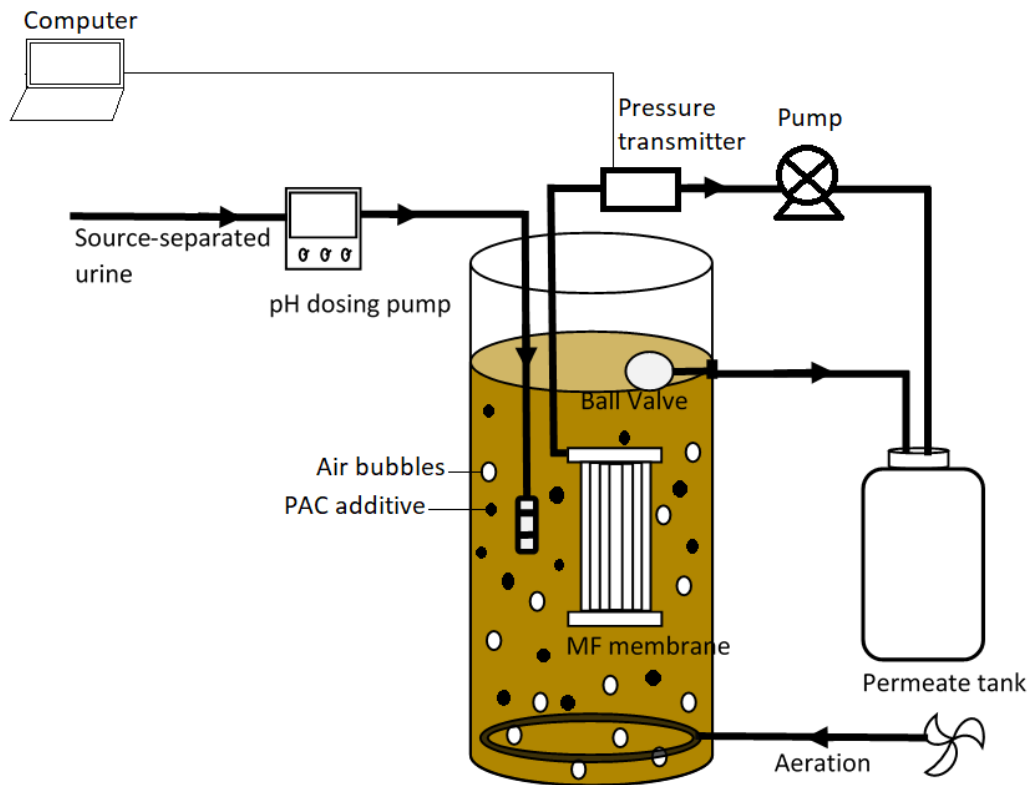


Figure 4.1 Schematic diagram of proposed hybrid PAC-MBR

4.1.2 Analytical methods

The sludge mixture samples and permeate samples were collected in every 24-hour cycle to monitor the performance of control MBR and proposed PAC-MBR. All samples were centrifuged and filtered through 0.2 μm filter immediately after collection, and then stored at 4°C for further analysis. The concentration of major cations (Na^+ , K^+ , Mg^{2+} , Ca^{2+}) and major anions (SO_4^{2-} , PO_4^- , Cl^-) were analysed by Ion Chromatography (IC, Thermo Fisher Scientific, USA) and Microwave Plasma Atomic Emission Spectroscopy (MP-AES 4100, Agilent, USA), respectively. The ammonia concentration in nitrogen ($\text{NH}_4\text{-N}$), nitrite concentration in nitrogen ($\text{NO}_2\text{-N}$), and nitrate concentration in nitrogen ($\text{NO}_3\text{-N}$) were

measured via test kit and UV-VIS spectrophotometer (Spectroquant^R NOVA 60, USA). The concentration of DOC was analysed by TOC analyser (Analytik Jena AG, Germany). The Hach HQD digital multimeter (HQ40D) was used to record readings of pH, conductivity, TDS and DO during operation.

For the analysis of presence of selected pharmaceuticals in stored urine and permeate, 1 M stock solution was prepared in methanol solution then stored at -30°C in dark. The standard solutions at various concentrations (0, 5, 10, 50, 75, 100, 250, 500, 750 and 1000 µg/L) were prepared by diluting stock solution with DI water. Collected samples were stored at 4°C and analysis within 2 weeks sampling. The pharmaceuticals in liquid samples were preconcentrated and separated by solid phase extraction (SPE) using Oasis MCX 3 cc Vac Cartridge (Waters, 60mg, 3cc) with 3 mL methanol and 3 mL deionised water. Then elute with methanol. 1 mL of individual final extract from SPE was used for liquid chromatography-mass spectrometry (LCMS-8060 Shimadzu).

The liquid chromatography was performed using ORTECS C18+Column, 2.7 µm, 2.1 mm ×75 mm (Waters). A sample injection volume of 10 µL was used at an optimized flow rate of 0.6 mL.min⁻¹. Mobile phases were 100% methanol (A) and ultrapure water (B). Optimised gradient elution conditions were concluded as follow: 50% mobile phase B between 0.01 and 0.10 min; a linear ramp from 50% to 95% from 0.10 to 1.50 min; stay at 95% from 1.50 to 3.5min; gradual back to 50% from 3.51 to 5.50 min. The multiple reaction modes (MRMs) selected for the analytes were: acetaminophen (152 >110, ES+), metronidazole (172 >128, ES+), carbamazepine (237 >194, ES+), ibuprofen (205 >161, ES-), naproxen (229 >185, ES-).

4.2 Results and discussion

4.2.1 Effect of PAC dosage on membrane permeate water quality

Table 4.1 shows the composition and corresponding ion concentrations in 0.5 g. L⁻¹ PAC-MBR and 2 g. L⁻¹ PAC-MBR. The urine nitrification performance was improved with increased PAC dosage. Average 42.8% of ammonia in feed urine was biological oxidized to stable nitrate in low PAC-MBR, while that number is increased by 5.2% to 48% in high PAC-MBR. This is due to the interception effect of the membrane and the adsorption and carrier properties of PAC sludge flocs increases the concentration and activity of nitrifying bacteria, resulting in an enhanced nitrification performance (Yang et al., 2016).

Table 4.1 Composition and corresponding ion concentrations in source-separated urine, low PAC-MBR permeate and high PAC-MBR permeate.

		Source- separated urine	0.5 g. L⁻¹ PAC-MBR	2 g. L⁻¹ PAC-MBR
NH ₄ -N	mg. L ⁻¹	4250 ± 216.5	1919.2 ± 146.62	1987.7 ± 205.5
NO ₃ -N	mg. L ⁻¹	N/A	1817.6 ± 102.43	1973.3 ± 178.9
NO ₂ -N	mg. L ⁻¹	N/A		N/A

PO ₄ -P	mg. L ⁻¹	264.1 ± 26.8	138 ± 4.24	235.5 ± 2.8
K ⁺	mg. L ⁻¹	1253.4 ± 120.5	1092.0 ± 24.6	1082.1 ± 4.7
Ca ²⁺	mg. L ⁻¹	2.9 ± 0.7	0	0
Mg ²⁺	mg. L ⁻¹	21.7 ± 0.2	19.0 ± 0.9	14.0 ± 0.2
Na ⁺	mg. L ⁻¹	1113.9 ± 41.1	701.8 ± 84.5	735.2 ± 69.3
Cl ⁻	mg. L ⁻¹	1475.9 ± 117.0	1379.9 ± 49.1	1377.6 ± 63.0
SO ₄ ²⁻	mg. L ⁻¹	899.3 ± 21.5	859.3 ± 5.7	813.7 ± 9.3
COD	mg. L ⁻¹	5013.0 ± 240.0	351.0 ± 70.0	202.0 ± 70.4
COD Removal rate	%	N/A	92.5 ± 4.7	96.0 ± 2.8
pH	-	9.2	6.2	6.2

4.2.2 Effect of PAC dosage on organic matter removal

Figure 4.2 shows COD removal performance overtime in proposed PAC-MBRs. It has been shown that the overall COD removal rate was improved with increased PAC dosage, i.e., the COD removal rates were 92.5 ± 4.7 % and 96.0 ± 2.8 % in low PAC-MBR and high PAC-MBR, respectively. It is worth noting that the highest COD removal rate in first 19 days of operation was achieved in high PAC-MBR, implying that the physical

adsorption of foulant to PAC was predominated in high PAC-MBR at the early stage to remove organic particles. In comparison, no obvious improvement of COD removal in low PAC-MBR was observed at that time. This was probably due to the relatively low concentration of PAC additive in the system, which leads to the rapid reaching of its equilibrium adsorbate concentrations. The increase of COD removal rate in low PAC-MBR up to 95.9% between day 1 and 31 is thereby resulted by simultaneous adsorption and biodegradation. This was consistent with the results reported in previous work regardless the treated water source (Ying and Ping, 2006, Hu et al., 2014a, Zhang et al., 2017)

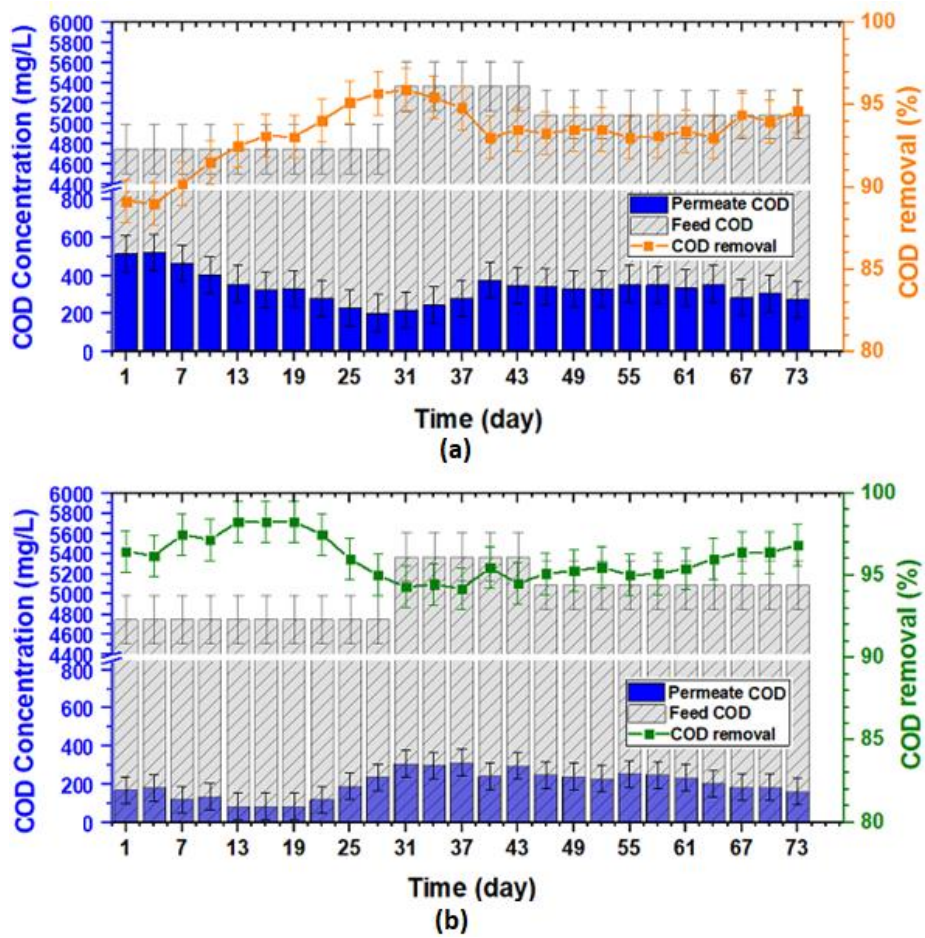


Figure 4.2 Variation of COD removal efficiencies in (a) low PAC-MBR and (b) high PAC-MBR overtime

4.2.3 Effect of PAC dosage on micropollutant removal

The removal efficiency of targeted pharmaceuticals and hormones between low PAC and high PAC additives MBR is discussed in this section. As can be seen in Figure 4.3, acetaminophen, naproxen, ibuprofen and estriol were fully removed in low PAC-MBR, while metronidazole and carbamazepine were removed at various removal efficiency. The removal of metronidazole and carbamazepine in low PAC-MBR were at $79 \pm 5\%$ and $97 \pm 1\%$, respectively. In contrast, greater than 99% removal efficiency was observed among all targeted micropollutants in high PAC-MBR, indicating that the addition of 2 g. L⁻¹ of PAC at 1.6% PAC replenishment rate was sufficient to remove targeted pharmaceuticals and hormones. The formation of biological powdered activated carbon (BPAC) over time via growth of stable microbial film on PAC is thereby the dominating removal mechanisms in micropollutants removal.

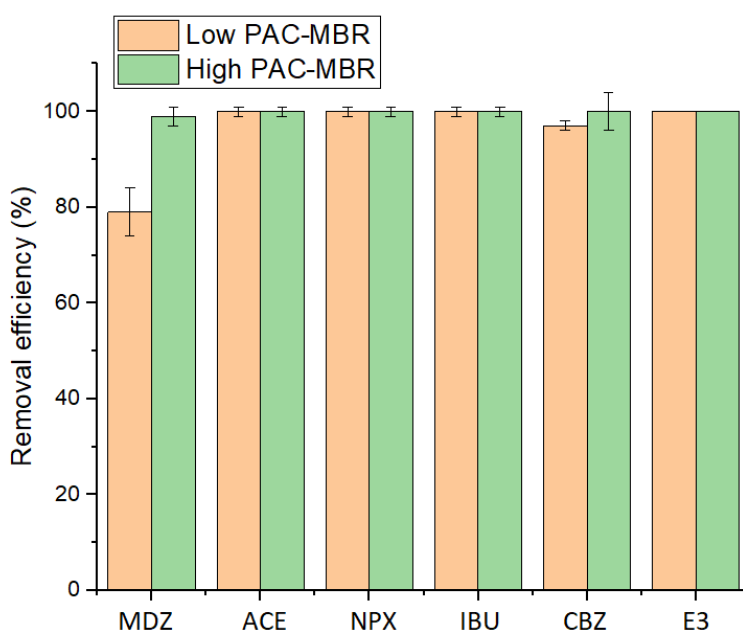


Figure 4.3 Overall micropollutants removal rate in low PAC-MBR and high PAC-MBR

4.2.4 Effect of PAC dosage on sludge mixture properties

Figure 4.4 shows the change of biomass concentrations and their corresponding MLVSS/MLSS ratio in each PAC-MBR. At day 73, the biomass concentration was increased from 4.4 to 6.2 g. L⁻¹ in low PAC-MBR, while that number increased from 5.1 g. L⁻¹ to 5.72 g. L⁻¹ in high PAC-MBR. The MLVSS/MLSS ratio in both PAC-MBRs did not change much and increased slightly over time indicating a stable biodiversity of microorganisms. Low MLVSS/MLSS ratio in the high PAC-MBR suggests that high PAC additive in MBR promotes the rapid growth of microorganisms, maintaining a relatively stable system operation without sacrificing the targeted micropollutants' removal efficiency. It was also noticed that, in both PAC-MBRs, the MLVSS concentration dropped immediately after PAC dosing, implying that the virgin PAC has a strong ability to physically adsorb organic or volatile foulants from the activate sludge mixture.

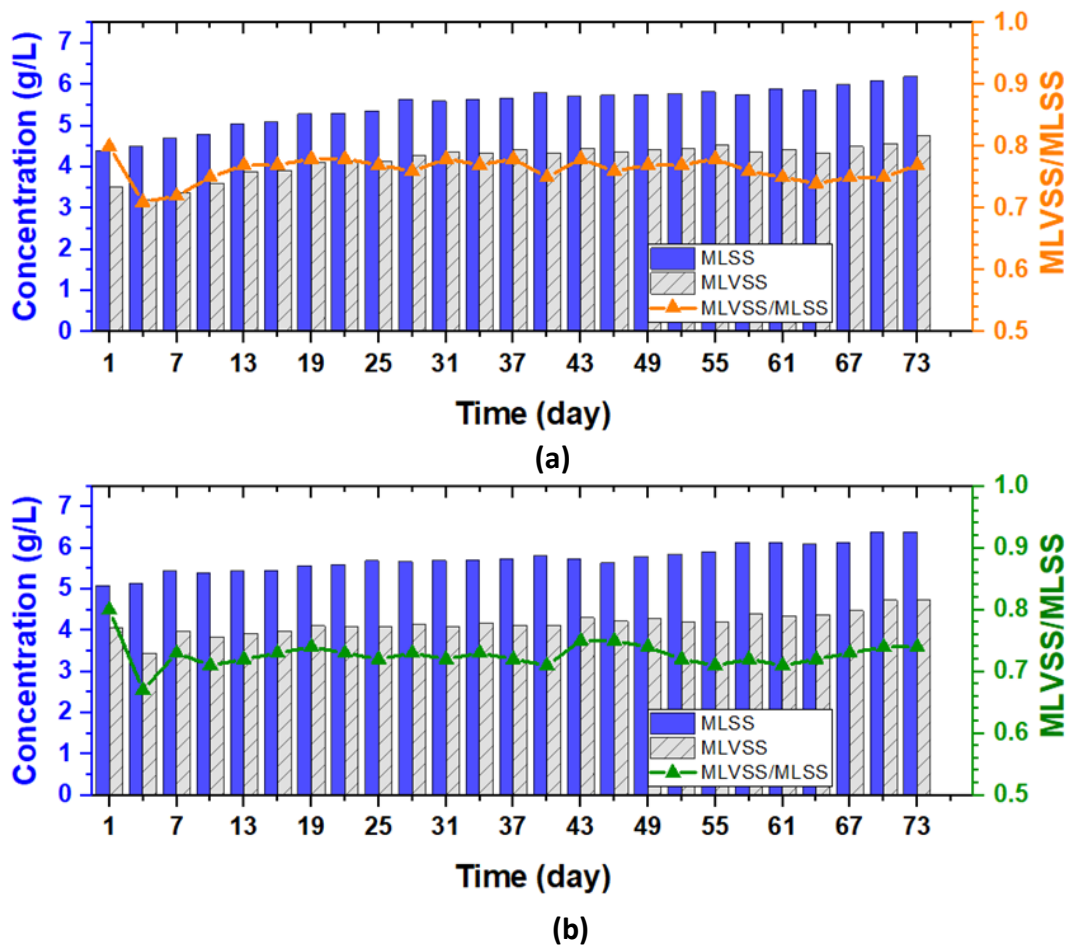


Figure 4.4 Variation of MLSS concentration and MLSS/MLVSS ratio in (a) low PAC-MBR and (b) high PAC-MBR overtime

4.3 Conclusions

In conclusion, high PAC dosage promote more rapid biomass growth, lower MLVSS/MLSS value and lower sludge viscosity compared to the low PAC dosage. The nitrification efficiency, COD removal performance and selected micropollutants removal efficiency were improved in high PAC additive. The addition of 2 g. L⁻¹ of PAC in MBR at 1.6% PAC replenishment rate could be beneficial for better removal of targeted pharmaceuticals and hormones without compromising the nutrient recovery efficiency.

5. Feasibility study of powdered activated carbon membrane bioreactor (PAC-MBR) for source-separated urine treatment: a comparison with MBR

[Notes: This chapter has been submitted for publication and is currently under review]

J. Jiang, A. Almuntashiri, W. Shon, S. Phuntsho, Q. Wang, S. Freguia, I. El-Saliby, H.K. Shon. (Under review). Feasibility study of powdered activated carbon membrane bioreactor (PAC-MBR) for source-separated urine treatment: a comparison with MBR.

5.1 Abstract

Micropollutants (MPs) such as pharmaceuticals and personal care products are a group of emerging environmental contaminants, which are structurally complex and can cause adverse physiological effects on human health at low concentration (Gavrilescu et al., 2015, Luo et al., 2014). This study demonstrated that a hybrid process of powdered activated carbon and microfiltration membrane bioreactor (PAC-MBR) could be utilized for efficient removal of metronidazole, acetaminophen, naproxen, ibuprofen, carbamazepine, estriol (> 99%) from source-separated urine via physical adsorption and biodegradation in a single step, without compromising the operating system stability. Further, it improved organic removal efficiency from $88.6 \pm 2.9\%$ to $96.0 \pm 1.2\%$, promoted rapid biomass growth, increased sludge floc size growth by 17% and reduced membrane fouling propensities.

Keywords: fouling; micropollutant; powdered activated carbon; urine; membrane bioreactor

5.2 Introduction

The presence of micropollutants (MPs) such as pharmaceuticals and personal care products in wastewater streams is an emerging health and environmental concern. These compounds are structurally complex and can cause adverse physiological effects on human health at low concentration (Gavrilescu et al., 2015, Luo et al., 2014). However, the current wastewater treatment technologies are not designed to remove these compounds, which leads to many residual pharmaceuticals and hormones in treated effluents. These further contaminate natural water systems and its aquatic ecosystems.

Microfiltration membrane bioreactor (MBR) technology is recommended in treating MPs with advantages such as compact operation space, less sludge waste production, longer sludge retention time (SRT), and improved effluent quality (Iorhemen et al., 2016, Grandclément et al., 2017, Caluwé et al., 2017). Previous studies on the removal of total antibiotics in five wastewater treatment plants (WWTPs) showed that 22.5% - 38.2% of total antibiotics were adsorbed on the surface of activated sludge particles, and 61.8% – 77.5% of which were degraded by bacteria. The removal efficiency of hydrophobic MPs ($\log K_{ow} > 3.2$) in aerobic MBR were greater than 85% while the removal capacity of hydrophilic MPs ($\log K_{ow} < 3.2$) varied significantly (Wang et al., 2020, Chtourou et al., 2018). For instance, the removal rate of carbamazepine, naproxen, metronidazole, acetaminophen, ibuprofen and estriol with MBR treatment of synthetic wastewater at pH

7 were $32 \pm 17\%$, $45 \pm 15\%$, $40 \pm 26\%$, $87 \pm 7\%$, $96 \pm 4\%$ and $97 \pm 2\%$, respectively (Gutiérrez et al., 2021, Nguyen et al., 2013b, Tufail et al., 2021). Therefore, post-treatment such as granular activated carbon (GAC) adsorption was introduced for additional MBR effluent purification, given that the physiochemical interactions between adsorbent and adsorbate can effectively remove MPs. However, such approach is unattractive due to high consumption of GAC, reduction in MPs removal efficiency due to the competitive adsorption between nutrients and MPs, decline of GAC adsorption capacity over time, and additional space requirement (Boehler et al., 2007, Almunashiri et al., 2021, Nguyen et al., 2013b, Asif et al., 2020).

The combined process of powdered activated carbon and microfiltration membrane bioreactor (PAC-MBR) seems to be an ideal approach to remove MPs via physical adsorption and biodegradation in a single step. This due to the continuous formation of biofilm on the adsorbent over time. To date, the removal efficiency of pharmaceuticals from urine in a PAC-MBR process and its effect on MBR biological and filtration performances have not yet been investigated. Therefore, this work studied the effect of powdered activated carbon (PAC) additive on biomass production, removal capacity of six selected MPs, and membrane fouling.

5.3 Materials and methods

5.3.1 Experimental setup

Two lab-scale membrane bioreactors, labelled ‘control MBR’ and ‘hybrid PAC-MBR’, were operated in parallel to treat hydrolysed urine - collected from the CB11 urine diversion system at the University of Technology Sydney, Australia - for 73 days. Each of them had 26 L effective working volume (Figure 5.1). The composition of stored urine is shown in Table 5.1. The dissolved oxygen (DO) level was controlled by DO meter at 4.3 mg. L⁻¹. The sludge retention time (SRT) was set at 62.5 days equivalent to discharge 415 mL of sludge mixture every day. The hydraulic retention time (HRT) was maintained at 3.5 days.

The commercial braid-reinforced polyvinylidene fluoride (PVDF) hollow fibre membrane with 0.1 µm nominal pore size, purchased from Lotte Chemical (South Korea), was used in this study. Each MF membrane module was then potted in UTS lab to a total effective area of 0.02 m². The Druck pressure transmitter PTX 1400 was used to measure the timely transmembrane pressure (TMP). The LogBox-AA (Novus Automation, UK) and LogChart II software were used for timely data logging and retrieval.

The powdered activated carbon, purchased from a local shop, had 1110 m²/g specific surface area and 34.2 µm mean particle size (D50). The PAC was initially rinsed with deionized (DI) water to remove loose dust particles, then it was dried in an oven at 105 °C for 1 hour. The PAC was allowed to cool down to room temperature inside a desiccator before being added at a dose of 2 g/L into the hybrid PAC-MBR. An extra 0.83 g pre-treated PAC was added into the proposed hybrid PAC-MBR every day, corresponding a PAC replenishment rate of 1.6% per day.

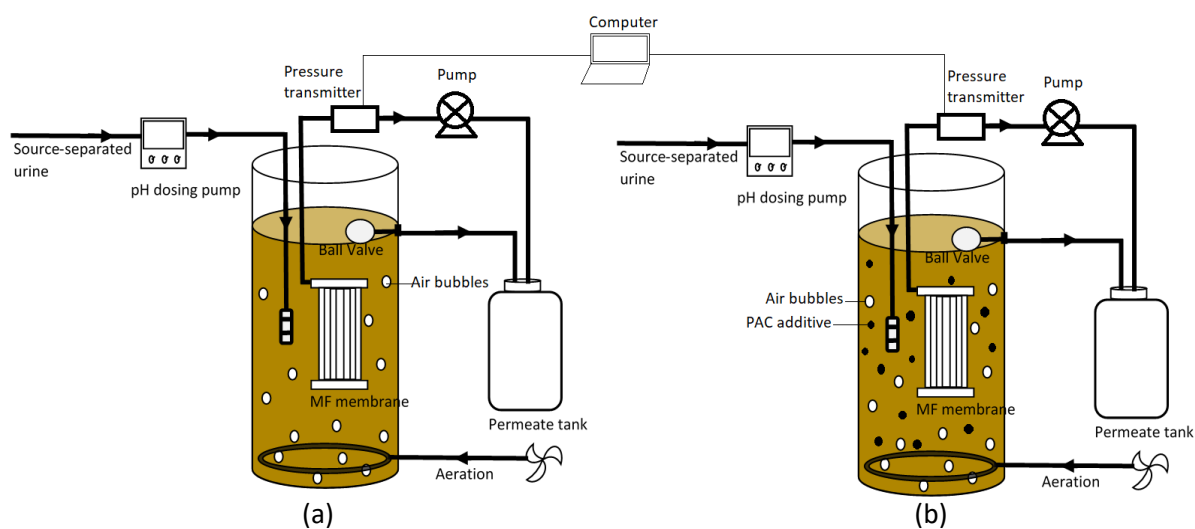


Figure 5.1 Schematic diagram of (a) control MBR and (b) hybrid PAC-MBR

Table 5.1 Composition and corresponding ion concentrations in source-separated urine, control MBR permeate, and hybrid PAC-MBR permeate

		Source-separated urine	Nitrified urine after control MBR	Nitrified urine after hybrid PAC-MBR
NH ₄ -N	mg/L	4250 ± 216.5	1894.5 ± 117.9	1987.7 ± 205.5
NO ₃ -N	mg/L	N/A	1796.0 ± 115.5	1973.3 ± 178.9
PO ₄ -P	mg/L	264.1 ± 26.8	238.5 ± 5.0	235.5 ± 2.8
K ⁺	mg/L	1253.4 ± 120.5	1099.7 ± 38.2	1082.1 ± 4.7
Ca ²⁺	mg/L	2.9 ± 0.7	3.4 ± 1.5	0.0
Mg ²⁺	mg/L	21.7 ± 0.2	22.6 ± 0.8	7.0 ± 0.2

Na ⁺	mg/L	1113.9 ± 41.1	809.3 ± 46.7	735.2 ± 69.3
Cl ⁻	mg/L	1475.9 ± 117.0	1338.3 ± 35.4	1377.6 ± 63.0
SO ₄ ²⁻	mg/L	899.3 ± 21.5	899.3 ± 3.1	813.7 ± 9.3
COD	mg/L	5013.0 ± 240.0	569.6 ± 50.0	202.0 ± 70.4
COD Removal rate	%	N/A	88.6 ± 2.9	96.0 ± 2.8
pH	-	9.2	6.2	6.2

5.3.2 Water quality analysis

The mixed liquor samples and permeate samples were collected every day to monitor the performance of control MBR and PAC-MBR. All samples were filtered through 0.2 µm filter and stored at 4°C prior to analysis. The concentration of major cations (Na⁺, K⁺, Mg²⁺, Ca²⁺) and major anions (SO₄²⁻, PO₄⁻, Cl⁻) was analysed by Ion Chromatography (IC, Thermo Fisher Scientific, USA) and Microwave Plasma Atomic Emission Spectroscopy (MP-AES 4100, Agilent, USA), respectively. Ammonia (NH₄-N), nitrite-nitrogen (NO₂-N) and nitrate-nitrogen (NO₃-N) were measured via test kit and UV-VIS spectrophotometer (Spectroquant^R NOVA 60, USA). The concentration of chemical oxygen demand (COD) was analysed by multi N/C 3100 TOC analyzer from Analytik Jena GmbH. The Hach HQD digital multimeter (HQ40D) was used to record readings of pH, conductivity (EC), total dissolved solids (TDS) and DO during operation.

5.3.3 Micropollutant analysis

Six representative MPs, purchased from Sigma Aldrich (Australia), were measured in the raw and treated urine: metronidazole (MDZ), acetaminophen (ACE), naproxen (NPX), ibuprofen (IBU), carbamazepine (CBZ), estriol (E3). They were chosen in this work according to their molecular structures and properties, acidity, hydrophobicity of molecular compounds, and likelihood in source-separated urine. A 1 M stock solution was used as standards for each MPs and was prepared in methanol solution and stored at -30°C in dark to avoid the photodegradation.

For the analysis of presence of selected MPs in stored urine and permeate, standard solutions at various concentrations (0, 5, 10, 50, 75, 100, 250, 500, 750, and 1000 µg/L) were prepared by diluting stock solutions with DI water. Collected samples were stored at 4°C and analysed within 2 weeks of sampling. The analytes in liquid samples were preconcentrated and separated by solid phase extraction (SPE) using Oasis MCX 3 cc Vac Cartridge (Waters, 60mg, 3cc) with 3 mL methanol and 3 mL DI water, then elute with methanol. 1 mL of individual final extract from SPE was used for liquid chromatography-mass spectrometry (LCMS-8060 Shimadzu). The liquid chromatography was performed using ORTECS C18+Column, 2.7 µm, 2.1 mm ×75 mm (Waters). A sample injection volume of 10 µL was used at an optimized flow rate of 0.6 mL/min. Mobile phases were 100% methanol (A) and ultrapure water (B). Optimised gradient elution conditions were concluded as follow: 50% mobile phase B between 0.01 and 0.10 min; a linear ramp from 50% to 95% from 0.10 to 1.50 min; stay at 95% from 1.50 to 3.5 min; gradual back to 50% from 3.51 to 5.50 min. The multiple reaction modes

(MRMs) selected for the analytes were: MDZ (172 >128, ES+), ACE (152 >110, ES+), NPX (229 >185, ES-), IBU (205 >161, ES-), CBZ (237 >194, ES+), E3 (287>171, ES-) (Table 5.2).

Table 5.2 MRM table for proposed LC-MS/MS analysis

Compound	Precursor (m/z)	Transition (m/z)	Polarity	Retention time
Metronidazole (MDZ)	172	128	+	0.39
Acetaminophen (ACE)	152	110	+	0.37
Naproxen (NPX)	229	185	-	1.9
Ibuprofen (IBU)	205	161	-	2.5
Carbamazepine (CBZ)	237	194	+	1.28
Estriol (E3)	287	171	-	1.15

The lipophilicity and hydrophilicity of MPs compounds were determined according to equation below. Specifically, logP represents the partition coefficient of unionised compound in neutral state in water-n-octanol system. logD is the distribution coefficient of ionised MPs molecule as a function of the pH between two phases. pK_a is the acid dissociation constant used to indicate the molecular acidity. The percent ionization (%) was used to measure the strength of acids/bases.

$$\log P = \log_{10} \frac{[\text{unionized-solute}]_{\text{octanol}}}{[\text{unionized-solute}]_{\text{water}}} \quad (5.1)$$

$$\log D_{\text{acids}} = \log P + \log \left(\frac{1}{1+10^{pH-pK_a}} \right) \quad (5.2)$$

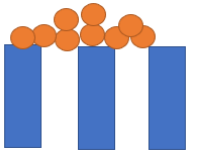
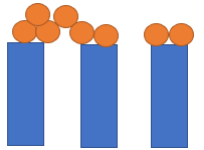


$$\log D_{\text{base}} = \log P + \log \left(\frac{1}{1+10^{pH-pK_a}} \right) \quad (5.3)$$

$$\% \text{ ionized} = \frac{100}{1+10^{pK_a-pH}} \quad (5.4)$$

5.3.4 Fouling models analysis

The membrane fouling mechanisms were evaluated based on four single models (Hermia's model) and five combined models. Briefly, cake filtration represents particles build up on the membrane surface as thickness increases over time; complete blocking means that the membrane pores are completely blocked by particles; intermediate blocking accounts for both cake filtration and complete blocking, where part of the membrane pores are blocked; and standard blocking occurs when particles accumulated within the membrane pores. The simulation between theoretical data and experimental data were performed and fitted in Python based on the fouling model equations (Table 5.3) and sum of squared error (SSE) value (Asif et al., 2020, Huang et al., 2020, Bolton et al., 2006)

Table 5.3 Membrane fouling models and corresponding equations at constant flux

Model	Equations	Fitted parameters	Fouling model illustrations
Single models			
Cake filtration	$\frac{P}{P_0} = 1 + K_c J_0^2 t$	$K_c (s \cdot m^{-2})$	
Intermediate blocking	$\frac{P}{P_0} = \exp(K_i J_0 t)$	$K_i (m^{-1})$	
Complete blocking	$\frac{P}{P_0} = \frac{1}{1 - K_b t}$	$K_b (s^{-1})$	
Standard blocking	$\frac{P}{P_0} = \left(1 - \frac{K_s J_0 t}{2}\right)^{-2}$	$K_s (m^{-1})$	
Combined models			
Cake-complete blocking	$\frac{P}{P_0} = \frac{1}{1 - K_b t} \left(1 - \frac{K_c J_0^2}{K_b} \ln(1 - K_b t)\right)$	$K_c (s \cdot m^{-2}),$ $K_b (s^{-1})$	

Cake-intermediate blocking	$\frac{P}{P_0} = \exp(K_i J_0 t) \left(1 + \frac{K_c J_0^2}{K_i} (\exp(K_i J_0 t) - 1)\right)$	$K_c (s \cdot m^{-2}),$ $K_i (m^{-1})$
Complete-standard blocking	$\frac{P}{P_0} = \frac{1}{(1 - K_b t) \left(1 + \frac{K_s J_0}{2K_b}\right) \ln(1 - K_b t)^2}$	$K_b (s^{-1}),$ $K_s (m^{-1}),$
Intermediate- standard blocking	$\frac{P}{P_0} = \frac{\exp(K_i J_0 t)}{\left(1 - \frac{K_s}{2K_i} \exp(K_i J_0 t) - 1\right)^2}$	$K_i (m^{-1}),$ $K_s (m^{-1}),$
Cake-standard blocking	$\frac{P}{P_0} = \left(1 - \frac{K_s J_0 t}{2}\right)^{-2} + K_c J_0^2 t$	$K_c (s \cdot m^{-2}),$ $K_s (m^{-1})$

5.4 Results and discussion

5.4.1 Comparison of permeate water quality

The composition and corresponding ion concentrations in source-separated urine, control MBR permeate, and hybrid PAC-MBR permeate were shown in Table 5.1. Compared to control MBR, the enhanced growth of ammonia oxidising bacteria (AOB) and nitrite oxidizing bacteria (NOB) on PAC surface was beneficial to urine nitrification and ammonia removal in hybrid PAC-MBR. For instance, on average, 43% of ammonia was converted into nitrate in control MBR, while 48% was biologically oxidised in PAC-MBR. This implied that the higher specific space introduced by PAC is more favourable to proliferation of nitrifying bacteria in a carbon-deficient environment, thereby enhancing the overall nitrification oxidation rate. The unfavourable nitrite accumulation was also mitigated at 2 g/L PAC dosage during the system operation because more sheltered space was created to protect sensitive nitrifying bacterial from losing their activity at the event of sudden change of temperature, pH, toxicity, or excessive nitrogen loading. This observation was consistent with other studies in that the nitrification occurs in higher efficiency with PAC addition to MBR (Ma et al., 2012, Thuy and Visvanathan, 2006, Hu et al., 2014b). As compared to the nutrient composition in permeate, since the PAC surface is negatively charged in aqueous solution with unpaired electron, positively charged compounds and ions were rapidly absorbed by strong electrostatic attraction, resulting in more favourable adsorption of calcium and magnesium (divalent cations) in PAC-MBR than control MBR (Mailler et al., 2015, Zhang et al., 2019).

5.4.2 Comparison of organic matter removal

Figure 5.2 shows chemical oxygen demand (COD) removal performance overtime in MBR with and without PAC dosage. The average COD removal rates in control MBR and PAC-MBR for 73 days operation was $88.6 \pm 2.9\%$ and $96.0 \pm 1.2\%$, respectively. The overall increased in COD removal by 7.4% with the PAC addition indicated that PAC additives were beneficial to effectively remove organic matter and consistently maintain a high quality permeate. It is worth to note that the COD removal rate in MBR slightly fluctuated between 87% and 90%, while that number in PAC-MBR initially increased from 96.5% to 98.5% at day 19, followed by a decrease in COD removal performance, then rebounded to 97% at the end of operation. The first 19-day's observations in PAC-MBR indicated that the organics were mainly removed by PAC adsorption rather than biodegradation. The reduced COD removal performance between day 19 and 31 could be explained by PAC surface saturation and the adsorption equilibrium of organic and inorganic pollutants on PAC surface. The increase in COD removal rate from day 31 implied the emergence and gradual adaptation of heterotrophic microorganisms in carbon-deficient environment, which attached to PAC surfaces as microbial communities and contributed to the elimination of biodegradable organics. As such, COD was likely removed through a combination effect of physical adsorption and biodegradation.

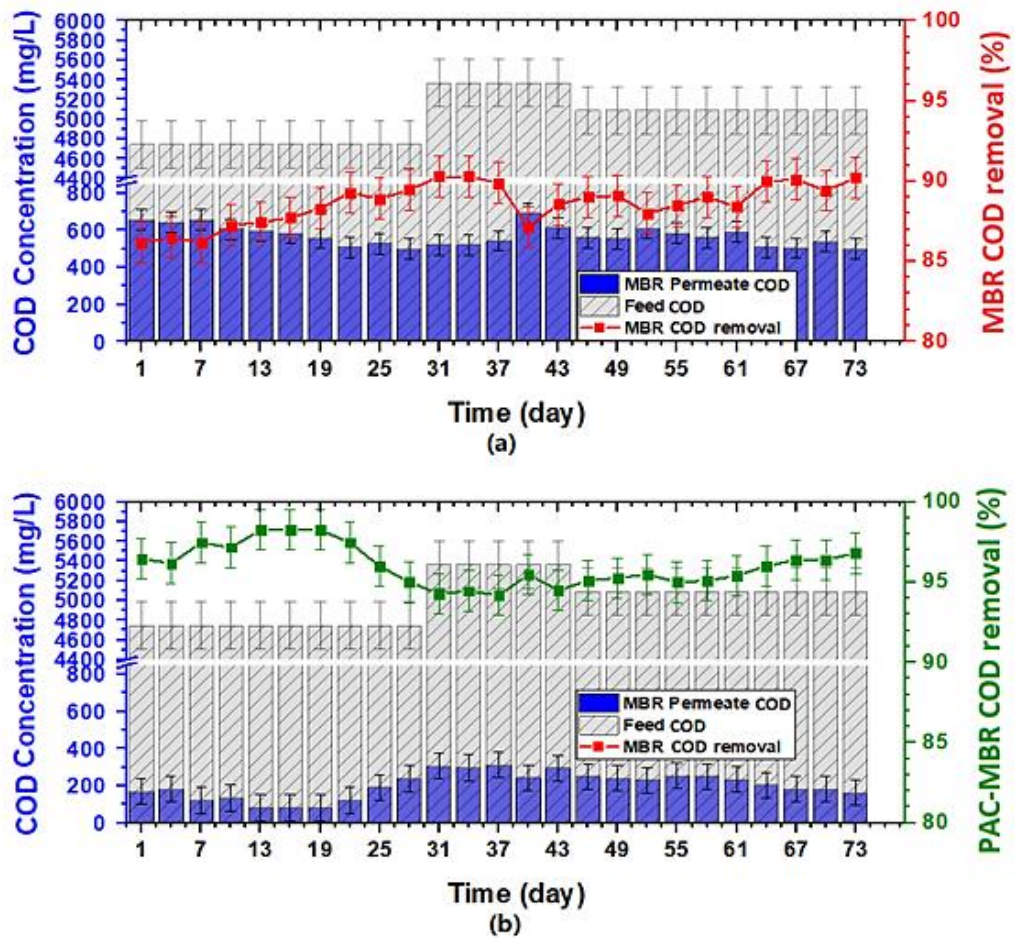


Figure 5.2 Variation of COD removal efficiencies in (a) control MBR, and (b) hybrid PAC-MBR in 73 days

5.4.3 Comparison of biomass growth

Figure 5.3 shows the change of biomass concentrations and their corresponding ratio of mixed liquor volatile suspended solids to mixed liquor suspended solids (MLVSS/MLSS) in each reactor. On day 73, 36.4% more rapid growth of biomass was observed in MBR, suggesting PAC provided large surface area for rapid microbial propagation. It's worth noting that the MLVSS/MLSS ratios in control MBR were consistently higher than that ratio in PAC-MBR. Between day 0 and day 73, the MLVSS/MLSS ratio in control MBR

slightly increased from 0.80 to 0.86, while that ratio maintained around 0.73 in PAC-MBR. This again indicated that PAC dosage had no impact on the stable operation of the membrane bioreactor. Compared to the control MBR, the floc size (D50) increased from $35 \pm 3 \mu\text{m}$ to $41 \pm 5 \mu\text{m}$ after introducing 2 g/L of PAC, corresponding to 17% growth of sludge floc size. Also, MLVSS concentration immediately dropped after PAC dosing in PAC-MBR, implying that the virgin PAC had higher capacity to physically adsorb organics or volatile foulants in activate sludge mixture at the early stage of the operation. Similar observations were reported in previous study regardless the treated wastewater types (Hu et al., 2014b, Alvarino et al., 2017).

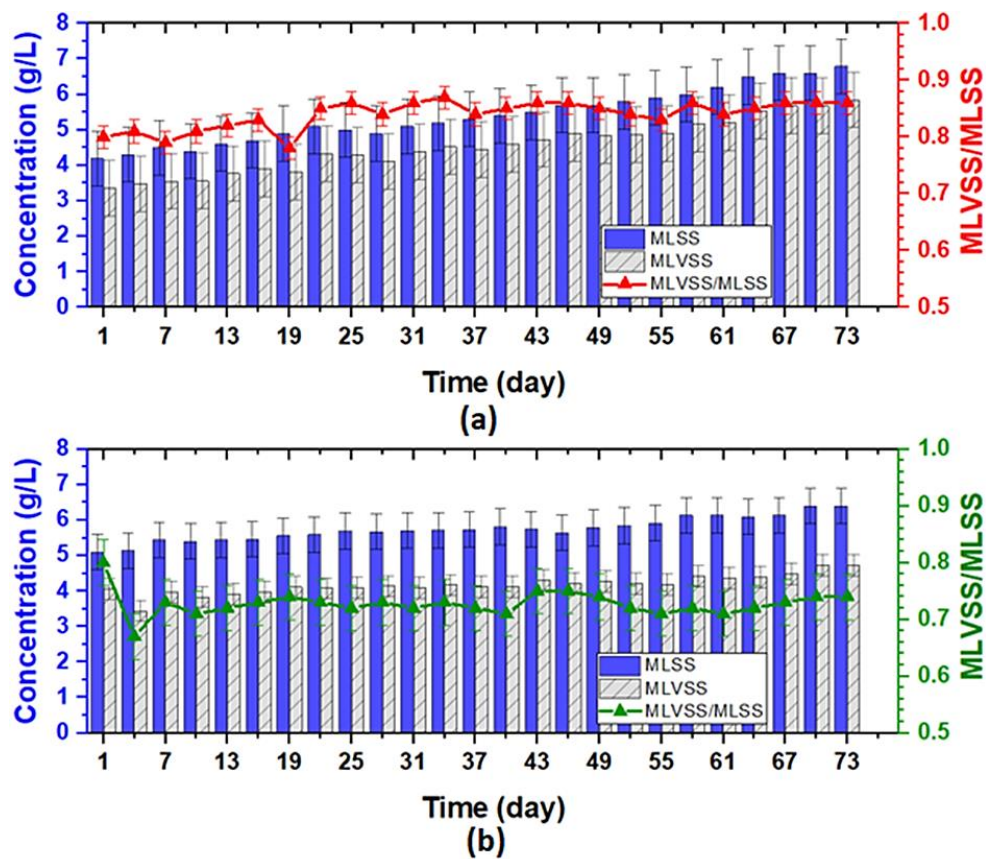


Figure 5.3 Variation of MLSS concentration and MLSS/MLVSS ratio in (a) control MBR and (b) hybrid PAC-MBR in 73 days

5.4.4 Membrane performance

As mentioned earlier, the occurrence of unfavourable membrane fouling is caused by four single fouling mechanisms (cake filtration, standard blocking, complete blocking, intermediate blocking,) and five combined fouling mechanisms (cake-complete blocking, cake-standard blocking, cake-intermediate blocking, complete-standard blocking, and intermediate standard blocking). As such, changes in TMP at any time (P_t) were measured periodically over 5 minutes and fitted to all fouling models to assess the membrane fouling propensities in control MBR and PAC-MBR. Membrane fouling mechanisms will be discussed in this section in accordance with Figure 5.4. and Table 5.4. The results in Table 5.4 shows that the cake-complete model was the best fitting model causing MBR membrane fouling with the minimal SSE value of 0.035. Given the value of fitting constant K_c in combined cake-complete fouling model was greater than K_b , it indicated that the membrane pore blocking led to the build-up of cake layer on the membrane surface at the early stage of filtration. Membrane fouling propensity was further exacerbated as the cake layer developed, the cake blocking became the dominant fouling model among other fouling models in MBR. This observation was consistent with previous studies where the cake-complete fouling mechanism plays a major role in MBR treating synthetic wastewater (Huang et al., 2020, Xiong et al., 2019).

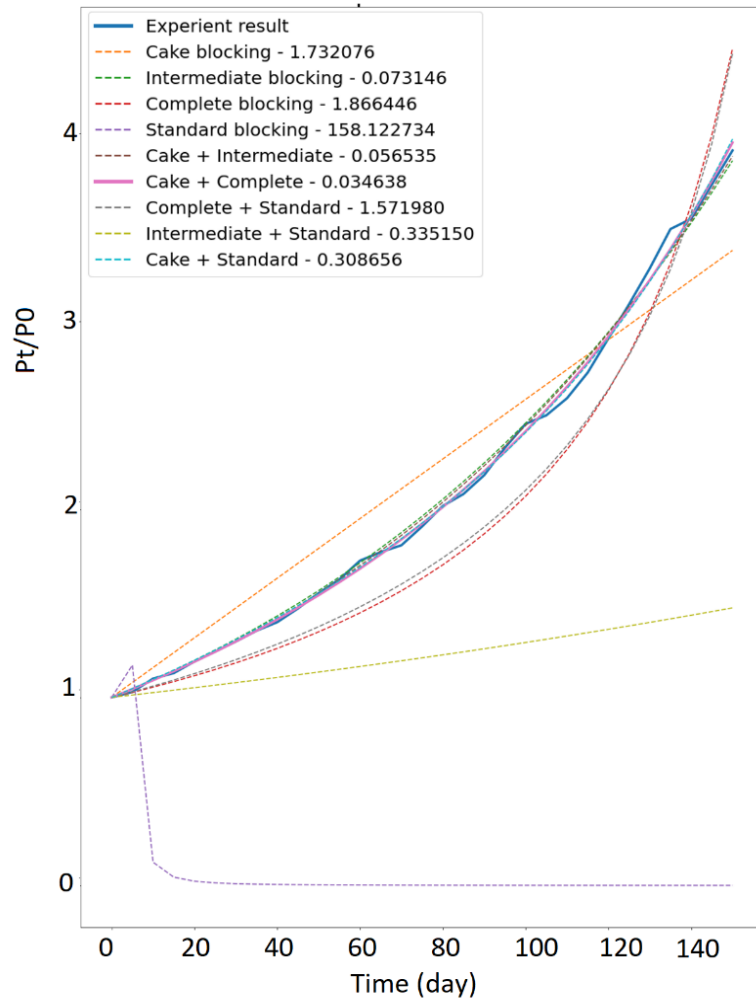
The TMP increase in control MBR was significantly faster than that in PAC-MBR. For instance, the change of TMP (P_t/P_0) in MBR at the end of 150-day operation was 2.26 times higher than that value in PAC-MBR, while there was no obvious TMP sharp jump in PAC-MBR throughout the experiment, suggesting that no severe irreversible fouling

was present after adding PAC (Figure 5.4). This could be explained by adsorption of organic foulants (polysaccharides and proteins) onto PAC which reduced the potential of pollutants deposition on the membrane surface and formation of thick cake layer. Besides, the sediment structure on membrane surface was improved as the cake layer attached on the membrane surface was continuously scrubbed out by PAC. Moreover, the 1.6% of PAC replenishment rate applied in proposed hybrid PAC-MBR also contributed to the decrease in number of organic pollutants in cake layer. Given the fact that continuously adding virgin PAC into the system maximized the interaction between PAC and activated sludge, thus, reducing the membrane fouling propensities from pore blocking or pore constriction caused by particles adsorption in the membrane. This observation was consistent with previous studies that the PAC addition in MBR reduced the activated sludge viscosity, resulting in lower membrane filtration resistance, improved critical flux and permeate quality, and longer system operation at higher flux in all types of wastewater treatment (Yang et al., 2016, Huang et al., 2021, Guo et al., 2008). This again proved the previous observations that 2 g/L of PAC addition reduced the MLVSS concentration in activated sludge mixture without affecting the stability of the system.

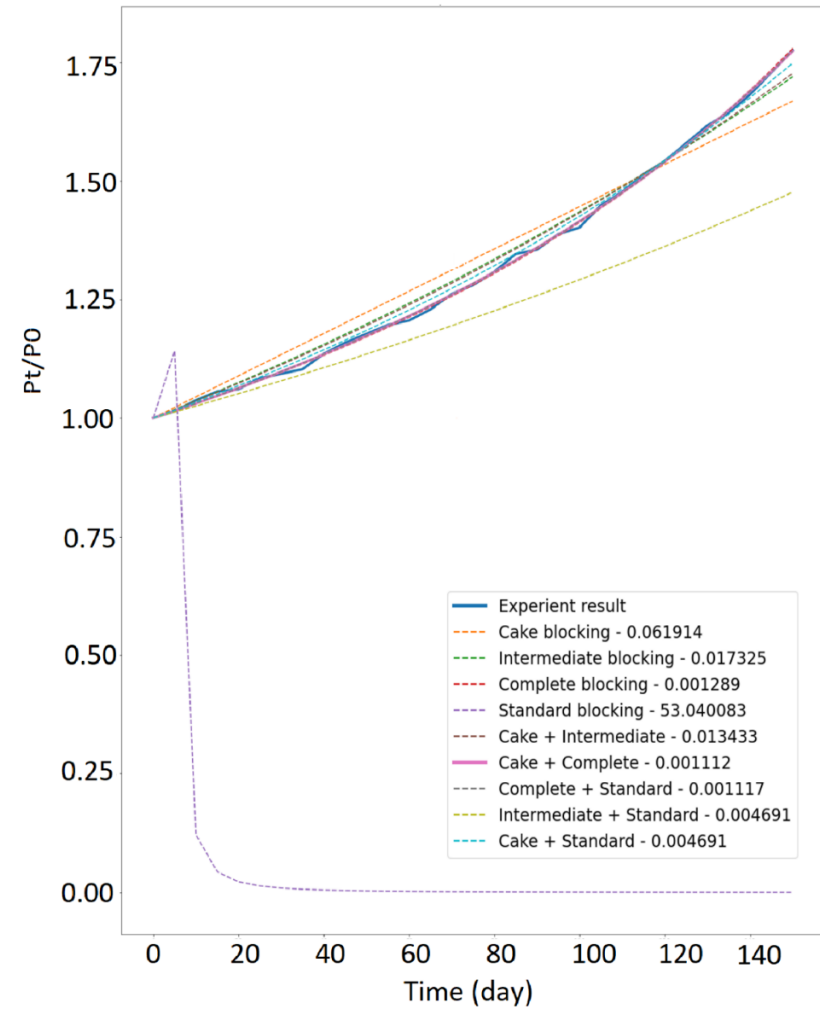
Table 5.4 Theoretical model fitting results and SSE values for the single and combined membrane fouling modules.

	Control MBR			PAC-MBR		
	Model fitting constants (10 ⁻⁵)	SSE	Model fitting constants (10 ⁻⁵)	SSE		
Single models						
	$K_c (s \cdot m^{-2})$			$K_c (s \cdot m^{-2})$		0.062
Cake blocking	670598213.71	1.73	188727671.08			
Intermediate blocking	$K_i (m^{-1})$	1850.53	0.07	$K_i (m^{-1})$	743.58	0.017
Complete blocking	$K_b (s^{-1})$	0.0052	1.87	$K_b (s^{-1})$	0.0029	0.0013
Standard blocking	$K_s (m^{-1})$	158393.96	158.12	$K_s (m^{-1})$	159330.60	53.04
Combined models						
	$K_c (s \cdot m^{-2})$	166265833.37	0.0567	$K_c (s \cdot m^{-2})$	33640386.53	
Cake-intermediate blocking	$K_i (m^{-1})$	1000.00		$K_i (m^{-1})$	560.73	0.013
	$K_c (s \cdot m^{-2})$	237237157.78	0.035	$K_c (s \cdot m^{-2})$	10466522.39	0.0011
Cake-complete blocking	$K_b (s^{-1})$	0.0031		$K_b (s^{-1})$	0.0027	
Complete-standard blocking	$K_b (s^{-1})$	0.0057	1.57	$K_b (s^{-1})$	0.0030	0.0011

	$K_s (m^{-1})$	359.75		$K_s (m^{-1})$	69.20	
	$K_i (m^{-1})$	400.00	0.34	$K_i (m^{-1})$	0.020	0.0047
Intermediate-standard blocking	$K_s (m^{-1})$	1000.00		$K_s (m^{-1})$	668.64	
	$K_c (s \cdot m^{-2})$	1.00	0.31	$K_c (s \cdot m^{-2})$	1.00	0.0047
Cake-standard blocking	$K_s (m^{-1})$	1397.42		$K_s (m^{-1})$	668.66	



(a)



(b)

Figure 5.4 Theoretical and experimental P_t/P_0 versus time profiles and corresponding SSE values for single and combined membrane fouling models in (a) control MBR and (b) hybrid PAC-MBR.

5.4.5 Removal of micropollutants by MBR

The influent concentration of metronidazole ($C_6H_9N_3O_3$), acetaminophen ($C_8H_9NO_2$), naproxen ($C_{14}H_{14}O_3$), ibuprofen ($C_{13}H_{18}O_2$), carbamazepine ($C_{15}H_{12}N_2O$), and estriol ($C_{18}H_{24}O_3$) in stored urine was measured at $1.2 \pm 0.7 \mu\text{g/L}$, $657.6 \pm 217 \mu\text{g/L}$, $15.0 \pm 2.7 \mu\text{g/L}$, $276.0 \pm 39.0 \mu\text{g/L}$, $24.5 \pm 2.7 \mu\text{g/L}$, and $8.0 \pm 1.2 \mu\text{g/L}$, respectively. The removal efficiency of micropollutant compounds and their hydrophobicity and persistent properties in control MBR and hybrid PAC-MBR at pH 6.2 are shown in Table 5.5 and Figure 5.5. As can be seen, there was significant variation in the removal efficiency of targeted pharmaceuticals and hormones in the control MBR, ranging from 41% to 97%. For instance, metronidazole, acetaminophen, naproxen, and carbamazepine with $\log D_{6.2}$ values less than 3.2 were not effectively removed through aerobic biological treatment, with the average removal efficiency of $82 \pm 6\%$, $83 \pm 7\%$, $73 \pm 12\%$, and $41 \pm 14\%$, respectively.

The low removal efficiency of carbamazepine in control MBR was probably due to its moderate hydrophobicity ($\log D_{6.2} = 1.89$) and strong resistance to biodegradation, resulting in its partial adsorption onto activated sludge. The lower removal efficiency of CBZ ($36.2 \pm 6.8\%$) by sorption on activated sludge in MBR operation was also reported by Chtourou et al. (2018) in treating industrial wastewater. In addition, it was suggested in literature that the molecular functional groups in the compound also influenced its removal efficiency (Nguyen et al., 2013a, Hai et al., 2011, Tadkaew et al., 2011). The presence of amide functional group - strong electron withdrawn group (EWG) – in CBZ thereby governed a low removal efficiency. The hydrophobic ibuprofen, on the other hand, containing strong electron donating group (EDG) was efficiently removed ($97 \pm 4\%$) in

control MBR. Furthermore, Tadkaew et al. (2010) reported that the pH in sludge mixture could significantly affect the removal performance of ionizable compounds (naproxen and ibuprofen) due to the change of their physicochemical properties. At 6.2 pH in this work, the ionization percentage in naproxen and ibuprofen was 95.82% and 98.4%, respectively. This indicated their hydrophobicity under proposed acidic condition and thereby they were rapidly adsorbed onto activated sludge. As compared to control MBR, greater than 99% removal efficiency was achieved among all targeted micropollutants in hybrid PAC-MBR. This observation was again consistent with literature that the dominating mechanism for removal of targeted hydrophilic compounds in MBR is biodegradation rather than sorption by activated sludge (Chtourou et al., 2018, Qrenawi and Rabah, 2023).

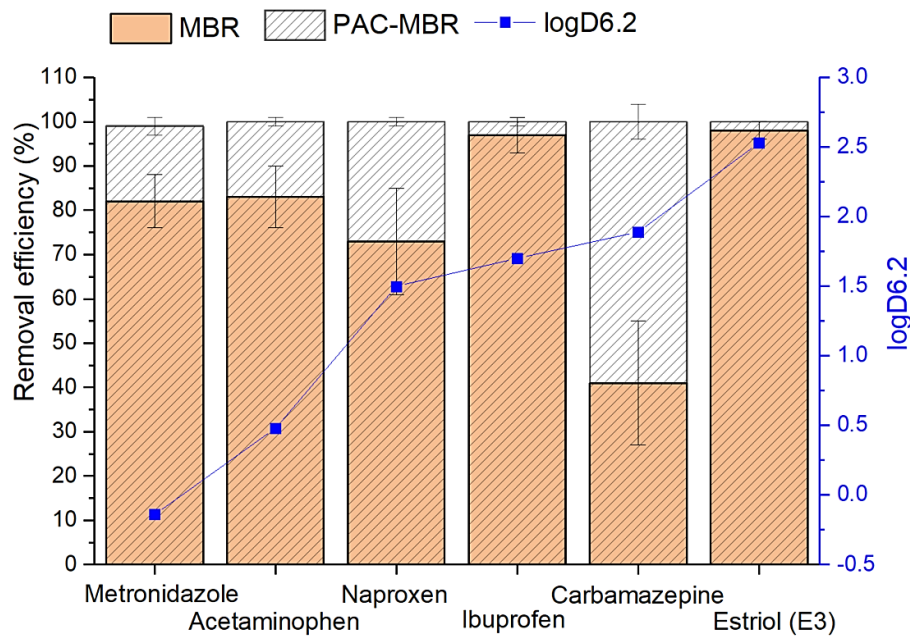
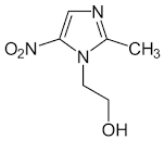
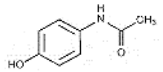
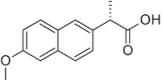
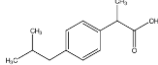
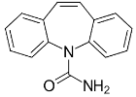
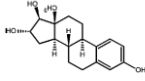


Figure 5.5 Targeted micropollutant removal rate and logD_{6.2} value in control MBR and hybrid PAC-MBR

Table 5.5 Physicochemical properties of targeted micropollutants and their corresponding removal efficiencies

Compound	Pharmaceutical classes	Structure	Molecular weight (g/mol)	pK _a	log P	logD _{6.2}	% Ionization	Concentration in stored urine (µg/L)	Concentration in control MBR (µg/L)	Concentration in PAC-MBR (µg/L)
Metronidazole (C ₆ H ₉ N ₃ O ₃)	Antibiotics		171.15	14.44	-0.14	0.00	1.2 ± 0.7	0.2 ± 0.04	0.01 ± 0.01	
Acetaminophen (C ₈ H ₉ NO ₂)	Pain reliever		151.16	9.86	0.48	0.02	657.6 ± 217	111.8 ± 15.2	0.12 ± 0.15	
Naproxen (C ₁₄ H ₁₄ O ₃)	Analgesics		230.26	4.84	1.58	95.82	15.0 ± 2.7	4.1 ± 0.3	0.004 ± 0.003	

Ibuprofen (C ₁₃ H ₁₈ O ₂)	Analgesics		206.28	4.41	3.5	1.7	98.40	276.0 ± 39.0	8.3 ± 1.6	0.008 ± 0.016
Carbamazepine (C ₁₅ H ₁₂ N ₂ O)	Antiepileptic		236.27	13.9 4	1.8 9	1.89	0.00	24.5 ± 2.7	14.5 ± 0.4	0.015 ± 0.016
Estriol (E3)	Hormones		288.38	10.2 5	2.5 3	2.53	0.01	8.0 ± 1.2	0.2 ± 0.02	0

5.5 Conclusion

In conclusion, the proposed hybrid PAC-MBR system was an ideal approach for complete nutrient recovery at the building level. To add 2 g. L⁻¹ PAC in MBR at 1.6% replenishment rate removed micropollutant via physical adsorption and biodegradation in a single step, without compromising the system operating stability. Furthermore, it improved organic matters removal efficiency from 88.6 ± 2.9 to 96.0 ± 1.2%, maintained consistent high-quality effluent, increased 17% growth of the mean sludge floc size, and promoted more rapid biomass growth. Compared to control MBR, the formation of biological powdered activated carbon (BPAC) over time via growth of stable microbial film on PAC guarantees >99% removal efficiency among targeted micropollutants. The removal efficiency of carbamazepine, for instance, was improved from 41 ± 14 % (control MBR-MF) to 100 ± 4% (hybrid PAC-MBR-MF).

6 Conclusions and recommendations

6.1 Conclusions

This study aimed at exploring the potential application of integrating membrane bioreactor with powdered activated carbon additive for simultaneous nutrient recovery and micropollutant removal from source-separated urine. The major findings from the work are summaries as below.

Chapter 3 studies the application of membrane bioreactor (MBR) for source-separated urine resource recovery. It concluded that the maximum nitrification rate of $447 \pm 50 \text{ mgN} \cdot \text{L}^{-1} \cdot \text{d}^{-1}$ was achieved, where approximately 50% of total ammonia (NH_3 and NH_4) in the feed is converted to nitrate by ammonia oxidation, without the introduction of additional alkalinity. Free ammonia (FA) and free nitrous acid (FNA) concentration are more critical than pH readings to control inhibitory effects and maintain the system stability. The influence of fouling on membrane can be alleviated by intermediate relaxation and/or moderate aeration intensity.

Chapter 4 studies the effect of PAC concentration in lab-scale PAC-MBR combination process on biological and micropollutant removal performance. It concluded that high PAC dosage promotes more rapid biomass growth, lower MLVSS/MLSS ratio and lower sludge viscosity. Compared to low PAC, the nitrification rate was increased by 5.2% to 48% with high PAC dosage and greater than 99% removal efficiency was observed among all targeted micropollutants. Thus, it is recommended to operate proposed PAC-

MBR at a high PAC concentration and a 1.6% replenishment rate to achieve better micropollutant removal efficiency and nitrification rate without compromising the nutrient recovery efficiency.

Chapter 5 compares the performance between a powdered activated carbon - membrane bioreactor (PAC-MBR-MF) and control MBR-MF for source-separated urine resource utilization in terms of treated permeate quality, emerging contaminants removal, membrane fouling control, membrane flux improvement, and biomass property. It concluded that the proposed hybrid PAC-MBR system was an ideal approach for complete nutrient recovery at the building level. Compared to control MBR, the formation of biological powdered activated carbon (BPAC) over time via growth of stable microbial film on PAC guarantees >99% removal efficiency among targeted micropollutants. Furthermore, it improved organic matters removal efficiency from 88.6 ± 2.9 to $96.0 \pm 1.2\%$, maintained consistent high-quality effluent, increased 17% growth of the mean sludge floc size, and promoted more rapid biomass growth.

6.2 Limitations and recommendations

The limitations and recommendations include,

- The filtration and biological performances were studied in laboratory scale. Although the proposed hybrid PAC-MBR-MF system were fed with full strength raw urine, the fouling behaviours and biodiversity of biomass community may not closely reflect the real case scenario.

- Although the PAC dosage in MBR was studied individually at low and high concentrations in terms of micropollutant removal, fouling mitigation, water quality, biomass growth and nitrification efficiency, the optimization of PAC concentration and its replenishment rate regarding long term operating cost is recommended in the next study.
- The use of PAC additive in MBR technology for effective removal of micropollutants from source-separated urine is quite recent, the acknowledgement of optimized system configurations and operational parameters, long term system stability, water treatment performance, and economic feasibility are unknown.
- The aged PAC in proposed hybrid PAC-MBR-MF system cannot be recycled or reused except landfilled, the proper waste treatment method with cost consideration for PAC amended sludge disposal is thereby needs to be considered.
- The storage cost and logistics cost in distortion urine-based fertilizer accounts to a large portion in expenses when consider the product commercialization. Therefore, it is recommended to combine proposed PAC-MBR-MF system with other technology, i.e., membrane capacitive deionization (MCDI) or membrane distillation (MD) technology for complete nutrient recovery and concentration from the source separated urine, concentrated urine-based fertilizer production, and clean water regeneration.

Bibliography

- ALKHUDHIRI, A., DARWISH, N. & HILAL, N. 2012. Membrane distillation: A comprehensive review. *Desalination*, 287, 2-18.
- ALMARZOOQI, F. A., AL GHAFERI, A. A., SAADAT, I. & HILAL, N. 2014. Application of capacitive deionisation in water desalination: a review. *Desalination*, 342, 3-15.
- ALMUNTASHIRI, A., HOSSEINZADEH, A., VOLPIN, F., ALI, S. M., DORJI, U., SHON, H. & PHUNTSHO, S. 2021. Removal of pharmaceuticals from nitrified urine. *Chemosphere*, 280, 130870.
- ALVARINO, T., TORREGROSA, N., OMIL, F., LEMA, J. & SUAREZ, S. 2017. Assessing the feasibility of two hybrid MBR systems using PAC for removing macro and micropollutants. *Journal of environmental management*, 203, 831-837.
- ANAND, C. K. & APUL, D. S. 2014. Composting toilets as a sustainable alternative to urban sanitation – A review. *Waste Management*, 34, 329-343.
- ANTHONISEN, A. C., LOEHR, R. C., PRAKASAM, T. & SRINATH, E. 1976. Inhibition of nitrification by ammonia and nitrous acid. *Journal (Water Pollution Control Federation)*, 835-852.
- ASIF, M. B., REN, B., LI, C., MAQBOOL, T., ZHANG, X. & ZHANG, Z. 2020. Powdered activated carbon – Membrane bioreactor (PAC-MBR): Impacts of high PAC concentration on micropollutant removal and microbial communities. *Science of The Total Environment*, 745, 141090.
- BAIRD, R. B. 2017. *Standard methods for the examination of water and wastewater, 23rd*, Water Environment Federation, American Public Health Association, American

- BASILE, A., CASSANO, A. & RASTOGI, N. K. 2015. *Advances in membrane technologies for water treatment: materials, processes and applications*, Elsevier.
- BHATTACHARYYAB, T. K. P. 2010. Human urine as a source of alternative natural fertilizer in agriculture:
A flight of fancy or an achievable reality. *Resources, Conservation and Recycling*, 55, 400-408.
- BOEHLER, M., JOSS, A., BUETZER, S., HOLZAPFEL, M., MOOSE, H. & SIEGRIST, H. 2007. Treatment of toilet wastewater for Re-Use in a MBR. *GEWASSERSCHUTZ WASSER ABWASSER*, 206, 12.
- BOLTON, G., LACASSE, D. & KURIYEL, R. 2006. Combined models of membrane fouling: Development and application to microfiltration and ultrafiltration of biological fluids. *Journal of Membrane Science*, 277, 75-84.
- BONNÉLYE, V., GUEY, L. & DEL CASTILLO, J. 2008. UF/MF as RO pre-treatment: the real benefit. *Desalination*, 222, 59-65.
- CALUWÉ, M., DOBBELEERS, T., D'AES, J., MIELE, S., AKKERMANS, V., DAENS, D., GEUENS, L., KIEKENS, F., BLUST, R. & DRIES, J. 2017. Formation of aerobic granular sludge during the treatment of petrochemical wastewater. *Bioresource Technology*, 238, 559-567.
- CHO, K., SHIN, S. G., LEE, J., KOO, T., KIM, W. & HWANG, S. 2016. Nitrification resilience and community dynamics of ammonia-oxidizing bacteria with respect to ammonia loading shock in a nitrification reactor treating steel wastewater. *Journal of Bioscience and Bioengineering*, 122, 196-202.
- CHTOUROU, M., MALLEK, M., DALMAU, M., MAMO, J., SANTOS-CLOTAS, E., SALAH, A. B., WALHA, K., SALVADÓ, V. & MONCLÚS, H. 2018. Triclosan,

- carbamazepine and caffeine removal by activated sludge system focusing on membrane bioreactor. *Process Safety and Environmental Protection*, 118, 1-9.
- COX, S. J., HANNA, J., ANTONY, A., NEGARESH, E., RICHARDSON, D. & LESLIE, G. Nanofiltration as pretreatment to reverse osmosis for paper and pulp mill effluent. IWA Regional Conference Membrane Technologies in Water and Waste Water Treatment, 2008. SIBICO International Ltd.
- FAO 2017. World fertilizer trends and outlook to 2020: Summary report. *Food and Agriculture organization of the United Nations (FAO), Rome*.
- FARMER, J. C., FIX, D. V., MACK, G. V., PEKALA, R. W. & POCO, J. F. The use of capacitive deionization with carbon aerogel electrodes to remove inorganic contaminants from water. Low level waste conference, Orlando, 1995.
- FIELD, R. W., WU, D., HOWELL, J. A. & GUPTA, B. B. 1995. Critical flux concept for microfiltration fouling. *Journal of Membrane Science*, 100, 259-272.
- FRY, D., MIDEKSA, D., AMBELU, A., FEYISA, Y., ABAIRE, B., CUNLIFFE, K. & FREEMAN, M. C. 2015. Adoption and sustained use of the arborloo in rural Ethiopia: a cross-sectional study. *Journal of Water, Sanitation and Hygiene for Development*, 5, 412-425.
- FUMASOLI, A., BUERGMANN, H., WEISSBRODT, D. G., WELLS, G. F., BECK, K., MOHN, J., MORGENROTH, E. & KAI, M. U. 2017. Growth of Nitrosococcus-Related Ammonia Oxidizing Bacteria Coincides with Extremely Low pH Values in Wastewater with High Ammonia Content. *Environmental Science & Technology*, 51, 6857-6866.
- FUMASOLI, A., ETTER, B., STERKELE, B., MORGENROTH, E. & UDERT, K. M. 2015. Operating a pilot-scale nitrification/distillation plant for complete nutrient recovery from urine. *Water Science and Technology*, 73, 215-222.

- GAVRILESCU, M., DEMNEROVÁ, K., AAMAND, J., AGATHOS, S. & FAVA, F. 2015. Emerging pollutants in the environment: present and future challenges in biomonitoring, ecological risks and bioremediation. *New Biotechnology*, 32, 147-156.
- GRANDCLÉMENT, C., SEYSSIECQ, I., PIRAM, A., WONG-WAH-CHUNG, P., VANOT, G., TILIACOS, N., ROCHE, N. & DOUMENQ, P. 2017. From the conventional biological wastewater treatment to hybrid processes, the evaluation of organic micropollutant removal: A review. *Water Research*, 111, 297-317.
- GRUNDITZ, C. & DALHAMMAR, G. 2001. Development of nitrification inhibition assays using pure cultures of Nitrosomonas and Nitrobacter. *Water research*, 35, 433-440.
- GUO, W., VIGNESWARAN, S., NGO, H. & XING, W. 2008. Comparison of membrane bioreactor systems in wastewater treatment. *Desalination*, 231, 61-70.
- GUTIÉRREZ, M., GRILLINI, V., PAVLOVIĆ, D. M. & VERLICCHI, P. 2021. Activated carbon coupled with advanced biological wastewater treatment: A review of the enhancement in micropollutant removal. *Science of The Total Environment*, 790, 148050.
- HAI, F. I., LI, X., PRICE, W. E. & NGHIEM, L. D. 2011. Removal of carbamazepine and sulfamethoxazole by MBR under anoxic and aerobic conditions. *Bioresource technology*, 102, 10386-10390.
- HANAK, D. P., KOLIOS, A. J., ONABANJO, T., WAGLAND, S. T., PATCHIGOLLA, K., FIDALGO, B., MANOVIC, V., MCADAM, E., PARKER, A. & WILLIAMS, L. 2016. Conceptual energy and water recovery system for self-sustained nano membrane toilet. *Energy conversion and management*, 126, 352-361.

- HU, J., SHANG, R., DENG, H., HEIJMAN, S. G. & RIETVELD, L. C. 2014a. Effect of PAC dosage in a pilot-scale PAC-MBR treating micro-polluted surface water. *Bioresour Technol*, 154, 290-6.
- HU, J., SHANG, R., DENG, H., HEIJMAN, S. G. J. & RIETVELD, L. C. 2014b. Effect of PAC dosage in a pilot-scale PAC-MBR treating micro-polluted surface water. *Bioresource Technology*, 154, 290-296.
- HUANG, C., LIU, H., MENG, S. & LIANG, D. 2020. Effect of PAC on the Behavior of Dynamic Membrane Bioreactor Filtration Layer Based on the Analysis of Mixed Liquid Properties and Model Fitting. *Membranes*, 10, 420.
- HUANG, W., ZHU, Y., WANG, L., LV, W., DONG, B. & ZHOU, W. 2021. Reversible and irreversible membrane fouling in hollow-fiber UF membranes filtering surface water: effects of ozone/powdered activated carbon treatment. *RSC Advances*, 11, 10323-10335.
- HUBE, S., ESKAFI, M., HRAFNKELSDÓTTIR, K. F., BJARNADÓTTIR, B., BJARNADÓTTIR, M. Á., AXELSDÓTTIR, S. & WU, B. 2020. Direct membrane filtration for wastewater treatment and resource recovery: A review. *Science of The Total Environment*, 710, 136375.
- IM, J., JUNG, J., BAE, H., KIM, D. & GIL, K. 2014. Correlation between nitrite accumulation and the concentration of AOB in a nitrification reactor. *Environmental Earth Sciences*, 72, 289-297.
- IORHEMEN, O. T., HAMZA, R. A. & TAY, J. H. 2016. Membrane Bioreactor (MBR) Technology for Wastewater Treatment and Reclamation: Membrane Fouling. *Membranes*, 6, 33.
- JANG, Y., KIM, H.-S., HAM, S.-Y., PARK, J.-H. & PARK, H.-D. 2021. Investigation of critical sludge characteristics for membrane fouling in a submerged membrane

- bioreactor: Role of soluble microbial products and extracted extracellular polymeric substances. *Chemosphere*, 271, 129879.
- JEON, S. I., PARK, H. R., YEO, J. G., YANG, S., CHO, C. H., HAN, M. H. & KIM, D. K. 2013. Desalination via a new membrane capacitive deionization process utilizing flow-electrodes. *Energy and Environmental Science*, 6, 1471-1475.
- JIANG, J., PHUNTSHO, S., PATHAK, N., WANG, Q., CHO, J. & SHON, H. K. 2021. Critical flux on a submerged membrane bioreactor for nitrification of source separated urine. *Process Safety and Environmental Protection*, 153, 518-526.
- KANG, X., SHUAI, L., XIAOMAO, W., CHUNSHENG, C. & XIA, H. 2018. Current state and challenges of full-scale membrane bioreactor applications: A critical review. *Bioresource Technology*, S0960852418313142-.
- KAYA, C., SERT, G., KABAY, N., ARDA, M., YÜKSEL, M. & EGEMEN, Ö. 2015. Pre-treatment with nanofiltration (NF) in seawater desalination—Preliminary integrated membrane tests in Urla, Turkey. *Desalination*, 369, 10-17.
- KHANZADA, N. K., FARID, M. U., KHARRAZ, J. A., CHOI, J., TANG, C. Y., NGHIEM, L. D., JANG, A. & AN, A. K. 2020. Removal of organic micropollutants using advanced membrane-based water and wastewater treatment: A review. *Journal of Membrane Science*, 598, 117672.
- KIM, Y.-J. & CHOI, J.-H. 2010a. Improvement of desalination efficiency in capacitive deionization using a carbon electrode coated with an ion-exchange polymer. *Water research*, 44, 990-996.
- KIM, Y. J. & CHOI, J. H. 2010b. Enhanced desalination efficiency in capacitive deionization with an ion-selective membrane. *Separation and Purification Technology*, 71, 70-75.

- KOOPS, H.-P., PURKHOLD, U., POMMERENING-RÖSER, A., TIMMERMANN, G. & WAGNER, M. 2006. The lithoautotrophic ammonia-oxidizing bacteria. *The Prokaryotes: Volume 5: Proteobacteria: Alpha and Beta Subclasses*, 778-811.
- KÖPPING, I., MCADELL, C. S., BOROWSKA, E., BÖHLER, M. A. & UDERT, K. M. 2020. Removal of pharmaceuticals from nitrified urine by adsorption on granular activated carbon. *Water research X*, 9, 100057.
- KUMARI, A., MAURYA, N. S. & TIWARI, B. 2020. Hospital wastewater treatment scenario around the globe. *Current developments in Biotechnology and Bioengineering*. Elsevier.
- KURISU, F., KURISU, F., SAKAMOTO, Y. & YAGI, O. 2007. Effects of ammonium and nitrite on communities and populations of ammonia-oxidizing bacteria in laboratory-scale continuous-flow reactors. *FEMS Microbiology Ecology*, 60, 501-512.
- KVARNSTRÖM, E., EMILSSON, K., STINTZING, A. R., JOHANSSON, M., JÖNSSON, H., AF PETERSENS, E., SCHÖNNING, C., CHRISTENSEN, J., HELLSTRÖM, D. & QVARNSTRÖM, L. 2006. *Urine diversion: one step towards sustainable sanitation*, EcoSanRes Programme.
- LAN, Y., GROENEN-SERRANO, K., COETSIER, C. & CAUSSERAND, C. 2017. Fouling control using critical, threshold and limiting fluxes concepts for cross-flow NF of a complex matrix: Membrane BioReactor effluent. *Journal of Membrane Science*, 524, 288-298.
- LARSEN, T. A., HOFFMANN, S., LÜTHI, C., TRUFFER, B. & MAURER, M. 2016. Emerging solutions to the water challenges of an urbanizing world. *Science*, 352, 928-933.

- LE CLECH, P., JEFFERSON, B., CHANG, I. S. & JUDD, S. J. 2003. Critical flux determination by the flux-step method in a submerged membrane bioreactor. *Journal of Membrane Science*, 227, 81-93.
- LE, V.-G., VU, C.-T., SHIH, Y.-J., BUI, X.-T., LIAO, C.-H. & HUANG, Y.-H. 2020. Phosphorus and potassium recovery from human urine using a fluidized bed homogeneous crystallization (FBHC) process. *Chemical Engineering Journal*, 384, 123282.
- LEE, J.-B., PARK, K.-K., EUM, H.-M. & LEE, C.-W. 2006. Desalination of a thermal power plant wastewater by membrane capacitive deionization. *Desalination*, 196, 125-134.
- LI, H. & ZOU, L. 2011. Ion-exchange membrane capacitive deionization: a new strategy for brackish water desalination. *Desalination*, 275, 62-66.
- LIU, Y. Q., LAN, G. H. & ZENG, P. 2015. Resistance and resilience of nitrifying bacteria in aerobic granules to pH shock. *Letters in applied microbiology*, 61, 91-97.
- LUO, Y., GUO, W., NGO, H. H., NGHIEM, L. D., HAI, F. I., ZHANG, J., LIANG, S. & WANG, X. C. 2014. A review on the occurrence of micropollutants in the aquatic environment and their fate and removal during wastewater treatment. *Science of The Total Environment*, 473-474, 619-641.
- MA, C., YU, S., SHI, W., TIAN, W., HEIJMAN, S. G. J. & RIETVELD, L. C. 2012. High concentration powdered activated carbon-membrane bioreactor (PAC-MBR) for slightly polluted surface water treatment at low temperature. *Bioresource Technology*, 113, 136-142.
- MAILLER, R., GASPERI, J., COQUET, Y., DESHAYES, S., ZEDEK, S., CRENOLIVÉ, C., CARTISER, N., EUDES, V., BRESSY, A. & CAUPOS, E. 2015. Study of a large scale powdered activated carbon pilot: Removals of a wide range

- of emerging and priority micropollutants from wastewater treatment plant effluents. *Water Research*, 72, 315-330.
- MAURER, M., PRONK, W. & LARSEN, T. A. 2006. Treatment processes for source-separated urine. *Water Research*, 40, 3151-3166.
- MAURER, M., SCHWEGLER, P. & LARSEN, T. A. 2003. Nutrients in urine: Energetic aspects of removal and recovery. *Water Science and Technology*.
- MEINZINGER, F., OLDENBURG, M., LISANWORK, A. A., GUTEMA, K., OTTERPOHL, R., KRUSCHE, P. & JEBENS, O. Implementation of urine-diverting dry toilets in multi-storey apartment buildings in Ethiopia. 3rd International Dry Toilet Conference, 2009a. 2009-15.08.
- MEINZINGER, F., OLDENBURG, M. & OTTERPOHL, R. 2009b. No waste, but a resource: Alternative approaches to urban sanitation in Ethiopia. *Desalination*, 248, 322-329.
- MITCHELL, C., FAM, D. & ABEYSURIYA, K. 2013. Transitioning to sustainable sanitation: a transdisciplinary pilot project of urine diversion.
- NGUYEN, L. N., HAI, F. I., KANG, J., PRICE, W. E. & NGHIEM, L. D. 2013a. Coupling granular activated carbon adsorption with membrane bioreactor treatment for trace organic contaminant removal: Breakthrough behaviour of persistent and hydrophilic compounds. *Journal of environmental management*, 119, 173-181.
- NGUYEN, L. N., HAI, F. I., KANG, J., PRICE, W. E. & NGHIEM, L. D. 2013b. Coupling granular activated carbon adsorption with membrane bioreactor treatment for trace organic contaminant removal: Breakthrough behaviour of persistent and hydrophilic compounds. *Journal of Environmental Management*, 119, 173-181.

- O'NEILL, M. 2015. Ecological Sanitation—A Logical Choice? *The Development of the Sanitation Institution in a World Society. Academic Dissertation in Natural Sciences, Tampere University of Technology. Juvenes Print, Tampere.*
- OGNIER, S., WISNIEWSKI, C. & GRASMICK, A. 2002. Characterisation and modelling of fouling in membrane bioreactors. *Desalination*, 146, 141-147.
- OGNIER, S., WISNIEWSKI, C. & GRASMICK, A. 2004. Membrane bioreactor fouling in sub-critical filtration conditions: a local critical flux concept. *Journal of Membrane Science*, 229, 171-177.
- ONSEKIZOGLU, P. 2012. Membrane distillation: principle, advances, limitations and future prospects in food industry. *Distillation-advances from modeling to applications*, 282.
- PANESAR, A., WERNER, C., MÜNCH, E. V., MAKSIMOVIC, C., SCHEINBERG, A., SCHERTENLEIB, R., BRACKEN, P. & GILBRICH, W. 2006. Capacity building for ecological sanitation-Concepts for ecologically sustainable sanitation in formal and continuing education. Published in.
- PARK, J., YAMASHITA, N. & TANAKA, H. 2018a. Membrane fouling control and enhanced removal of pharmaceuticals and personal care products by coagulation-MBR. *Chemosphere*, 197, 467-476.
- PARK, S., YEON, K.-M., MOON, S. & KIM, J.-O. 2018b. Enhancement of operating flux in a membrane bio-reactor coupled with a mechanical sieve unit. *Chemosphere*, 191, 573-579.
- PEKALA, R., FARMER, J., ALVISO, C., TRAN, T., MAYER, S., MILLER, J. & DUNN, B. 1998. Carbon aerogels for electrochemical applications. *Journal of non-crystalline solids*, 225, 74-80.

- PREISNER, M., NEVEROVA-DZIOPAK, E. & KOWALEWSKI, Z. 2021. Mitigation of eutrophication caused by wastewater discharge: A simulation-based approach. *Ambio*, 50, 413-424.
- QRENAWI, L. I. & RABAH, F. K. 2023. Membrane Bioreactor (MBR) as a Reliable Technology for Wastewater Treatment. *Journal of Membrane Science and Research*, 9.
- RANDALL, D. & NAIDOO, V. 2018a. Urine: the liquid gold of wastewater. *Journal of Environmental Chemical Engineering*.
- RANDALL, D. G., KRÄHENBÜHL, M., KÖPPING, I., LARSEN, T. A. & UDERT, K. M. 2016. A novel approach for stabilizing fresh urine by calcium hydroxide addition. *Water Research*, 95, 361-369.
- RANDALL, D. G. & NAIDOO, V. 2018b. Urine: the liquid gold of wastewater. *Journal of Environmental Chemical Engineering*.
- SAMAL, K., MAHAPATRA, S. & HIBZUR ALI, M. 2022. Pharmaceutical wastewater as Emerging Contaminants (EC): Treatment technologies, impact on environment and human health. *Energy Nexus*, 6, 100076.
- SIMHA, P. & GANESAPILLAI, M. 2017. Ecological Sanitation and nutrient recovery from human urine: How far have we come? A review. *Sustainable Environment Research*, 27, 107-116.
- SIMPSON-HEBERT, M. 2007. Low-cost Arborloo offers Ethiopians health and agriculture benefits. *Waterlines*, 26, 12-14.
- STOQUART, C., SERVAIS, P., BÉRUBÉ, P. R. & BARBEAU, B. 2012. Hybrid Membrane Processes using activated carbon treatment for drinking water: A review. *Journal of Membrane Science*, 411-412, 1-12.

- SUSS, M. E., BAUMANN, T. F., BOURCIER, W. L., SPADACCINI, C. M., ROSE, K. A., SANTIAGO, J. G. & STADERMANN, M. 2012. Capacitive desalination with flow-through electrodes. *Energy and Environmental Science*, 5, 9511-9519.
- TADKAEW, N., HAI, F. I., MCDONALD, J. A., KHAN, S. J. & NGHIEM, L. D. 2011. Removal of trace organics by MBR treatment: The role of molecular properties. *Water Research*, 45, 2439-2451.
- TADKAEW, N., SIVAKUMAR, M., KHAN, S. J., MCDONALD, J. A. & NGHIEM, L. D. 2010. Effect of mixed liquor pH on the removal of trace organic contaminants in a membrane bioreactor. *Bioresource technology*, 101, 1494-1500.
- THUY, Q. T. T. & VISVANATHAN, C. 2006. Removal of inhibitory phenolic compounds by biological activated carbon coupled membrane bioreactor. *Water science and technology*, 53, 89-97.
- TIAN, X., GAO, Z., FENG, H., ZHANG, Z., LI, J. & WANG, A. 2019. Efficient nutrient recovery/removal from real source-separated urine by coupling vacuum thermal stripping with activated sludge processes. *Journal of Cleaner Production*, 220, 965-973.
- TILLEY, E., ULRICH, L., LÜTHI, C., REYMOND, P. & ZURBRÜGG, C. 2014. Compendium of sanitation systems and technologies.
- TIRANUNTAKUL, M., SCHNEIDER, P. A. & JEGATHEESAN, V. 2011. Assessments of critical flux in a pilot-scale membrane bioreactor. *Bioresource Technology*, 102, 5370-5374.
- TUFAIL, A., PRICE, W. E., MOHSENI, M., PRAMANIK, B. K. & HAI, F. I. 2021. A critical review of advanced oxidation processes for emerging trace organic contaminant degradation: Mechanisms, factors, degradation products, and effluent toxicity. *Journal of Water Process Engineering*, 40, 101778.

- UDERT, K. M., BUCKLEY, C. A., WÄCHTER, M., MCARDELL, C. S., KOHN, T., STRANDE, L., ZÖLLIG, H., FUMASOLI, A., OBERSON, A. & ETTER, B. 2015. Technologies for the treatment of source-separated urine in the eThekweni Municipality. *Water Sa*, 41, 212-221.
- UDERT, K. M., LARSEN, T. A., BIEBOW, M. & GUJER, W. 2003a. Urea hydrolysis and precipitation dynamics in a urine-collecting system. *Water Research*, 37, 2571-2582.
- UDERT, K. M., LARSEN, T. A. & GUJER, W. 2003b. Biologically induced precipitation in urine-collecting systems. *Water Science and Technology: Water Supply*, 3, 71-78.
- UDERT, K. M. & WÄCHTER, M. 2012. Complete nutrient recovery from source-separated urine by nitrification and distillation. *Water Research*, 46, 453-464.
- VAN DER MAREL, P., ZWIJNENBURG, A., KEMPERMAN, A., WESSLING, M., TEMMINK, H. & VAN DER MEER, W. 2009. An improved flux-step method to determine the critical flux and the critical flux for irreversibility in a membrane bioreactor. *Journal of Membrane Science*, 332, 24-29.
- VOLPIN, F., JIANG, J., EL SALIBY, I., PREIRE, M., LIM, S., HASAN JOHIR, M. A., CHO, J., HAN, D. S., PHUNTSHO, S. & SHON, H. K. 2020. Sanitation and dewatering of human urine via membrane bioreactor and membrane distillation and its reuse for fertigation. *Journal of Cleaner Production*, 270, 122390.
- WANG, S., MA, X., LIU, Y., YI, X., DU, G. & LI, J. 2020. Fate of antibiotics, antibiotic-resistant bacteria, and cell-free antibiotic-resistant genes in full-scale membrane bioreactor wastewater treatment plants. *Bioresource Technology*, 302, 122825.

- WILSENACH, J. A. & LOOSDRECHT, M. C. V. 2006. Integration of Processes to Treat Wastewater and Source-Separated Urine. *Journal of Environmental Engineering*, 132, 331-341.
- WILSENACH, J. A. & VAN LOOSDRECHT, M. C. M. 2004. Effects of Separate Urine Collection on Advanced Nutrient Removal Processes. *Environmental Science & Technology*, 38, 1208-1215.
- WINKER, M. & SAADOUN, A. 2011. Urine and brownwater separation at GTZ main office building Eschborn, Germany; Case study of sustainable sanitation projects. Retrieved Jan, 17, 2012.
- WREMO 2013. Report on a trial of emergency compost toilets. Hamilton & Gauden-Ing, Business & Development Wellington Region Emergency Management Office, New Zealand.
- WU, X., ZHOU, C., LI, K., ZHANG, W. & TAO, Y. 2018. Probing the fouling process and mechanisms of submerged ceramic membrane ultrafiltration during algal harvesting under sub- and super-critical fluxes. *Separation and Purification Technology*, 195, 199-207.
- WU, Z., WANG, Z., HUANG, S., MAI, S., YANG, C., WANG, X. & ZHOU, Z. 2008. Effects of various factors on critical flux in submerged membrane bioreactors for municipal wastewater treatment. *Separation and Purification Technology*, 62, 56-63.
- XIONG, J., ZUO, X., ZHANG, S., LIAO, W. & CHEN, Z. 2019. Model-based evaluation of fouling mechanisms in powdered activated carbon/membrane bioreactor system. *Water Science and Technology*, 79, 1844-1852.

- YANG, J., SONG, Y. & ZHANG, J. The combined process of PAC-MBR on wastewater treatment. 6th International Conference on Mechatronics, Materials, Biotechnology and Environment (ICMMBE 2016), 2016. Atlantis Press, 68-75.
- YING, Z. & PING, G. 2006. Effect of powdered activated carbon dosage on retarding membrane fouling in MBR. *Separation and Purification Technology*, 52, 154-160.
- ZAKARIA, F., ĆURKO, J., MURATBEGOVIC, A., GARCIA, H. A., HOOIJMANS, C. M. & BRDJANOVIC, D. 2018. Evaluation of a smart toilet in an emergency camp. *International Journal of Disaster Risk Reduction*, 27, 512-523.
- ZHANG, F., YANG, H., WANG, J., LIU, Z. & GUAN, Q. 2018. Effect of free ammonia inhibition on NOB activity in high nitrifying performance of sludge. *RSC advances*, 8, 31987-31995.
- ZHANG, Q., SUN, F.-Y., DONG, W.-Y., ZHANG, G.-M. & HAN, R.-B. 2015. Micro-polluted surface water treatment and trace-organics removal pathway in a PAC-MBR system. *Process Biochemistry*, 50, 1422-1428.
- ZHANG, S., XIONG, J., ZUO, X., LIAO, W., MA, C., HE, J. & CHEN, Z. 2019. Characteristics of the sludge filterability and microbial composition in PAC hybrid MBR: Effect of PAC replenishment ratio. *Biochemical Engineering Journal*, 145, 10-17.
- ZHANG, S., ZUO, X., XIONG, J., MA, C. & BO, H. 2017. Effect of powdered activated carbon dosage on sludge properties and membrane bioreactor performance in a hybrid MBR-PAC system. *Environmental Technology*, 40, 1-29.
- ZHANG, Y. K., WANG, S. Y., DONG, Y. J. & PENG, Y. Z. 2014. Effect of FA and FNA on activity of nitrite-oxidising bacteria. *Zhongguo Huanjing Kexue/China Environmental Science*, 34, 1242-1247.

ZHOU, Q., SUN, H., JIA, L., WU, W. & WANG, J. 2022. Simultaneous biological removal of nitrogen and phosphorus from secondary effluent of wastewater treatment plants by advanced treatment: A review. *Chemosphere*, 296, 134054.

Appendix A Code for fouling model simulations and automatically calculating sum of squared error (SSE) and model fitting constants

[Notes: Appendix A has been submitted for publication and is currently under review]

J. Jiang, A. Almuntashiri, W. Shon, S. Phuntsho, Q. Wang, S. Freguia, I, El-Saliby, H.K. Shon. (Under review). Feasibility study of powdered activated carbon membrane bioreactor (PAC-MBR) for source-separated urine treatment: a comparison with MBR.

Code:

```
j0 = data[~np.isnan(data).any(axis=3)]
```

```
data = np.genfromtxt('./data.csv', delimiter=',')
```

```
data = data[~np.isnan(data).any(axis=1)]
```

```
T, P = np.transpose(data)
```

```
# T *= 86400
```

```
V = P / P[0]
```

```
T = T.astype('float128')
```

```
V = V.astype('float128')
```

```
assert len(T) == len(V)
```

```
assert np.isnan(T).any() == False
```

```
assert np.isnan(V).any() == False
```

```
assert np.isinf(T).any() == False
```

```
assert np.isinf(V).any() == False
```

```
minimum_error, minimum_function = np.inf, ""
```

```
functions, function_names = [], []
```

```
def cake_blocking(t, kc):
```

```
    return 1 + kc * j0**2 * t
```

```
def predict_and_plot_cake_blocking():
```

```
    kc = curve_fit(cake_blocking, T, V, bounds=(0, 1e10))[0][0]
```

```
    _ = plt.plot(T, prediction(cake_blocking, [kc]))
```

```
    return kc
```



```

functions.append(predict_and_plot_cake_blocking)

function_names.append('Cake blocking')

_ = plt.plot(T, V)

kc = predict_and_plot_cake_blocking()

error = sse(cake_blocking, kc)

if error < minimum_error:

    minimum_error = error

    minimum_function = function_names[-1]

print("Kc:\t\t\t", kc)

print("SSE with predicted Kc:\t", error)

def intermediate_blocking(t, ki):

    return np.exp(ki * j0 * t)

def predict_and_plot_intermediate_blocking():

    ki = curve_fit(intermediate_blocking, T, V, bounds=(0, 1e4))[0][0]

    _ = plt.plot(T, prediction(intermediate_blocking, [ki]))

```

```

    return ki

functions.append(predict_and_plot_intermediate_blocking)

function_names.append('Intermediate blocking')

_ = plt.plot(T, V)

ki = predict_and_plot_intermediate_blocking()

error = sse(intermediate_blocking, ki)

if error < minimum_error:

    minimum_error = error

    minimum_function = function_names[-1]

print("Ki:\t\t\t", ki)

print("SSE with predicted Ki:\t", error)

def complete_blocking(t, kb):

    return 1 / (1 - kb * t)

def predict_and_plot_complete_blocking():

```

```

kb = curve_fit(complete_blocking, T, V, bounds=(0, 1 / T[-1]))[0][0]

_ = plt.plot(T, prediction(complete_blocking, [kb]))

return kb

functions.append(predict_and_plot_complete_blocking)

function_names.append('Complete blocking')

_ = plt.plot(T, V)

kb = predict_and_plot_complete_blocking()

error = sse(complete_blocking, ki)

if error < minimum_error:

    minimum_error = error

    minimum_function = function_names[-1]

print("Kb:\t\t\t", kb)

print("SSE with predicted Kb:\t", error)

def standard_blocking(t, ks):

    return (1 - (ks * j0 * t) / 2)**-2

```

```

def predict_and_plot_standard_blocking():

    ks = curve_fit(standard_blocking, T, V, bounds=(0, 1e6))[0][0]

    _ = plt.plot(T, prediction(standard_blocking, [ks]))

    return ks

functions.append(predict_and_plot_standard_blocking)

function_names.append('Standard blocking')

_ = plt.plot(T, V)

ks = predict_and_plot_standard_blocking()

error = sse(standard_blocking, ks)

if error < minimum_error:

    minimum_error = error

    minimum_function = function_names[-1]

print("Ks:\t\t", ks)

print("SSE with predicted Ks:\t", error)

```

```

def cake_intermediate(t, kc, ki):

    return np.exp(ki * j0 * t) * (1 + (kc * j0 / ki) * (np.exp(ki * j0 * t) - 1))

def predict_and_plot_cake_intermediate():

    kc, ki = curve_fit(cake_intermediate, T, V, bounds=((0, 0), (1e10, 1e3)))[0][:2]

    _ = plt.plot(T, prediction(cake_intermediate, [kc, ki]))

    return kc, ki

functions.append(predict_and_plot_cake_intermediate)

function_names.append('Cake + Intermediate')

_ = plt.plot(T, V)

kc, ki = predict_and_plot_cake_intermediate()

error = sse(cake_intermediate, kc, ki)

if error < minimum_error:

    minimum_error = error

    minimum_function = function_names[-1]

print("Kc, Ki:\t\t\t\t", (kc, ki))

```

```

print("SSE with predicted Kc, Ki:\t", error)

def cake_complete(t, kc, kb):

    return 1 / (1 - kb * t) * (1 - kc * j0**2 / kb * np.log(1 - kb * t))

def predict_and_plot_cake_complete():

    kc, kb = curve_fit(cake_complete, T, V, bounds=((0, 0), (1e10, 1 / T[-1])))

    _ = plt.plot(T, prediction(cake_complete, [kc, kb]))

    return kc, kb

functions.append(predict_and_plot_cake_complete)

function_names.append('Cake + Complete')

_ = plt.plot(T, V)

kc, kb = predict_and_plot_cake_complete()

error = sse(cake_complete, kc, kb)

if error < minimum_error:

    minimum_error = error

    minimum_function = function_names[-1]

```

```

print("Kc, Kb:\t\t\t", (kc, kb))

print("SSE with predicted Kc, Kb:\t", error)

def complete_standard(t, kb, ks):

    return 1 / ((1 - kb * t) * (1 + ks * j0 / 2 / kb * np.log(1 - kb * t)**2))

def predict_and_plot_complete_standard():

    kb, ks = curve_fit(complete_standard, T, V, bounds=((0, 0), (1 / T[-1], 1e10)))[0][:2]

    _ = plt.plot(T, prediction(complete_standard, [kb, ks]))

    return kb, ks

functions.append(predict_and_plot_complete_standard)

function_names.append('Complete + Standard')

_ = plt.plot(T, V)

kb, ks = predict_and_plot_complete_standard()

error = sse(complete_standard, kb, ks)

if error < minimum_error:

    minimum_error = error

```

```

    minimum_function = function_names[-1]

print("Kb, Ks:\t\t\t", (kb, ks))

print("SSE with predicted Kb, Ks:\t", error)

def intermediate_standard(t, ki, ks):

    return np.exp(ki * j0 * t) / ((1 - ks / 2 / ki * (np.exp(ki * j0 * t) - 1))**2)

def predict_and_plot_intermediate_standard():

    ki, ks = curve_fit(intermediate_standard, T, V, bounds=((0, 0), (4e2, 1e2)))[0][:2]

    _ = plt.plot(T, prediction(intermediate_standard, [ki, ks]))

    return ki, ks

functions.append(predict_and_plot_intermediate_standard)

function_names.append('Intermediate + Standard')

_ = plt.plot(T, V)

ki, ks = predict_and_plot_intermediate_standard()

error = sse(intermediate_standard, ki, ks)

```



```

if error < minimum_error:

    minimum_error = error

    minimum_function = function_names[-1]

print("Ki, Ks:\t\t\t\t", (ki, ks))

print("SSE with predicted Ki, Ks:\t", error)

def cake_standard(t, kc, ks):

    return (1 - ks * j0 * t / 2)**-2 + kc * j0**2 * t

def predict_and_plot_cake_standard():

    kc, ks = curve_fit(cake_standard, T, V, p0=(1,1), bounds=(0, 1e10))[0][:2]

    _ = plt.plot(T, prediction(cake_standard, [kc, ks]))

    return kc, ks

functions.append(predict_and_plot_cake_standard)

function_names.append('Cake + Standard')

_ = plt.plot(T, V)

kc, ks = predict_and_plot_cake_standard()

```

```
error = sse(cake_standard, kc, ks)

if error < minimum_error:

    minimum_error = error

    minimum_function = function_names[-1]

print("Kc, Ks:\t\t\t", (kc, ks))

print("SSE with predicted Kc, Ks:\t", error)
```

Appendix B Theoretical fouling models results (Control MBR)

[Notes: Appendix B has been submitted for publication and is currently under review]

J. Jiang, A. Almuntashiri, W. Shon, S. Phuntsho, Q. Wang, S. Freguia, I, El-Saliby, H.K. Shon. (Under review). Feasibility study of powdered activated carbon membrane bioreactor (PAC-MBR) for source-separated urine treatment: a comparison with MBR.

Single model

	Cake blocking	Intermediate blocking	Complete blocking	Standard blocking
Time (day)	Pt/p0 (kPa)	Pt/p0 (kPa)	Pt/p0 (kPa)	Pt/p0 (kPa)
0	1.00	1.00	1.00	1.00
5	1.08	1.05	1.03	1.17
10	1.16	1.09	1.05	0.12
15	1.24	1.14	1.08	0.04
20	1.32	1.20	1.12	0.02
25	1.40	1.25	1.15	0.01
30	1.48	1.31	1.18	0.01
35	1.55	1.37	1.22	0.01
40	1.63	1.43	1.26	0.00
45	1.71	1.50	1.30	0.00
50	1.79	1.57	1.35	0.00

55	1.87	1.64	1.40	0.00
60	1.95	1.72	1.45	0.00
65	2.03	1.79	1.51	0.00
70	2.11	1.88	1.57	0.00
75	2.19	1.96	1.63	0.00
80	2.27	2.05	1.70	0.00
85	2.35	2.15	1.78	0.00
90	2.43	2.25	1.87	0.00
95	2.50	2.35	1.96	0.00
100	2.58	2.46	2.07	0.00
105	2.66	2.57	2.19	0.00
110	2.74	2.69	2.32	0.00
115	2.82	2.81	2.47	0.00
120	2.90	2.94	2.63	0.00
125	2.98	3.08	2.83	0.00
130	3.06	3.22	3.05	0.00
135	3.14	3.37	3.31	0.00
140	3.22	3.52	3.62	0.00
145	3.30	3.68	3.99	0.00
150	3.38	3.85	4.45	0.00

Combined models

	Cake- complete blocking	Cake- intermediate blocking	Complete- standard blocking	Intermediate- standard blocking	Cake- standard blocking
Time (day)	Pt/p0 (kPa)	Pt/p0 (kPa)	Pt/p0 (kPa)	Pt/p0 (kPa)	Pt/p0 (kPa)
0	1.00	1.00	1.00	1.00	1.00
5	1.04	1.04	1.03	1.03	1.03
10	1.09	1.09	1.06	1.07	1.07
15	1.14	1.14	1.09	1.11	1.11
20	1.19	1.19	1.13	1.15	1.15
25	1.24	1.25	1.16	1.19	1.19
30	1.30	1.30	1.20	1.24	1.24
35	1.35	1.36	1.24	1.29	1.29
40	1.41	1.43	1.28	1.34	1.34
45	1.48	1.49	1.33	1.39	1.39
50	1.54	1.56	1.38	1.45	1.45
55	1.61	1.63	1.43	1.51	1.51
60	1.68	1.70	1.48	1.57	1.58
65	1.76	1.78	1.54	1.64	1.65
70	1.84	1.87	1.60	1.71	1.72
75	1.92	1.95	1.67	1.79	1.80
80	2.01	2.04	1.74	1.87	1.89
85	2.10	2.14	1.82	1.96	1.98
90	2.20	2.24	1.91	2.06	2.07

95	2.30	2.34	2.00	2.16	2.18
100	2.41	2.45	2.10	2.27	2.29
105	2.53	2.56	2.21	2.39	2.42
110	2.65	2.68	2.34	2.51	2.55
115	2.78	2.81	2.48	2.65	2.69
120	2.92	2.94	2.64	2.80	2.85
125	3.06	3.08	2.82	2.96	3.02
130	3.22	3.22	3.03	3.14	3.21
135	3.39	3.37	3.28	3.33	3.41
140	3.56	3.53	3.58	3.54	3.63
145	3.75	3.70	3.95	3.77	3.88
150	3.95	3.87	4.42	4.02	4.15

Appendix C Theoretical fouling models results (Hybrid PAC-MBR)

[Notes: Appendix C has been submitted for publication and is currently under review]

J. Jiang, A. Almuntashiri, W. Shon, S. Phuntsho, Q. Wang, S. Freguia, I. El-Saliby, H.K. Shon. (Under review). Feasibility study of powdered activated carbon membrane bioreactor (PAC-MBR) for source-separated urine treatment: a comparison with MBR.

Single model

	Cake	Intermediate	Complete	Standard
Time	blocking	blocking	blocking	blocking
(day)	Pt/p0 (kPa)	Pt/p0 (kPa)	Pt/p0 (kPa)	Pt/p0 (kPa)
0	1.00	1.00	1.00	1.00
5	1.02	1.02	1.01	1.14
10	1.04	1.04	1.03	0.12
15	1.07	1.06	1.05	0.04
20	1.09	1.07	1.06	0.02
25	1.11	1.09	1.08	0.01
30	1.13	1.11	1.10	0.01
35	1.16	1.13	1.11	0.01
40	1.18	1.16	1.13	0.00
45	1.20	1.18	1.15	0.00
50	1.22	1.20	1.17	0.00

55	1.25	1.22	1.19	0.00
60	1.27	1.24	1.21	0.00
65	1.29	1.26	1.23	0.00
70	1.31	1.29	1.26	0.00
75	1.33	1.31	1.28	0.00
80	1.36	1.34	1.30	0.00
85	1.38	1.36	1.33	0.00
90	1.40	1.38	1.36	0.00
95	1.42	1.41	1.38	0.00
100	1.45	1.44	1.41	0.00
105	1.47	1.46	1.44	0.00
110	1.49	1.49	1.47	0.00
115	1.51	1.52	1.51	0.00
120	1.53	1.54	1.54	0.00
125	1.56	1.57	1.57	0.00
130	1.58	1.60	1.61	0.00
135	1.60	1.63	1.65	0.00
140	1.62	1.66	1.69	0.00
145	1.65	1.69	1.73	0.00
150	1.67	1.72	1.78	0.00

Combined models

Time (day)	Cake- complete blocking Pt/p0 (kpa)	Cake- intermediate blocking Pt/p0 (kpa)	Complete- standard blocking Pt/p0 (kpa)	Intermediate- standard blocking Pt/p0 (kpa)	Cake- standard blocking Pt/p0 (kpa)
0	1.00	1.00	1.00	1.00	1.00
5	1.02	1.02	1.02	1.02	1.02
10	1.03	1.04	1.03	1.03	1.03
15	1.05	1.05	1.05	1.05	1.05
20	1.06	1.07	1.06	1.07	1.07
25	1.08	1.09	1.08	1.09	1.09
30	1.10	1.11	1.10	1.11	1.11
35	1.12	1.13	1.12	1.12	1.12
40	1.13	1.15	1.13	1.14	1.14
45	1.15	1.17	1.15	1.16	1.16
50	1.17	1.19	1.17	1.18	1.18
55	1.19	1.22	1.19	1.21	1.21
60	1.22	1.24	1.22	1.23	1.23
65	1.24	1.26	1.24	1.25	1.25
70	1.26	1.28	1.26	1.27	1.27
75	1.28	1.31	1.28	1.30	1.30
80	1.31	1.33	1.31	1.32	1.32
85	1.33	1.36	1.33	1.35	1.35
90	1.36	1.38	1.36	1.37	1.37

95	1.39	1.41	1.39	1.40	1.40
100	1.42	1.43	1.41	1.43	1.43
105	1.44	1.46	1.44	1.45	1.45
110	1.48	1.49	1.47	1.48	1.48
115	1.51	1.51	1.51	1.51	1.51
120	1.54	1.54	1.54	1.54	1.54
125	1.58	1.57	1.57	1.57	1.57
130	1.61	1.60	1.61	1.61	1.61
135	1.65	1.63	1.65	1.64	1.64
140	1.69	1.66	1.69	1.68	1.68
145	1.73	1.69	1.73	1.71	1.71
150	1.77	1.73	1.77	1.75	1.75